

On the Characteristics of Fires in Tunnels

Doctoral Thesis

Anders Lönnermark

Submitted for the degree of Doctor of Philosophy
at the
Department of Fire Safety Engineering
Lund Institute of Technology
Lund University

Lund 2005

Department of Fire Safety Engineering
Lund Institute of Technology

Lund University
Box 118, SE-221 00 Lund
Sweden

Report 1033
ISSN 1402-3504
ISRN LUTVDG/TVBB--1033--SE
ISBN 91-628-6637-0

© Anders Lönnermark, 2005
Printed by Tryckeriet i E-huset, Lund University, Lund, Sweden
September 2005

Front page photo: Large-scale fire test carried out in the Runehamar tunnel, Norway,
2003 (photo by Haukur Ingason)

“I will tell you what knowledge is.
To know when you know something,
and to know when you do not,
that is knowledge.”

Konfucius

Abstract

Important phenomena related to tunnel fires are presented including both experimental and theoretical work. The main focus is on the large-scale fire tests performed in 2003, in the Runehammar tunnel in Norway. During these tests heat release rate (HRR), temperatures, gas concentrations (O_2 , CO_2 , CO , HCN , and H_2O), velocities, radiation, and smoke were measured. Four tests with a set-up simulating HGV cargos were performed with fuel loads constituting of different mixtures of cellulose and plastic. The fuel load ranged from 2850 kg to 11010 kg giving maximum HRRs between 66 MW and 202 MW.

The results showed that ordinary (non-hazardous) cargo can give HRRs and temperatures normally expected to be related only to hazardous goods (e.g. tanker fires). Thus, the highest HRR and gas temperature were far higher than that suggested by most tunnel design guidelines. A close correlation between the maximum HRR and energy content is presented for passenger cars and HGVs. It has also been shown in the Runehammar tests that the fire in an HGV can spread a long distance downstream in a tunnel, of the order of 100 m. Based on the test results and real incidents one must emphasize the importance of the incident operation during the first five to ten minutes of the fire. The actions of the people inside the tunnel and the rescue personnel during this time period can be crucial to the outcome.

During two of the fire tests, large pulsations of the gas flow inside the tunnel were observed. These pulsations were registered only when the measured heat release rate was higher than 125 MW - 135 MW. Two different periods of pulsations were registered, short periods of approximately 4 s and longer periods of approximately 18 s. The pulsations are presented and explanations are given, using two different approaches: an acoustic approach and a frequency response analysis based on an impedance approach. The intrinsic resonances of the system proved to be close to the periods found in the experiments. Several factors can affect the pulsations, but the calculations show that the oscillation periods are properties of the system.

Other issues discussed include backlayering and the effect of the ventilation on the HRR, flame length, and the conditions in the tunnel. Literature data are, where relevant, compared with the results from the Runehammar tests. In this analysis toxicity and the effect of the ventilation conditions on the gas composition in the tunnel are also included. Special attention was paid to the CO/CO_2 ratio and its dependence on the ventilation and combustion conditions. In this context results from a detailed study of the emissions from an enclosure fire under varied ventilation conditions are used as the basis for a discussion of the impact of ventilation on the acute toxicity of the fire gases.

Key words: tunnel fire, experiments, heat release rate, temperature, fire spread, ventilation, backlayering, pulsations, thermoacoustic instability, equivalence ratio, emissions, gas concentrations, toxicity.

Acknowledgements

First of all I would like to thank my colleague and friend Dr Haukur Ingason at SP Fire Technology, who acted as deputy supervisor and has inspired me during the work with guidance, collaboration, and interesting discussions. His hard work during the initial phase was essential for making it possible to perform the tests in the Runehammar tunnel.

I would also like to thank my supervisor Professor Göran Holmstedt at the Department of Fire Safety Engineering, Lund University for advices and SP, Professor Ulf Wickström, and Dr Margaret Simonson for making it possible for me to perform my PhD studies. Dr Bror Persson is acknowledged for being the person who made me start with the studies in the first place and also for interesting discussions regarding the pulsations in the Runehammar tunnel.

Special thanks go to Mr Henry Persson who was my first head of section at SP and since then has been a partner in many research project and a good friend and mentor. Per Blomqvist is the co-author of two of the papers in this thesis. In addition to this work, we have collaborated in a number of research projects, both experimental and otherwise. I would like to thank him for an interesting journey of collaboration so far and I hope for more co-operation in the future.

Much of the work has been experimental and would not have been possible without the fantastic technicians at SP Fire Technology. They always see the solutions instead of the problems in their work and thereby have always managed to accomplish my requests regarding experimental set-ups. Therefore, Joel Blom, Michael Magnusson, Joel Blom, Markus Lönnmark, and Ari Palo-Oja are acknowledged for their invaluable help. The rest of my colleagues at SP Fire Technology are acknowledged for being a part of the nice and inspiring atmosphere, making the work easier to perform. I am also indebted to SP's librarian Helene Ekström, who in a nice and quick manner has helped me to obtain copies of different kinds of literature, stretching back to the 19th century. Dr Sven-Inge Möller at Combustion Physics, Lund University is acknowledged for describing the use of pulse combustors today.

All the papers, upon which this thesis is based, contain large experimental parts. This work would not have been possible without funding. The following organizations are gratefully acknowledged for the financial support and co-operation: the Swedish Rescue Services Agency, the Swedish Fire Research Board, the Swedish Road Administration, the Swedish Rail Administration, the European Commission, Promat International, Gerco Beveiligingen B.V., B I G Brandschutz Innovationen, and the Norwegian Road Administration.

Finally, my special thanks go to my wonderful wife Anne who has supported me all through this work and for having patience with me covering the dinner table with papers and having the lap top on the coffee table, and to my son Andreas and daughter Johanna who have been understanding when their father has been abroad or generally absent-minded.

List of publications

This thesis is based on the following papers:

- I. Lönnermark, A. and Ingason, H., “Gas Temperatures in Heavy Goods Vehicle Fires in Tunnels”, *Fire Safety Journal*, **40**, 506-527, 2005.
- II. Ingason, H. and Lönnermark, A., “Heat Release Rates from Heavy Goods Vehicle Trailer Fires in Tunnels”, *Fire Safety Journal*, (in press).
- III. Blomqvist, P. and Lönnermark, A., “Characterization of the Combustion Products in Large-scale Fire Tests: Comparison of Three Experimental Configurations”, *Fire and Materials*, **25**, 71-81, 2001.
- IV. Lönnermark, A. and Blomqvist, P., “Emissions from an Automobile Fire”, *Chemosphere*, (in press).
- V. Lönnermark, A. and Ingason, H., “Acoustic Considerations Regarding Pulsations during Large-Scale Fire Tests in a Tunnel”, *Fire Safety Science - Proceedings of the Eighth International Symposium, Beijing, China, 18-23 September, 2005*, (in press).
- VI. Lönnermark, A., Persson, B., and Ingason, H., “Pulsations during Large-Scale Fire Tests in the Runehamar Tunnel”, (submitted to *Fire Safety Journal*).
- VII. Lönnermark, A. and Ingason, H., “Fire Spread and Flame Length in Large-Scale Tunnel Fires”, *Fire Technology*, (in press).

In addition to the papers included in the thesis the author has also contributed to the following publications:

- VIII. Blomqvist, P., Lönnermark, A., Månsson, M., and Persson, H., “Fire Characteristics and Detailed Smoke Gas Analyses in Controlled Under-Ventilated Large-Scale Combustion Experiments”, *Proceedings of the INDUSTRIAL FIRES III Workshop, Risø, Denmark*, pp. 7-16, 1996.
- IX. Blomqvist, P., Lönnermark, A., Månsson, M., and Persson, H., “Methodology for Measurements of Fire Characteristics and Smoke Gas Composition in Controlled Under-ventilated Large-scale Combustion Experiments”, *Proceedings of the Second International Conference on Fire Research and Engineering, Gaithersburg, Maryland, USA*, pp. 314-324, 1997.
- X. Blomqvist, P., Lönnermark, A., Månsson, M., and Persson, H. “Chemical characterization of the smoke gases in large-scale combustion experiments”, *Proceedings of the 8th International Fire Science & Engineering Conference (Interflam '99), Edinburgh, Scotland, Volume 1*, pp. 143-153, 1999.

- XI. Lönnermark, A., Persson, B., and Persson, H., “Modelling of Foam Spread on a Burning Liquid”, Proceedings of the 9th International Fire Science & Engineering Conference (Interflam 2001), 291-302, Edinburgh, Scotland, 17-19 September, 2001.
- XII. Axelsson, J., Andersson, P., Lönnermark, A., Van Hees, P., and Wetterlund, I., “Uncertainty of HRR and SPR Measurements in SBI and Room/corner Test”, 9th International Fire Science & Engineering Conference (Interflam 2001), 507-518, Edinburgh, Scotland, 17-19 September, 2001.
- XIII. Lönnermark, A., “CFD Modelling of Small Biomass-Fired Boilers”, Thesis for the degree of licentiate of engineering, Department of Energy Conversion, Chalmers University of Technology, Göteborg, Sweden, 2002.
- XIV. Persson, B., Lönnermark, A., and Persson, H., “Modelling of Foam Spread on a Burning Liquid Fuel Surface”, Fire Safety Science - Proceedings of the Seventh International Symposium, 667-678, Worcester, USA, 16-21 June, 2002.
- XV. Persson, B., Lönnermark, A., and Persson, H., “FOAMSPEX: Large Scale Foam Application - Modelling of Foam Spread and Extinguishment”, *Fire Technology*, **39**, 4, 347-362, 2003.
- XVI. Ingason, H. and Lönnermark, A., “Large-scale Fire Tests in the Runehammar tunnel - Heat Release Rate (HRR)”, International Symposium on Catastrophic Tunnel Fires (CTF), SP Report 2004:05, p.81-92, Borås, Sweden, 2003.
- XVII. Lönnermark, A. and Ingason, H., “Large Scale Fire Tests in the Runehammar Tunnel - Gas Temperature and Radiation”, International Symposium on Catastrophic Tunnel Fires (CTF), SP Report 2004:05, p. 93-103, Borås, Sweden, 20-21 November, 2003.
- XVIII. Ingason, H. and Lönnermark, A., “Recent Achievements Regarding Measuring of Time-heat and Time-temperature Development in Tunnels”, 1st International Symposium on Safe & Reliable Tunnels, Prague, Czech Republic, 4-6 February, 2004.
- XIX. Lönnermark, A. and Ingason, H., “Fires in Heavy Goods Vehicle (HGV) Cargos in Tunnels”, 10th International Fire Science & Engineering Conference (Interflam 2004), 1529-1540, Edinburgh, Scotland, 5-7 July, 2004.
- XX. Ingason, H. and Lönnermark, A., “Fire development of Large Vehicles in Road Tunnels”, Proceedings of the Fifth International Conference on Tunnel Fires, 203-212, London, UK, 25-27 October, 2004.
- XXI. Lönnermark, A. and Ingason, H., “Recent Achievements Regarding Heat Release and Temperatures during Fires in Tunnels”, Safety in Infrastructure - Svédületes!, Budapest, Hungary, 20-21 October 2004, 2004.

Nomenclature

a	Correlation constant (see Eq. (5.17)) [depends on b]
A	Area [m^2]
A_i	Constants in the exponential expression of the general natural fire curve (Eq. (3.5)) [-]
b	Correlation constant (see Eq. (5.17)) [-] Distance [m]
B	Buoyancy factor [m/s]
c	Correlation constant (see Equation (5.3)) [-] Speed of sound [m/s]
C	Concentration (by volume) [%]
c_p	Specific heat capacity [kJ/(K kg)]
D	Diameter [m]
D_H	Hydraulic diameter [m]
E	Amount of energy developed per consumed kilogram of oxygen [kJ/kg]
f	Frequency [1/s]
F_1	Fraction of an incapacitating dose [-]
FI	Total fraction of an incapacitating dose [-]
\bar{F}_{ws}	View factor between the walls and the fire source [-]
Fr	Froude number [-]
g	Acceleration of gravity [m/s^2]
h	Convective heat transfer coefficient [$\text{kW}/(\text{m}^2 \text{K})$]
h_b	Beam depth [m]
h_f	Flame height of free burning flame [m]
h_r	Radial extension of flame beneath a ceiling [m]
Δh_c	Heat of combustion per unit mass [kJ/kg]
H	Height [m]
H_f	Distance between top of fuel and ceiling [m]
I	COHb concentration at incapacitation [%]
k	Time width coefficient (in Equation (3.3)) [1/min] Correlation constant (see Equation (5.2)) [-] Wave number [1/m]
K	Correlation constant (see Equation (5.3)) [-]
K_g	Grade factor [-]
L	Length [m]
L_b	Half the width between two beams [m]
L_f	Flame length [m]
\dot{m}	Mass flow rate [kg/s]
M	Molecular weight [g/mol]
n	Retard index (in Equation (3.3)) [-] Acoustic mode [-] Time step number [-]
N	A non-dimensional group (see Equation (4.1)) [-]
p	Pressure [Pa]
P	Perimeter [m]
Q	Energy [GJ]
\dot{Q}	Heat release rate [kW] in most equations, but [MW] in some relationships

\dot{Q}^*	Non-dimensional heat release rate [-]
\dot{Q}''	Heat release rate divided by plan area of the fire [kW/m ²] Heat flux [kW/m ²]
r	Amplitude coefficient (in Equation (3.3)) [°C] Stoichiometric mass ratio of air to volatiles [-] Radius [m]
R	Correlation coefficient [-]
Re	Reynolds number [-]
Ri	Richardson number [-]
RMV	Breathing rate [L/min]
St	Strouhal number [-]
t	Time [s] or [min] (depending on specific application)
T	Temperature [K] or [°C] (depending on specific application) Period [s]
ΔT_0^*	Dimensionless constant (see Eq. (5.8))
Tr	Heat transfer function [-]
u	Velocity [m/s]
u_{cr}^*	Non-dimensional critical velocity [-]
\dot{V}''	Volumetric surface burning rate [m ³ /(m ² s)]
V_{CO_2}	Multiplying factor for the enhanced uptake of asphyxiant gases due to hyperventilation [-]
W	Width [m]
x	Distance [m]
X	Mole fraction [-]
y	Yield [g/g]
Y	Concentration [ppm]

Greek symbols

α	Ratio between the number of moles of combustion products including nitrogen and the number of moles of reactants including nitrogen (expansion factor) [-] Blockage ratio [-] Thermal diffusivity [m ² /s]
α_i	Constants in the exponential expression of the general natural fire curve (Eq. (3.5)) [1/min] Correlation constant in Eq. (5.15) [-]
β	Correlation constant in Eq. (5.15) [-] Correlation coefficient in Eq. (6.2)
γ	Specific heat ratio [-]
ε	Emissivity [-]
ν	Kinematic viscosity [m ² /s]
η_w	Ratio between the temperature rise of the surface and the fire [-]
η_x	Ratio between the temperature rise of an interior point and the surface [-]
ρ	Density [kg/m ³]
σ	Stefan-Boltzmann constant (kW/(m ² K ⁴))
τ	Time delay (s)

φ	Phase [rad]
ϕ	Equivalence ratio [-]
χ	Combustion efficiency [-]
ξ	Correlation coefficient in Eq. (6.2) [-]
ψ	Downhill slope of the tunnel [%]
ω	Angular frequency [rad/s]

Subscripts

0	Referring to ambient conditions or to the Runehamar tunnel without protection
1	Referring to the protection tunnel near the fire in the Runehamar tests
b	Beating
B	Flame holder
c	Convective
cr	Critical
f	Fire, flame
g	Gas
l	Loss
r	Radiation
	Resting
sl	Smoke layer
t	Tunnel
w	Wall
wv	Well ventilated
x	Referring to a certain distance

Abbreviations

BA	Breathing apparatus
CFD	Computational fluid dynamics
HC	Hydrocarbon
HGV	Heavy goods vehicle
HRR	Heat release rate
imp	Impingement
ITA	International Tunnelling Association
NA	Not available
OD	Optical density
PAH	Polycyclic aromatic hydrocarbons
PBDD/F	Polybrominated dibenzo-p-dioxins and -furans
PCDD/F	Polychlorinated dibenzo-p-dioxins and -furans
PE	Polyethene
PS	Polystyrene
PUR	Polyurethane
RABT	Richtlinien für die Ausstattung und den Betrieb von Straßentunneln
RWS	Rijkswaterstaat
THC	Total hydrocarbon content
ZTV	Zusätzliche Technische Vertragsbedingungen und Richtlinien für den Bau von Straßentunneln

Table of contents

	Abstract	i
	Acknowledgements	ii
	List of publications	iii
	Nomenclature	v
	Table of contents	ix
1	Introduction	1
1.1	Aim of this thesis	1
1.2	The outline of the thesis	2
2	Background	3
2.1	Tunnel accidents	3
2.2	Guidelines	7
2.2.1	Heat release rate	7
2.2.2	Temperature	9
3	Fire experiments in tunnels	13
3.1	Different methods of estimating the HRR and some factors influencing the results	13
3.2	Summary of experiments	16
3.3	Summary of results from fire experiments	19
4	Flame length and fire spread in a tunnel	29
5	Ventilation	41
5.1	Different types of ventilation	41
5.2	Effects of ventilation on the fire	42
5.3	Backlayering	47
5.4	Pulsations	53
6	Gas concentrations in the tunnel	65
6.1	Emissions from fires	65
6.2	Influence of ventilation on the gas composition	67
6.3	Toxicity	76
7	Application of the results	83
7.1	Effects on the tunnel structure	83
7.2	Rescue operations	83
7.3	Sprinkler and other water-based extinguishment systems	85
8	Conclusions	87
9	Future work	89
10	References	91

1 Introduction

1.1 Aim of this thesis

The author of this thesis has during his employment at SP Swedish National Testing and Research Institute (1995-) been involved in a number of research project, both national and international (financed by the European Commission). Most of this work has been experimental, but several of the projects have also involved mathematical and numerical modelling (e.g. computational fluid dynamics, CFD).

Regarding the articles included in this thesis (I-VII): in those cases where the author of this thesis appears as the first name, he was responsible for writing the article, with help and input from the co-authors. In those cases where the author of this thesis does not appear as first name, he took an active part in the writing process and wrote selected parts of the articles.

Papers I, II, V, VI, and VII concern the large-scale fire tests performed in the Runehammar tunnel in Norway. In this test series, the author of the thesis took an active part in the planning of the tests together with the initiator and project leader Dr Haukur Ingason. The author was responsible for the preparation, performing, and evaluation of the tests in close collaboration with Dr Ingason. In Papers V and VI, the author has performed the calculations, although Dr Bror Persson developed the theory behind the calculations presented in Paper VI. In Paper III and IV, the author was responsible for planning, performing, and evaluating the tests. He was also responsible for the measurements of physical properties (e.g. mass loss rate, heat release rate, mass flow, temperature etc.), while Per Blomqvist was responsible for the sampling of gases and gas analyses. In the work presented in Paper III, the author was responsible for the construction, calibration, and use of the phi meter.

The aim of this thesis is to describe different phenomena that can be observed in connection with fires in tunnels. Some features are common to other types of fires or fires in other situations than tunnels, while some are specific to fires in tunnels. The latter will obtain the most attention.

Much of the information concerns all types of fires in tunnels, although the focus is on fires in heavy goods vehicles (HGV), since several of the papers, upon which this thesis is based, concern the results from the large-scale fire tests performed in the Runehammar tunnel in 2003. As will be discussed, HGVs have had a very important role in determining the ultimate outcome of the fire in all the major tunnel fires during recent years. Previously, there has also been a lack of information regarding the magnitude and effect of fires in HGVs in tunnels. The cargo in the HGVs is of special interest, since it is this cargo that constitutes the majority of the fire load. This thesis will show that there have previously been some misconceptions concerning the size and nature of fires in loads of seemingly innocuous goods.

The thesis focuses on the physical (and to some extent chemical) processes in connection with fires in tunnels. Many of the properties found and effects discussed can be very important for the evacuation of people and the ability of the rescue service to help people or to come close enough to the fire to make extinguishment

feasible. The processes of evacuation and extinguishment are, however, not discussed in detail, but are only mentioned to illustrate the importance of different parameters

Much interest within the field of tunnel fires is focused on the smoke movement and verification of the ability of different installations to evacuate smoke or to meet certain conditions. Some specific aspects of ventilation and smoke (e.g. backlayering) are discussed, but ventilation of smoke is not a focal point of this thesis.

The importance of the thermal insult on the structure (e.g. spalling) will be discussed briefly, although the factors behind the response of the structure to the high temperatures associated with fires in tunnels are outside the scope of this thesis.

1.2 The outline of the thesis

This thesis is based on seven papers (see list above). These papers are not presented separately, but the results are described and discussed in the different sections of the thesis when suitable. Below follows a description of the different chapters in the thesis.

Chapter 2 provides the background and the reason for performing the large-scale fire tests in the Runehamar tunnel in 2003. The Runehamar tests are a central part of the thesis and the results from these tests will be compared with the information presented in Chapter 2.

Chapter 3 provides an overview of results from fire experiments in tunnels or fire tests with vehicles. The focus is on the heat release rate (HRR) and temperature and in this chapter the main results from Papers I and II are presented and compared with experimental results from other test series.

Chapter 4 gives information on flame lengths and fire spread in tunnels. The result from Paper VII are summarized and compared with results from models and experiments found in the literature.

In Chapter 5 different types of ventilation strategies are discussed briefly. The main focus of the chapter is on the pulsations observed in the Runehamar tests (Paper V and VI) and on the effect the ventilation has on the fire. The phenomenon backlayering is discussed and the results from the Runehamar tests are compared to some correlations found in the literature.

In Chapter 6 different factors affecting the production of different gases are discussed, in particular the effect of ventilation and the equivalence ratio, ϕ . The combustion gases produced in a fire are important for the severity of the hazard to people in a tunnel during a fire.

In Chapter 7 how the results presented in this thesis correlate with different applications in a real fire situation, is discussed briefly.

2 Background

This chapter contains background information on which the decision to perform the tests in the Runehamar tunnel in 2003 was based. In Section 2.1 selected tunnel accidents are presented and discussed while in Section 2.2 some existing guidelines regarding tunnel fire safety are presented and how their content correlate with occurred accidents, especially those involving HGVs.

2.1 Tunnel accidents

Fires in tunnels have obtained special attention during recent years due to several catastrophic fires in alp tunnels. There were, however, fires in tunnels also prior to these accidents. In Table 2.1 a summary is given of fires in road tunnels of special interest. A more extensive list is given by Carvel and Marlair [1].

Table 2.1 Summary of fires in road tunnels [1, 2]

Year	Tunnel, length	Location	Vehicle at origin of the fire	Cause of fire	Duration	Consequences for		
						people	vehicles	structure
1949, 13 May	Holland L = 2 550 m	New York, USA	1 HGV loaded with 11 ton carbon bisulfur	Load falling of HGV	4 h	66 injured (smoke)	10 HGVs 13 cars	Serious damage 200 m
1978, 11 Aug	Velsen L = 770 m	Velsen, Netherlands	2 HGVs and 4 cars	Front-back collision	1 h 20 min	5 dead 5 injured	2 HGVs 4 cars	Serious damage 30 m
1979, 11 July	Nihonzaka L = 2 045 m	Shizuoka, Japan	4 HGVs and 2 cars	Front-back collision	4 days	7 dead 2 injured	127 HGVs, 46 cars	Serious damage 1100 m
1980, 17 Apr.	Kajiwara L = 740 m	Japan	1 truck (4 t) with 3600 L paint and 1 truck (10 t)	Collision with side wall and over-turning	1 h 20 min	1 dead	2 trucks	Damage 280 m
1982, 7 Apr.	Caldecott L = 1 083 m	Oakland, USA	1 car, 1 bus, 1 tanker with 33 000 L petrol	Front-back collision	2 h 40 min	7 dead 2 injured	3 HGV 1 bus 4 cars	Serious damage 580 m
1983, 3 Feb.	Fréjus L = 12 868 m	Modane, France-Italy	1 HGV loaded with plastic material	Gear box breaking	1 h 50 min	none	1 HGV	Serious damage 200 m
1986, 9 Sept.	L'Arme L=1100 m	France		Collision		3 dead 5 injured		
1987, 18 Feb.	Gumefens L = 340 m	Bern, Switzerland	1 HGV	Mass collision on slippery road	2 h	2 dead	2 HGV 1 van	Slight damage
1993	Serra a Ripoli L=442 m	Bologna, Italy	Car and HGV with rolls of paper	Vehicle out of control and collision	2 h 30 min	4 dead 4 injured	4 HGV 11 cars	Serious damage to lining
1993	Fréjus L=12870 m	France	1 HGV	Engine fire	2 h	none	1 HGV	

Year	Tunnel, length	Location	Vehicle at origin of the fire	Cause of fire	Duration	Consequences for		
						people	vehicles	structure
1994, 5 July	St. Gotthard L=16322 m	Goeschenen, Switzerland	1 HGV with trailer loaded with 750 bicycles wrapped in carton and plastics	Friction wheel	2 h	none	1 HGV (with trailer)	Serious damage to ceiling, pavement and equipment 50 m, tunnel closed for 2.5 days
1994, 27 Feb.	Huguenot L=4000 m	South Africa	Bus	Fire in gearbox	1 h	1 dead 28 injured	bus	Damage to installations
1996, 18 Mar.	Isola delle Femmine L=150 m	Sicilia, Italy	1 tanker with liquid gas + 1 small bus	Bus crashed into back of tanker (stopped due to previous collision)		5 dead 34 injured	1 tanker 1 bus 18 cars	Damage to lining and lighting
1997, 31 Oct.	St. Gotthard L=16322 m	Switzerland	1HGV loaded with cars	Fire in engine	1 h 20 min	none	1 HGV	Serious damage 100 m
1999, 24 Mar.	Mont Blanc L=11 600 m	France-Italy	Fire starts in a HGV	Not known	53 h	39 dead	23 HGVs 1 small truck 9 cars 1 motorcycle	Severe damage (900 m), the tunnel closed for three years
1999, 29 May	Tauern L=6400 m	Austria	Multiple collision due to maintenance work	Leakage of paints and varnishes	15 h	12 dead	16 HGVs 24 cars	Closed for three months
2000, 14 July	Seljestads-tunn L=1272 m	Norway	Multiple collision	Diesel fire in engine compartment	45 min	6 injured	1 lorry 6 cars 1 MC	Severe damage
2001, 24 Oct.	St. Gotthard ^{a)} L=16322	Switzerland	Collision between two HGVs	Collision	2 days	11 dead	13 HGVs 10 cars	Severe damage 230 m, additionally damage 700 m, closed for two months
2003, 10 Nov.	Fløfjell 3100 m	Norway	Fire in car spread to the tunnel lining	Collision between car and wall		1 dead	1 car	
2005, 4 June	Fréjus 12900 m	France/Italy	1 HGV carrying tyres	Engine fire		2 dead, 21 injured	4 HGV	10 km of equipment to be repaired

a) The actual tunnel length is 16322 m, but another 596 m is motorway protected by an enclosing gallery giving a total length of 16918 m.

Not all tunnel fires reach catastrophic proportions. As shown in Table 2.1 there have been fires in both the St. Gotthard tunnel and the Fréjus tunnel prior to the most recent ones. The same is true for the Mont Blanc tunnel (not reported in the table). The question remains: when will a fire spread to other vehicles, resulting in a major hazard for occupants and the tunnel structure? The aim of this thesis is to spread

some light on some of the important parameters and phenomena governing the passage from a “benign” fire to a catastrophe.

Table 2.2 Summary of fires in rail tunnels [1, 3].

Year	Tunnel, length	Location	Vehicle at origin of the fire	Cause of fire	Duration	Consequences for		
						people	vehicles	structure
1903, 10 Aug	Couronnes underground	Paris, France		Electrical fault		≥84 dead		
1921, 21 Oct	Batignolles, L = 1000 m	Paris, France		Collision resulting in a large fire; discharging gases from the gaslight system		≥28 dead, most due to the fire		
1958, 28 July	London underground Holland Park	UK	train	Sparkover in electro-technical equipment		1 dead, 51 injured		
1971, 14 Feb.	Wranduk, L=1500 m	Yugoslavia		Fire in engine		34 dead, 120 injured		
1972, 6 Nov.	Hokoriku	Japan	Restaurant car			30 dead, 690 injured	2 carriages	
1979, 17 Jan.	San Fransisco underground	USA	underneath a metro car	Short circuit		1 dead, 58 injured		
1987, 18 Nov	Kings Cross Station	London, UK	Escilator 4 (wooden)		6 h	31 dead, many injured		
1990, 28 Dec	New York underground	USA	Cable in tunnel			2 dead, 200 injured		
1991, 1 June	Moscow underground	Russia	Under a train	Electrical fire		7 dead, ≥10 injured		
1995, 28 Oct.	Baku underground	Azerbaijan	At the rear of the fourth car (out of five)	Electrical fault		289 dead (245 in train, 40 in tunnel), 265 injured	2 rail cars completely damaged	Cables; No visible damage to the structure
1996, 18 Nov	Channel tunnel L=50 000 m	England-France	1 HGV	Suspected arson	2.5 h	30 injured by the smoke	10 HGVs	Severe damage to the tunnel ceiling
1998, 10 July	Gueizhou, L=800 m	China	Train	Explosion in gas canisters		≥80 dead		
1999, 23 May	Salerno, L = 9000 m	Italy	Train	Smoke bomb		4 deaths, 9 injured		
2000, 11 Nov	Kitzsteinhorn funicular tunnel	Austria	The rear driver's cab	Hydraulic oil leakage into the heater	3 h	155 dead	train completely burnt out	
2003, 18 Feb	Jungangno underground	Daego, South Korea	Petrol and cigarette in train	Arson	3.75 h	198 dead, 146 (+ 20 fire fighters) injured		

In Table 2.2, a summary of selected fires in rail tunnels is presented. More comprehensive lists of fires in rail tunnels have been published by Carvel [1] and Andersen and Paaske [3].

As can be seen from the Tables 2.1 and 2.2, there is a larger risk for fatalities in accidents in rail tunnels/metros than in road tunnels, the reason for this being the large number and concentration of people being transported. On the other hand one can also see the pattern that more recent fire incidents in road tunnels have involved an increased number of fatalities compared to previous events. This is no doubt due, at least in part, to the increasing transportation of goods on roads and through road tunnels. It is expected that the heavy goods transport on roads and through road tunnels will increase with between 40 % and 60 % over the period between 2000 and 2010 [4].

A common factor for catastrophic fires is the fire spread to a large number of vehicles, making it very difficult for firefighters to reach the seat of the fire or even to come close enough to extinguish the fire. The heat release rate (HRR) is commonly used to describe the size of a fire (most often presented in kW or MW). Ingason estimated the heat release rates (based on available information) from some of the more recent large fires in European tunnels [5]. A summary of the results are presented in Table 2.3 together with estimations made by Bettelini for the St. Gotthard fire [6]. The estimates range from more than 100 MW to 400 MW. In all these fires at least 10 HGVs were involved.

Table 2.3 Summary of estimated energy content and peak HRR in tunnel fires involving HGVs [5, 6].

Accident	Vehicle type	Estimated heat content [GJ]	Estimated peak HRR [MW]	Conseq. for people	Conseq. for tunnel
Eurotunnel	10 HGV	2200	370	30 injured	Damage to ceiling
Mont Blanc	14 HGV, 9 cars	5000-7000	380	39 deaths	Closed for 3 years
Tauern	16 HGV, 24 cars	4000-4500	300-400	12 deaths	Closed for 3 months
St Gotthard	13 HGV, 10 cars	1400-2700 ^{a)}	"More than 100"	11 deaths	Closed for 2 months

a) Assumption: 100 GJ - 200 GJ per HGV and 5 GJ per car.

From the above summary of the recent fires with fatalities in road tunnels it is obvious that HGVs play an important role in determining the outcome of a fire in a tunnel. This becomes even more significant when one considers that road transportation of goods through road tunnels will increase in the future. Indeed, the traffic through the Mont Blanc tunnel is increasing and will soon be back at the same level as it was at the time for the latest accident in 1999. The fire in the Fréjus tunnel on 4 June, 2005, has put the spotlight on traffic across the Alps and the EU sees the transferring part of the traffic on roads to railways as one solution [7], potentially significantly increasing the fire load on railways.

From Table 2.1 it can be seen that HGVs often are involved in the fires and often lead to fatalities if two or more HGVs are involved. The importance of the HGVs led to the need for a comparison with different existing guidelines (see below) and a decision to study the potential size of fires in HGVs with ordinary cargos. This led to the decision to perform the tests in the Runehamar tunnel, the results of which are summarized in Section 3.3 together with results from other tests series.

2.2 Guidelines

An important step towards safety in tunnels in Europe was the tunnel directive (2004/54/EC) from the European Parliament which has recently entered into force (30 April 2004) [8]. One can argue that the directive has not gone far enough and is not as detailed as many of the existing guidelines. However, these guidelines are recommendations and not binding. The strength of the directive is that it is mandatory through legislation. The directive applies to all tunnels in the Trans-European Road Network with lengths of over 500 m. The directive states requirements of minimum safety, but cannot be used for designing of safety measures (except for minimum requirements, e.g. for emergency exits) during the construction or design stage of the tunnel. For this task different types of guidelines and standards are of more use and therefore some of these will be discussed below.

A number of standards and guidelines exist, both national and international, regarding transportation and construction of safe tunnels. One can say that there are two main issues to be resolved when designing a safe tunnel. One is the safety of the people inside the tunnel, where the hot smoke in the tunnel is of great concern. The designing of ventilation as pertains to smoke movement, for example, is based on the HRR of the fire. The second main issue is the endurance of the structure under the effect of a fire. In this case the temperature is important and different types of temperature-time curves (see below) are used to represent the potential heat load on the structure. The temperature curves and HRR values chosen are, however, not always directly related to each other. Note that guidelines and requirements exist for a large variety of parts of a tunnel construction, including installations, but the information given below focuses mainly on the HRR and the expected maximum temperature from fires in different types of vehicle fires in tunnels. Summaries of the various requirements in different countries are available for road tunnel [9], rail tunnels [10], and metros [11]. When it comes to the ventilation in particular, Bendelius has presented lists and information on handbooks and guidelines [12].

2.2.1 Heat release rate

Heselden assumed HRR for different design fires as a basis for calculations of smoke and fire spread in tunnels [13, 14]. He used fires of the sizes 3, 10, 20, 50, and 100 MW and referred to these as motor car, van, lorry, coach, and large petrol spill fires, respectively. The value for a lorry (20 MW) has long been thought to be representative for HGVs and has even been included in several guidelines. In Table 2.4 recommended design values for the HRR from different types of vehicle fires are presented and some of the values assumed by Heselden can still be recognized. Note that the values in Table 2.4 are those which were valid at the time when the tests in the Runehamar tunnel were performed in 2003. Since then some guidelines have been updated, e.g. NFPA 502 where a value for HGV (in the NFPA standard called

heavy goods truck) has been included, 20 MW to 30 MW [15]. The next version of NFPA 502 is scheduled to 2009 and a call for comments has already been released. PIARC (Technical Committee C3.3, Working group 6) has also prepared an updated version on their guidelines (System and Equipment for Fire and Smoke Control in Road Tunnels). This is still to be published. The design values for the maximum HRR are the same as in Table 2.4, with the exception of fires involving dangerous goods, which are estimated to range from 200 MW to 300 MW [16].

Table 2.4 Design values for HRR for tunnel fires according to different guidelines (in 2003). The HRR values are given in MW.

Type of vehicle	PIARC [2]	French rules [17]	NFPA [18]
1 small car	2.5	2.5	-
1 large car	5	5	5
2 to 3 cars	8	8	-
Van	15	15	-
Bus	20	20	20
HGV	20-30	20-30	-
Tanker	100	100	100

The catastrophic fires in European tunnels in recent years show that fires involving several HGVs, even those with “non-hazardous” cargo, produce a great deal of smoke and heat and are extremely difficult to combat. The tunnel fires described above, all gave HRR well over 100 MW. In three cases the HRR was estimated to be between 300 MW and 400 MW [5] (see Table 2.3). In contrast, regulations and recommendations for design of safety systems in tunnels, assume that HGVs with ordinary cargos (not liquid fuels or other hazardous products) to give relatively low HRR in the event of a fire (see Table 2.4).

In light of the conclusions drawn from catastrophic fires, the HRR values for HGVs presented in Table 2.4 seem low. This was one of the reasons which prompted SP Fire Technology to initiate a project where the HRRs from HGV loads, consisting of typical, non-hazardous commodity mixtures, were measured. The set-up of and result from these tests are summarized in the following sections. One of the main results from the Runehamar tests was that HGV trailers with ordinary cargoes (mixtures of cellulose and plastics) can give very high peak HRR, 66 MW – 202 MW, i.e. far above the assumed value in the guidelines and of the same order of magnitude as for tanker fires. These values have already been discussed by authorities and representatives for standardization (e.g. for NFPA 502 at the first International Symposium on Tunnel Safety and Security in Greenbelt, MD, USA in November 2004). The standards and guidelines are continuously revised and it is anticipated that the maximum value for typical HGVs will increase over time.

When it comes to railways a number of international groups of experts exist, whose focus is on the harmonization of the railway infrastructure and operation, and an increase in safety. Examples of such groups are the International Union of Railways (Union Internationale des Chemins de fer, UIC), the UN ECE group of experts, and the European Association for Railway Interoperability (Association Européenne pour l’Interopérabilité Ferroviaire, AEIF) [19]. For the fire resistance of rolling

stock, a new European standard is on its way [20]. The aim of the standard is that “the design of rolling stock and the materials used shall be aimed at limiting fire development should an ignition event occur”. This is an important aim since an early phase of slow fire development is essential to escape a fire. As soon as the rate of fire/flame spread increases beyond a certain level the situation becomes more severe. The standard for rolling stock, prEN45545-2, is a complex document with requirements on different objects found in rolling stock, where the specific requirements depend on the object, material, orientation and size. The standard does not, however, give any guidance on design fires for tunnels. The standard was also recently voted down and will therefore be revised and delayed. One standard giving information on heat release per object is the NFPA 130 standard [21]. Again, the document does not give any guidance on the time evolution of the fire and maximum HRR.

Due to the overall increase of cargo transportation, the need for transportation of cargo on rail will also increase. There are, however, no standards, similar to those for passenger transportation, for cargo trains. This issue is presently under discussion and some suggestions for values of design fires for this type of ‘vehicle’ (e.g. see reference [22]), have also been proposed, especially after the Runehamar tests.

2.2.2 Temperature

Road tunnels are often covered with some type of lining, but the purpose of this lining can vary from one tunnel application to another. In some cases the lining is a thin layer of concrete to prevent dripping water, which both causes mechanical wear on the road and can cause problems with ice. There are also aesthetical issues and issues regarding the perception of a driver in a tunnel. In other cases the lining is installed to protect the construction or installations in the case of a fire. One problem has, however, been to decide which fire load to use for the engineering of the tunnel construction. This involves both the type of fire and the distribution (both in time and space) of the temperature exposure to the construction. A standard curve used when testing the temperature exposure is the cellulose curve defined in several standards, e.g. ISO 834 [23]. This curve applies to materials found in typical buildings. This has been used for many years, also for tunnels, but it is clear that this curve does not represent all materials, e.g. petrol, chemicals, etc., and therefore a special curve, the hydrocarbon curve (the HC curve) [24], which was developed in the 1970s for use in the petrochemical and off-shore industries, has been applied to tunnels. The main difference between these two curves is that the HC curve exhibits a much faster fire development and consequently is associated with a faster temperature increase than the standard ISO 834 fire curve and has traditionally been seen to be more relevant for a petroleum fire.

Specific temperature curves have been developed in some countries to simulate hydrocarbon fires in tunnels. Examples of such curves are the RABT/ZTV Tunnel Curve in Germany [25] and the Rijkswaterstaat Tunnel Curve (RWS curve) in The Netherlands (based on laboratory scale tunnel tests performed by TNO in 1979 [26, 27]). In connection with the RWS curve, the Dutch authorities require that the temperature of the interface between the concrete and the protective covering does not exceed 380 °C and that the temperature of the reinforcement does not exceed 250 °C. In France a modified version of the hydrocarbon curve is used

(HCmod), which is the traditional hydrocarbon curve increased by a factor 1300/1100.

In Figure 2.1 the five, above mentioned, fire temperature curves are presented graphically (the first two hours).

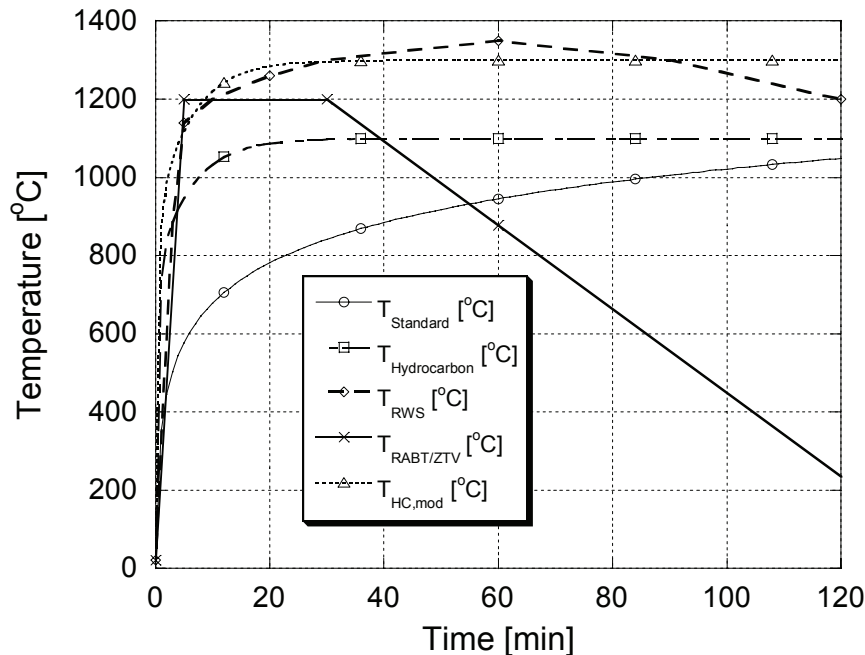


Figure 2.1 Fire temperature curves used for testing reaction of structures to heat exposure (the first two hours).

PIARC recommends the use of the ISO 834 curve (60 min) for cars and vans and the RWS curve or the modified HC curve (120 min) for trucks and tankers [28, 29]. The recommendations are particularly for tunnels that are immersed, under/inside superstructures, or in unstable ground. For cut and cover tunnels or tunnels in stable ground the recommendations can be decreased depending on the situation, but in most cases the same curves are used. These recommendations are agreed on together with the International Tunnelling Association, ITA [30]. According to NFPA 502, the following maximum temperatures are assumed for different types of vehicle fires: Passenger car = 400 °C, Bus = 700 °C, Heavy goods truck = 1000 °C, and Tanker = 1200 °C – 1400 °C. In Swedish guidelines for road tunnels the gas temperature in the tunnel is assumed to follow the HC curve [31]. The different fire curves and their expressions are further discussed in Section 3.3, where they are compared to the results from the Runehamar tests.

It should be noted that temperature measurements are associated with measurement uncertainties as other types of measurement. In fire experiments thermocouples are commonly used. In addition to ordinary sensor uncertainties, thermocouples can be affected by radiation. The significance of this effect varies between situations depending on several conditions, e.g dimension and position of thermocouple, temperature distribution, conditions of the flames and smoke, temperature of the surroundings, etc. This means that that it can be difficult to compare temperature meas-

urements not corrected for radiation effects. In many cases the description of the conditions for a certain test series is such that a correction of the measurement results is difficult to perform. This should be kept in mind when comparing the temperature measurements from different test series and during the discussion of flame lengths presented in this thesis. Reference to this type of uncertainty is not made in each specific case. Some further details on this problem and the influence on the measurements in the Runehamar tunnel are, however, given in Paper I.

3 Fire experiments in tunnels

3.1 Different methods of estimating the HRR and some factors influencing the results

The Heat Release Rate (HRR) is a very central and important parameter when studying and defining safety in connection with tunnel fires. In fact it is seen as the most important parameter used to define fire hazard [32]. It relates to several of the other parameters of importance, i.e. temperature, ventilation of smoke (e.g. the critical velocity that will be discussed below), flame length, radiation, fire spread etc. Therefore, different methods have been used to determine the HRR from tunnel fire experiments. These methods can be summarized as:

1. Extrapolation from values of the HRR from free burning tests, to tunnel conditions.
2. Measuring of the mass loss rate, either by load cells (or scales of some kind) or for liquid fires determining the flow of fuel needed to keep the liquid surface at a certain defined level.
3. Calorimetry by measuring either the consumption of oxygen [33, 34] (see Eq. (3.1)) or the production of carbon dioxide and carbon monoxide [35]. If the fire is under-ventilated and significant amounts of other carbon containing compounds are generated, these can also be included in the analyses [36]. The advantage of the method based on the production of CO and CO₂ is that the changes in concentration of these species is relatively large compared to the decrease in oxygen concentration. The disadvantage is that it is more fuel dependent than the method based on oxygen consumption.

A common way to express the heat release rate based on oxygen consumption calorimetry is by the following expression:

$$\dot{Q} = \frac{E \cdot \dot{m} \cdot (M_{O_2} / M_{air}) \cdot (1 - X_{H_2O}^0)}{\alpha - 1 + \frac{1 - (X_{O_2} / (1 - X_{CO_2}))}{X_{O_2}^0} + \frac{X_{O_2}^0 - (X_{O_2} \cdot (1 - X_{CO_2}^0)) / (1 - X_{CO_2})}{X_{O_2}^0}} \quad (3.1)$$

where

- \dot{Q} = the heat release rate from the fire, HRR [kW]
- E = amount of energy developed per consumed kilogram of oxygen [kJ/kg]
- \dot{m} = mass flow in exhaust duct [kg/s]
- M_{O_2} = molecular weight for oxygen [g/mol]
- M_{air} = molecular weight for the gas flow in the duct, [g/mol]
- α = ratio between the number of moles of combustion products including nitrogen and the number of moles of reactants including nitrogen (expansion factor) [-]
- $X_{O_2}^0$ = mole fraction for O₂ in the ambient air, measured on dry gases [-]
- $X_{CO_2}^0$ = mole fraction for CO₂ in the ambient air, measured on dry gases [-]

$X_{H_2O}^0$ = mole fraction for H₂O in the ambient air [-]

X_{O_2} = mole fraction for O₂ in the flue gases, measured on dry gases [-]

X_{CO_2} = mole fraction for CO₂ in the flue gases, measured on dry gases [-]

All methods are assigned different uncertainties. Using free burning results can lead to an underestimation of the HRR, since both the fire growth and fire spread rate and the maximum HRR can increase in a tunnel, relative to free-burning, due to the increased feedback from the flames and the hot smoke layer. This is a well known phenomenon from enclosure fires [37], but has also been seen in tunnel fire tests [38]. Takeda and Akita studied this phenomenon and showed that it is also related to the ventilation factor [39]. Carvel *et al.* have studied both the effect of the tunnel on the HRR [40] and the effect of the ventilation on the HRR from a fire in a tunnel. The former is further discussed in this section, while the effect of the ventilation is discussed in Section 5.2.

Saito *et al.* showed that the mass loss rate for liquid fires increased in a tunnel compared to free-burning conditions [41]. The tests were performed with pool fires with methanol (0.1 m, 0.15 m, 0.2 m, and 0.25 m in diameter) and heptane (0.15 m in diameter). For the two smallest pools the effect of the tunnel (with an air velocity 0.08 m/s) on the mass loss rate of methanol was only a few percent, while for the 0.25 m diameter pool the mass loss rate in the tunnel was increased by a factor 2.7 compared to free-burning conditions. For heptane, the tunnel (with an air velocity of 0.43 m/s) increased the mass loss rate approximately by a factor 4. For both fuels the mass loss rate was significantly decreased with increasing air velocity. This illustrates the importance of the heat feed back from the flames, hot gases, and tunnel structure on the mass loss rate. This issue is further discussed in Section 5.2.

Ingason performed pool fire tests in a model scale tunnel, using heptane, methanol, and xylene as fuels [42, 43]. For methanol the free burning mass loss rate was 0.017 kg/s/m². This value should be compared to 0.015 kg/s/m² for a natural ventilated test in a tunnel and 0.020 kg/s/m² for a test with forced ventilation (4.8 m/s). If the forced ventilated case is considered (an increase of 18 %), the result is comparable to the results of Saito *et al.* (for the case 0.20 m diameter pool and an air velocity of 0.2 m/s; or 0.25 m diameter pool and an air velocity of 0.39 m/s or higher). In the test with natural ventilation the mass loss rate, however, decreased compared to the free-burning case. For heptane, the maximum increase due to the tunnel was by a factor of 3.3 (0.13 kg/s/m² (u = 1 m/s) compared to 0.04 kg/s/m² (free-burning)).

Carvel *et al.* performed an analysis of different experiments in tunnels and showed that the width of the tunnel has a significant influence on the HRR from a fire in a tunnel [40]. This result can be explained by the radiation to the pool (from walls and from the ceiling layer), the temperature inside the tunnel, and also the flow pattern near the fire. The work includes an extensive summary of experiments involving liquid pool, wood cribs, and cars and how the HRR from these tests in tunnels is compared to similar free burning tests. The same authors gave a relationship for the influence of the width of the tunnel on the HRR [44], i.e.:

$$\dot{Q}_{tunnel} = \left(1 + 24 \left(\frac{W_f}{W_t} \right)^3 \right) \dot{Q}_{open} \quad (3.2)$$

where W_f is the width of the fire and W_t is the width of the tunnel. It should be noted that there were some restrictions in the development of the equation. The first is that it is not valid for methanol fires. The main reasons for this is that methanol burns differently, with lower HRR, than other liquid fuels and that it produces much less smoke (which means both less radiation to the walls and less radiation to the fuel) than other fuels. The effect of the walls comes first when the width of the methanol pool constitute a larger part of the tunnel width (starting when $W_f/W_t > 0.5$ and the enhancement factor passes 2 when W_f/W_t is approximately 0.75) [45]. On the other hand this might also mean that methanol is not as relevant as other fuels when studying safety in tunnels. The other restriction is that the relationship does not hold when the fire becomes so large that the ventilation can be said to be limited and thereby the HRR is not developing in the same way. This is an important restriction since this means that other parameters also need to be included in the analyses to determine whether the relationship holds for the situation of interest. The general conclusion was, however, that for the same type of fire, a wider tunnel is safer than a narrower one.

The same analysis showed that the tunnel height is not significant. However, the use of some of the experimental results to support this statement is questionable. In one case [41], the HRR in the tunnel tests compared to open air tests increased significantly with pool dimensions. This is expected since the radiation impact will be larger as the temperature is increased. The distance to the ceiling was not changed during this test series. Despite this, the result was taken as evidence contradicting the hypothesis of the influence of the ceiling height. This interpretation is not correct, however; instead a value corresponding to “no information” should be used.

In another test series [46], the increase in HRR for pool fires in the tunnel compared to open air tests was approximately the same as the increase in HRR for wood crib fires compared to open air tests. Again this was taken as evidence that the ceiling height is not important. This is, however, for several reasons also a misleading conclusion. First, one cannot compare pool fires with wood crib fires in this way since they burn very differently and thereby react very differently to radiation. Second, the top of the wood crib was at a higher level than the pool fire, but a wood crib is not solely burning on the upper surface but is burning three-dimensionally and the position of the lower level of the wood crib is also important. This has, for example, been shown by Heskestad who showed that the flame height for 3D fires are best correlated measured to the base of the fire [47]. To verify or undermine the hypothesis of the importance of the ceiling height or the distance between the fuel and the ceiling, identical tests with varied elevation of the fuel need to be performed.

All together, there are several factors that affect the HRR from a fire in a specific tunnel, both compared to fires in the open and compared to a fire in the same type of object in another tunnel. Some important factors are the type of fuel (e.g. chemical composition; liquid or solid), geometry (2D such as pool fire, 3D such as wood crib,

or something in between such as a 3D object mainly burning on the outer surfaces), radiation from walls, ceiling and upper layer, amount of fuel (i.e. is the fire easily reaching a fuel controlled situation or is the flame/fire spread a long phase that can be speeded up by the tunnel), and ventilation. To complicate the situation, several of these factors interact and can have different effects depending on the situation. Many of the comparisons performed are, unfortunately, made between test series where more than one parameter has varied making direct conclusions concerning the significance of a specific parameter difficult.

Using the mass loss rate for determining the HRR involves two uncertainties in particular: it can be difficult to measure the mass loss rate accurately (load cells can be affected by the environment (high temperatures) and the signal can start to drift (a situation of instability or similar can also arise)) and it can be difficult to keep a constant level of the fuel surface and accurately measure the flow rate of fuel needed to keep this level in a large-scale test, even if there are methods to solve this (see for example [41] or [48]). The second important source of error, when calculating the HRR from the mass loss rate, is the value of the effective heat of combustion. This is not a constant value; the combustion efficiency is not one and it can vary both in time and between different experimental set-ups and conditions.

The calorimetry technique is, if used under controlled conditions, the most accurate method to calculate the HRR. Therefore, this method is used in most standard applications for fire testing in laboratories. One reason for the broad application of the oxygen consumption calorimetry is the fact that many common fuels release approximately the same amount of energy per kg O₂ consumed, i.e. 13.1 MJ/kg O₂ [33]. This gives a good estimate of the HRR even if the fuel composition is not completely known. If the fuel composition is known the method can be used with constants for the specific fuel.

There are, however, some sources of uncertainties connected to the calorimetric method. In Eq. (3.1), the HRR is linearly dependent on the mass flow rate and therefore this needs to be accurately estimated. In a tunnel there are two important sources of errors, one is the calculation of the mean velocity from velocity measurements and the other is the determination of the cross-section of the tunnel when the roughness is large and the cross-sectional area can vary (for a further discussion of these issues see Paper II and reference [49]). Further, the gas concentrations need to be analysed in a representative manner. Other aspects of the uncertainty related to the calorimetric method are described in the literature, e.g. by Enright and Fleischmann [50, 51] and by Axelsson *et al.* [52, 53].

3.2 Summary of experiments

The first extensive large-scale tunnel test series where the HRR and gas temperatures from various large vehicles (passenger cars, train wagons, subway cars, and HGV trailer) were measured was in the EUREKA 499 –FIRETUN test series in 1990 to 1992 [54]. The peak HRRs measured varied between 6 and 128 MW and the gas temperatures at ceiling height above the vehicles between 200 °C and 1100 °C. Another major series of fire test in tunnels was performed in the Memorial Tunnel in Massachusetts in 1995 [48]. However, the fire load in this test series did not consist

of vehicles, but of liquid pool fires of different sizes, varying between 20 and 100 MW with a maximum gas temperatures at the ceiling of approximately 1360 °C. The main purpose of the Memorial tests was to investigate the effects of different ventilation systems on the smoke control in tunnels. The test series included a large number of well instrumented tests. In order to simulate the cross-section of vehicles (pool fires were used in all tests) and their effect on the ventilation, movable steel plates were placed in different positions.

Other important test series include the one in the Offeneegg tunnel (Switzerland, 1965) using petrol pools from 6.6 to 95 m² [55], a disused railway tunnel in Glasgow (Scotland, 1970) [13], the Zwenberg tunnel (Austria, 1975) [56] using petrol pool fires from 6.8 to 13.6 m², and the P.W.R.I. experiments (Japan, 1980) using pool fires of 4 and 6 m², passenger cars and buses [57]. No HRR measurements based on calorimetry were performed in any of these tests. In the Ofeneegg tunnel tests gas temperatures up to 1325 °C were measured. In the Netherlands, small-scale tests using petrol pans were performed in an 8 m long tunnel, 2 m high and 2 m wide [27]. In these tests, gas temperatures in the range of 900 – 1360 °C were measured. The Rijkswaterstaat Tunnel Curve (the RWS Curve) in the Netherlands is based on these tests. The RWS curve represents a worst-case scenario of a 300 MW petrol tanker burning in a tunnel for two hours.

In 1985 two large-scale tests in a tunnel using wood cribs as fuel to simulate a fire in a subway car (80 GJ), and in two passenger cars (11.7 GJ) colliding in a tunnel, were performed [58, 59].

In 2002, a series of tests were performed in the Second Benelux tunnel in the Netherlands [60]. HRR and temperatures from pan fires (5, 20 MW) and vehicle fires such as passenger cars, vans and HGV fire loads, were measured. The peak HRR (based on weight loss) varied between 4.5 and 26 MW and the maximum gas temperatures at the ceiling did not exceed 600 °C.

In 2003, large-scale tunnel tests were carried out with HGV cargos in the Runehamar tunnel in Norway (see Paper I and II). The tunnel is a 1600 m long two-way, asphalted road tunnel that was taken out of use in the late 1980s. It is 6 m high and 9 m wide, with a slope varying between 0.5 % uphill and 1 % downhill (in relation to the air flow direction). In total, four tests were performed with fires in a HGV trailer set-up. In three tests mixtures of different chosen cellulose and plastic materials were used, and in one test a “real” commodity consisting of furniture and fixtures was used. In all tests the mass ratio was approximately 80 % cellulose and 20 % plastic. A polyester tarpaulin covered the cargo in all cases (in test T4 only the upstream end and the downstream end of the set-up were covered). The four tests are summarized in Table 3.2. The maximum heat release rates varied between 66 MW and 202 MW. The maximum gas temperatures varied between 1250 °C and 1365 °C.

Table 3.1 Overview of selected tunnel fire test series, indicating performed measurements [13, 27, 48, 54, 57, 60-65] and Papers I-II and V-VII.

Location	No of tests	Length [m]	Height [m]	Cross section [m ²]	Objects	Measurements	Comments
Ofenegg, CH 1965	11	190	6	23	Petrol (6.6, 47.5, 95 m ²)	T, u, CO, O ₂ , smoke spread, \dot{m}_f (estimated)	Single track rail tunnel, dead end, sprinkler
Glasgow, UK, 1970	5	620	5.2	39.5	Kerosine (1.44, 2.88, 5.76 m ²)	T, smoke spread	Disused railway tunnel
Zwenberg, AT 1975	30	390	3.9	20	Petrol (6.8, 13.6 m ²), wood, rubber	T, u, CO, CO ₂ , O ₂ , NO _x , THC, visibility	Disused railway tunnel
TNO, NL, 1979-80	2	8	2	4	Petrol (~3 m ²)	T, humidity	Experimental tunnel
P.W.R.I, Japan 1980	16	700	~6.8	57.3	Petrol (4, 6 m ²), passenger car, bus	T, u, CO, OD, \dot{m}_f , radiation	Special test tunnel, sprinkler
Takeihigasi Tunnel, P.W.R.I, Japan 1980	8	3277	~6.8	58	Petrol (4 m ²), bus	T, u, CO, O ₂ , OD, \dot{m}_f , radiation	In use road tunnel, sprinkler
TUB-VTT, Finland, 1985	2	140	5	24-31	Wood cribs (simulating subway coach and collision of two cars)	T, u, \dot{m}_f , CO, CO ₂ , O ₂ , visibility, smoke height	Disused cavern system
Repparfjord, NO EUREKA 1990-92	21	2300	4.8-5.5	25-35	Wood cribs, cars, metro car, rail cars, heptane, HGV	HRR, T, u, CO, CO ₂ , O ₂ , SO ₂ , C _x H _y , NO, OD, visibility, soot, smoke spread, PCDD/F, PAH, PBDD/F, \dot{m}_f	Disused transportation tunnel
Memorial, USA 1993-95	98	853	4.4 and 7.9	36 and 60	Fuel oil (4.5 – 45 m ²)	T, u, CO, CO ₂ , CH ₄ , THC, \dot{m}_f , visibility, stratification	853 m, 8.8x4.3, foam
Shimizu No. 3, Japan, 2001	10	1120	8.5	115	Petrol (1, 4, 9 m ²), cars, bus	T, u, OD, radiation	New road tunnel, sprinkler
2 nd Benelux, NL, 2002	14	872	5.1	50	n-heptane+ toluene, car, van, wood pallets (HGV mock-up)	T, u, \dot{m}_f , CO, OD, radiation, smoke front, visibility, fire detection	New road tunnel, sprinkler
Runehamar, NO 2003	4	1600	5-6	32-47	Cellulose, plastic, furniture	HRR, T, PT, u, CO, CO ₂ , O ₂ , HCN, H ₂ O, isocyanates, OD, radiation	Disused road tunnel

The results from some of the tests series described here are discussed in the next section. Furthermore, results from a reduced scale test series are presented in Section 5.2, on the effect of the ventilation on the HRR. More details on the test series presented in Table 3.1 are given by Ingason and Lönnemark [66]. A comprehensive list of experimental test series in large-scale, reduced-scale, or laboratory scale tunnel is given by Carvel and Marlair [67].

Table 3.2 Description of the commodities used in the Runehamar tests.

Test nr	Description of the fire load ^{a)}	Target	Total weight, excl target [kg]	Total weight, incl target [kg]	Theoretical calorific energy [GJ]
T1	360 wooden pallets measuring 1200 × 800 × 150 mm, 20 wooden pallets measuring 1200 × 1000 × 150 mm and 74 PE plastic pallets measuring 1200 × 800 × 150 mm, 122 m ² polyester tarpaulin	32 wooden pallets and 6 PE pallets	10160	11010	247
T2	216 wood pallets and 240 PUR mattresses measuring 1200 × 800 × 150 mm, 122 m ² polyester tarpaulin	20 wooden pallets and 20 PUR mattresses	6390	6930	135
T3	Furniture and fixtures (tightly packed plastic and wood cabinet doors, upholstered PUR arm rests, upholstered sofas, stuffed animals, potted plant (plastic), toy house of wood, plastic toys). 10 large rubber tyres (800 kg), 122 m ² polyester tarpaulin	Upholstered sofa and arm rests	8330	8550	179
T4	600 corrugated paper cartons with interiors (600 mm × 400 mm × 500 mm ; L × W × H) and 15 % of total mass of unexpanded PS cups (18000 cups) and 40 wood pallets (1200 × 1000 × 150 mm), 10 m ² polyester tarpaulin	-	2850	-	62

a) PE = Polyethylene, PUR = Polyurethane, PS = Polystyrene

3.3 Summary of results from fire experiments

The details regarding the results from the Runehamar tests are given in Papers I, II, V, VI, and VII. In this section these results are compared to results from other test series with a focus on temperature and HRR measurements.

Ingason and Lönnemark presented energy content, peak HRR, and time to peak HRR for different types of road vehicles (mostly passenger cars and simulated HGV trailers) from a number of test series [68]. Included in that summary were also results from the Runehamar tests. The values from the Runehamar tests were later somewhat altered due to a more thorough analysis of the HRR calculations (see Paper II). A summary of the data from the above mentioned vehicle fire tests is presented in Table 3.3.

Table 3.3 Summary of HRR data from fires in different types of vehicles [64, 65, 68-75] and Paper II.

Vehicle	No. of tests	Energy [GJ]	Peak HRR [MW]	Average peak HRR [MW]	Time to Peak [min]
Passenger car	15	2 – 8	1.5 – 8.5	4.1	10 – 38
2 cars	7	5 – 10	5.6 – 10	7.6	13 – 55
3 cars	1	NA	8.9	8.9	33
Bus	2	41 ^{a)}	29 – 30	29.5	7 – 8
HGV trailers	10	10 – 244	13 – 202	- ^{b)}	8 – 18

a) Information on energy content available only for one of the buses; the value 41 GJ corresponds to the bus giving a peak HRR of 29 MW.

b) The test set-ups were too different for an average to be of interest.

The vehicle data shows that there is a correlation between the energy content and the maximum HRR developed. In Figure 3.1 this is shown graphically. There is a scatter in the data and there are differences in test conditions, but there is clear relationship between the maximum HRR and the energy content. The correlations were derived separately for passenger cars (include tests both with one and two cars) and HGVs, respectively. This was done due to the difference in scale. However, the relationship between the maximum HRR and the energy content is very similar for the two groups. For passenger cars $\dot{Q}_{\max}/Q_{\text{tot}} = 0.868 \text{ MW/GJ}$ ($R = 0.840$) and for HGVs $\dot{Q}_{\max}/Q_{\text{tot}} = 0.866 \text{ MW/GJ}$ ($R = 0.910$). Note that the regression lines have been forced to pass the origin. Considering the limited amount of test data available for HGVs, the assumption that the line passes the origin is considered to be valid. For the only case with a bus, with enough data, the relationship is approximately 0.7 MW/GJ.

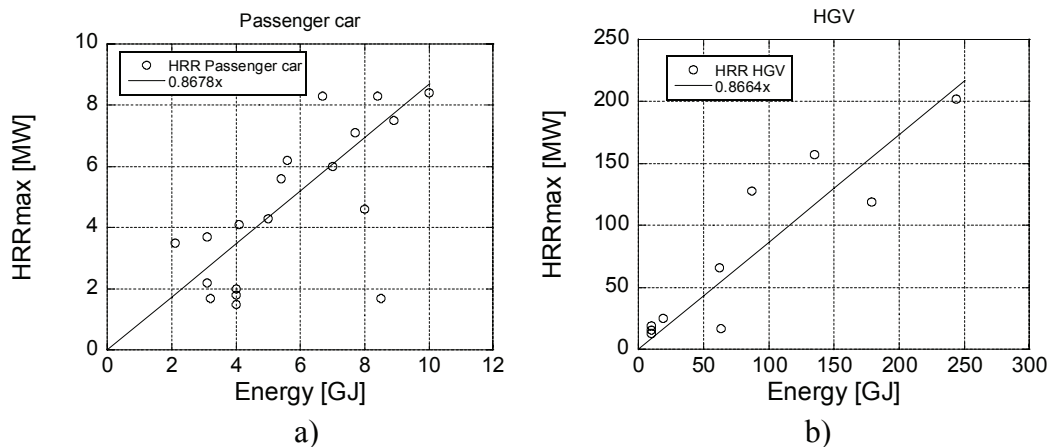


Figure 3.1 Relationship between maximum HRR and total calorific content for a) passenger cars and b) HGVs. The straight lines are linear regression through the origin. In the case of passenger cars, the outlier [8.5 GJ; 1.7 MW] has not been included since the test was ventilation controlled.

One of the data points in Figure 3.1a is very far from the regression line and this point was not included in the regression as this test had restricted ventilation to give a maximum possible HRR of 2 MW. This shows the importance of the ventilation and that the actual situation affects how well the results will agree with the correla-

tion in Figure 3.1. The type and geometry of the fuel are also important for the maximum HRR in a specific case.

In Paper IV, car fire test data containing an extensive analysis of fire gases and extinguishing water is presented. Actually, three tests were performed: a fire started in the engine compartment, and two started in the coupé. However, these three tests are presented as a single test in the paper as they were performed consecutively, with some of the cumulative measurements being conducted across all three tests. During these tests the maximum HRR was approximately 3.5 MW. All fires were extinguished. The third test, which was the largest one, was extinguished when the HRR had passed its maximum value. The total developed energy was calculated to be 3.8 GJ. Due to the extinguishments the values cannot be used in deriving the correlation between the maximum HRR and the energy content, but assuming that both the HRR and the total energy would have been higher if the tests had not been interrupted, the values indicate that these results would also fit well into the correlation.

In Figure 3.2 time resolved HRR data is presented graphically for the HGV simulation tests summarized in Table 3.3 [68]. From the results several conclusions can be drawn. Prior to the Runehamar test series, only one fire test in a tunnel had been performed where a HRR higher than 100 MW was registered, i.e. the HGV tests in the EUREKA test series. In the Runehamar tests, three tests had higher HRR than 100 MW and one tests (T4) had a maximum HRR of 66 MW. In other words, all the Runehamar tests had maximum HRR higher, and in most cases much higher, than those suggested in the guidelines described in Section 2.2.1. Indeed, the maximum HRR in the tests with wooden and plastic pallets was higher than 200 MW. This is in the same order of magnitude as the HRR often estimated for tanker fires. One should keep in mind that in all the Runehamar tests and in the EUREKA HGV test, ordinary (i.e. non-hazardous) cargoes were used. Thus, these values cannot be explained as related only to hazardous goods. When loaded on HGVs, ordinary goods can be considered to be hazardous in terms of the potential for HRR. This is also in line with the results of real tunnel fires where fires involving HGVs often lead to dramatic consequences, either for occupants, the tunnel structure, or both. The importance of the HGVs for the consequences of a tunnel fire is illustrated in Table 2.1.

The total calorific content in each test in the Runehamar test series is given in Table 3.2. The total developed energy for each commodity, calculated through integration of the HRR curve, was 243 MW, 141 MW, 131 MW, and 56.7 MW. These values correspond to combustion efficiencies of 0.98, 1.04, 0.73, and 0.91 for T1, T2, T3, and T4, respectively. The value above one can probably be explained by uncertainties in the estimation of the calorific content and uncertainties in the method of estimating the HRR. This is further discussed in Paper II. Three of the values of combustion efficiency are relatively close to one, while the value for T3 is lower. This can be explained by the more compact set-up of the fuel in T3 than in the other tests; both the cabinet doors and the wooden toy houses were packed in a very compact way and these commodities constituted more than 50 % of the total weight of the commodities used in test T3.

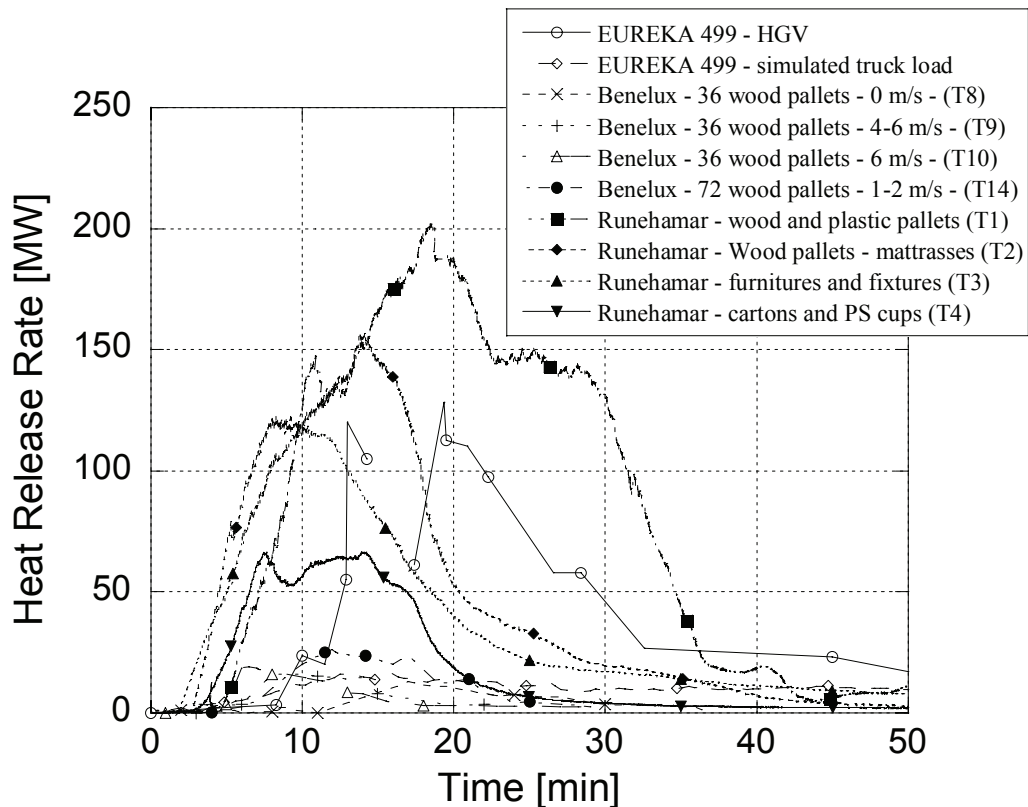


Figure 3.2 The time resolved HRR for the HGV trailer simulation tests from three different test series.

The furniture tests in Runehammar reached a similar maximum HRR as was the case in the EUREKA furniture test. However, according to the correlation in Figure 3.1, the HRR in the Runehammar should be higher than the EUREKA test due to the higher energy content. A probable reason for this not being the case is that in the Runehammar test much of the cellulose was very densely packed (e.g. the cardboard doors) as noted above.

Another feature shown in Figure 3.2 is that for the large tests there exists an initial delay with a slow increase in the HRR before the HRR increases rapidly. This initial delay depends on the ignition source, position of ignition, type of fuel, geometry of fuel etc. When the HRR increases, the risk for fire spread and the hazard to people also increases. Therefore, slow initial fire development, early detection, and fast reaction to the evolving situation, are very important for successful escape from a HGV fire in a tunnel. The increase in HRR is almost linear and was estimated to be 20.5 MW/min, 29 MW/min, 17 MW/min, and 17.7 MW/min for test T1, T2, T3, and T4, respectively [76]. The values were calculated in the HRR range from 5 MW to 100 MW, except for T4 where it was calculated to its maximum HRR. Similar rates of increase in HRR for the tests in the 2nd Benelux tunnel (Test 8, 9, 10, and 14) ranged from 2.6 MW/min to 14.4 MW/min.

Ingason and Lönnemark summarized values of calorific potential and peak HRR from tests performed with rail vehicles in the Repparfjord tunnel [68]. These values

are given in Table 3.4 together with values presented by Barber *et al.* [77]. For the rail vehicles, the scatter in data on maximum HRR as a function of the energy content is large. Especially for the German Intercity-Express railway cars, the correlation coefficient is low. A reason for the differences can be the importance of the ventilation conditions inside the vehicles for the HRR developed, i.e. the number and sizes of openings has a major effect on the ventilation and combustion situation inside the vehicle. Since this can vary significantly between different types of vehicles (e.g. type and mounting of windows) and different incidents, large variations in HRR are to be expected.

Table 3.4 Large-scale experimental heat release data from rail vehicles [68]

Type of vehicle, test series	Calorific value [GJ]	Peak HRR [MW]	HRR/Energy [MW/GJ]	Reference
Rail				
A Joined Railway car; two half cars, one of aluminium and one of steel, EUREKA 499	55	43	0.78	Steinert [71]
German Intercity-Express railway car (ICE), EUREKA 499	63	19	0.30	Steinert [71]
German Intercity passenger railway car (IC), EUREKA 499	77	13	0.17	Ingason <i>et al</i> [78]
British Rail 415, passenger railway car ^{a)}	NA	16	NA	Barber <i>et al.</i> [77]
British rail Sprinter, passenger railway car, fire retardant upholstered seatings ^{a)}	NA	7	NA	Barber <i>et al.</i> [77]
Metro				
German subway car, EUREKA 499	41	35	0.85	Ingason <i>et al</i> [78]

a) The test report is confidential and no information is available on test set-up, test procedure, measurement techniques, ventilation, etc.

In Paper I (Table 5), a summary is given of peak gas temperatures near the ceiling during different fire tests in road tunnels. The temperatures range from 250 °C to 1360 °C for pool fires, from 110 °C to 480 °C for car fires, and from 290 °C to 1365 °C for simulated HGV fires. The temperature is a function of the HRR, but the results are also dependent on the type of ventilation, air speed, geometry of the tunnel, fuel set-up and elevation, type of fuel etc. There are significant differences both within and between the different test series and direct comparisons and correlations can be difficult. Therefore, a separate test series is planned where these relationships can be studied.

A similar summary was presented by Ingason and Lönnemark for rail vehicles [68]. The peak gas temperatures range from 680 °C to 1050 °C. The end values of the span correspond to a German subway steel car and a German subway aluminium car, respectively. The air velocity was somewhat higher in the latter case (0.5 m/s compared to 0.3 m/s). The results, however, show the importance of the material in the vehicle and whether the fire is able to burn through the material.

As shown in Paper I, the best correlation between the nominal fire curves and the temperatures measured in the Runehamar tests was found to be a combination of the HC curve and the RWS curve (see Figure 3.3). This correlation is described by

$$T = 20 + \sum_i^N n_i \cdot r_i \cdot (1 - e^{-k_i t})^{n_i - 1} e^{-k_i t} \quad (3.3)$$

with $i=2$, $n_1=1.2$, $r_1=1920$ °C , $k_1 = 0.00385$ min⁻¹, $n_2=30$, $r_2=300$ °C, and $k_2 = 0.62$ min⁻¹. The temperature is given in degrees Celcius and the time in minutes. More details regarding the correlation and the temperature-time curves can be found in Paper I.

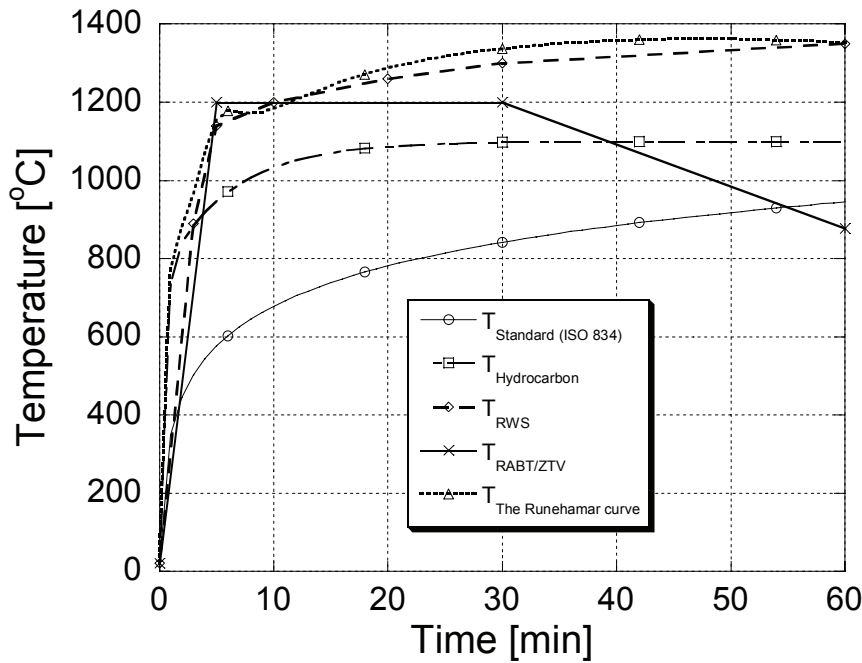


Figure 3.3 The temperature curve corresponding to a best fit of the Runehammar data described by Equation (3.3) is compared with four different fire temperature curves often used for testing structures.

In the discussion of different fire curves it can be of interest to discuss how these curves relate to each other. Wickström suggested that the expression for the standard fire curve:

$$\Delta T = 345 \log_{10}(8t + 1) \quad (3.4)$$

can be exchange by an expression used in the former Swedish building code [79]:

$$\Delta T = T_{\max} \left[1 - \sum_{i=1}^3 A_i e^{-\Gamma \alpha_i t} \right] \quad (3.5)$$

where the constants α_i have been converted to correspond to a time, t , in minutes and Γ is the dimensionless compartment time factor. There were mainly two reasons for

this suggestion. The expression in Eq. (3.5) is more suitable for calculation purposes and it does not increase infinitely as Eq. (3.4) does. The values of the constants in Eq. (3.5) are presented in Table 3.5 and Table 3.6. This curve is called the general natural fire curve. During the work with the revision of the standard ISO 834, Eq. (3.5) was included in the discussions [80].

This expression was also the starting point for the development of the HC curve and the values of the constants for this curve is also included in Table 3.6 [81]. The expression for the HC curve was later changed losing the direct connection between the two curves. It is presented in several standards (e.g. EN 1363-2:1999):

$$\Delta T = 1080 \left[1 - 0.325e^{-0.167t} - 0.675e^{-2.5t} \right] \quad (3.6)$$

Table 3.5 Values of the constants in the summation in Eq. (3.5).

<i>i</i>	1	2	3
A_i [-]	0.324	0.204	0.472
α_i [1/min]	0.0033	0.028	0.32

Table 3.6 Values of T_{\max} and Γ used in Eq. (3.5) to describe different fire curves.

Curve	T_{\max} [°C]	Γ [-]
ISO 834	1325	1
HC	1080	50
Runehamar	1330	35

In Figure 3.4 different fire curves are presented. The ISO curve based on a logarithmic expression (Eq. (3.4)) is compared to the expression suggested by Wickström (Eq. (3.5)). In addition the HC curve and a suggested curve based on the Runehamar results (and a combination of the HC curve and the RWS curve) are presented. The curves are based on the same summation constants given in Table 3.5. The differences between the curves are the T_{\max} and the value of Γ . In the case of the curve representing the results from the Runehamar tests, the value of T_{\max} is based on a maximum absolute temperature of 1350 °C and an assumed ambient temperature of 20 °C. Note that the curve is approaching a constant value. Therefore, only the first 60 minutes are included. After this time, the RWS curve and the correlation based on this decrease. This can be seen in Figure 3.5, where two different correlations (Eq. (3.3) and Eq. (3.5) with $\Gamma=35$ and $T_{\max} = 1330$ °C) are compared to temperature measurements from test T1 in the Runehamar tunnel and to a combination of the HC curve and the RWS curve. Both correlations well represent the experiments and both are somewhat higher than the RWS curve between 20 min and 60 min. After the time 60 min the correlations differ where the Eq. (3.3) follows the RWS curve while Eq (3.5) is approaching its constant value. The advantage of Eq. (3.3) is the fact that it first follows the HC curve and then the RWS curve and the transition between them is supported by the experiment. The advantage of Eq. (3.5) is the simplicity of the expression and that the ISO curve, the HC curve and the Runehamar experiments can be represented with the same expression, only changing the value of two parameters, T_{\max} and Γ .

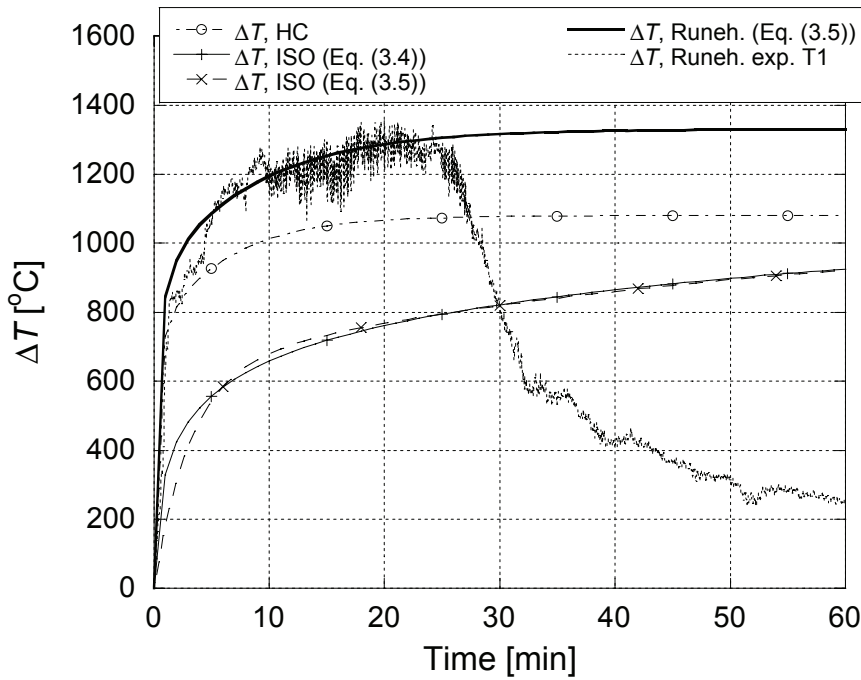


Figure 3.4 Comparison of different fire curves based on Eq (3.4) and Eq (3.5) with results from the results from the Runehammar tunnel.

Using the finite element computer code TASEF, Wickström derived relationships for the ratio between the temperature rise of the surface (ΔT_w) and the fire (ΔT_f), and of an interior point (ΔT_x) and the surface, respectively [82]:

$$\Delta T_x = \eta_x \eta_w \Delta T_f \quad (3.7)$$

where

$$\eta_w = \frac{\Delta T_w}{\Delta T_f} = 1 - 0.0616(t/60)^{-0.88} \quad (3.8)$$

is the ratio between the temperature rise of the surface and the fire and

$$\eta_x = \frac{\Delta T_x}{\Delta T_w} = 0.10 \ln\left(\frac{t}{60x^2}\right) - 0.81 \quad (3.9)$$

is the ratio between the temperature rise of an interior point and the surface. The time, t , is given in minutes and x is the distance below the surface of the interior point.

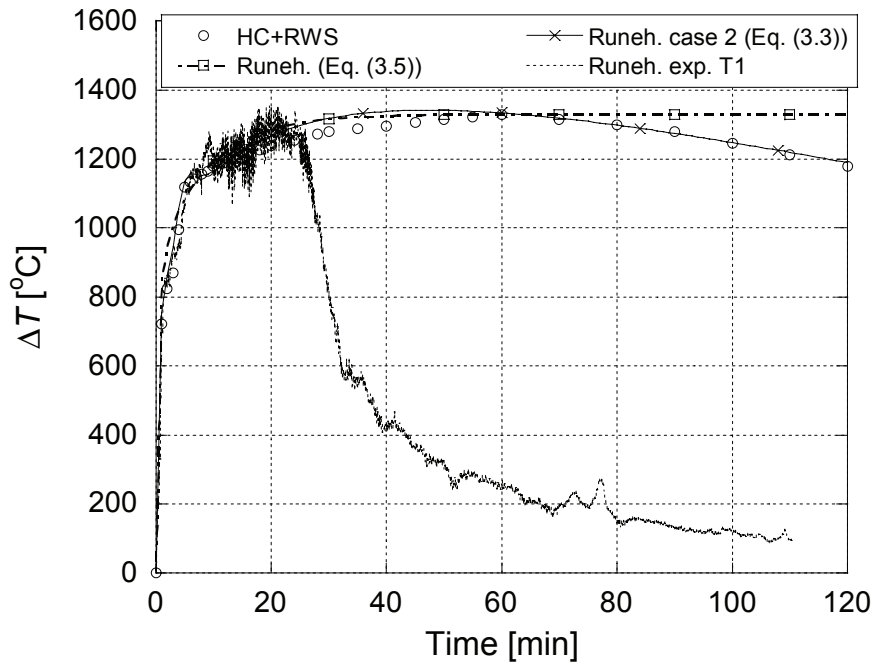


Figure 3.5 Comparison of two different correlations (Eq. (3.3) and Eq. (3.5), respectively) to a combination of the HC curve and the RWS curve, and the experimental results from test T1.

In Figure 3.6, Eq. (3.7) has been used to calculate the temperature at the depth 0.04 m inside normal-weight concrete exposed to three different fire temperatures according to expression Eq. (3.5) and the values presented in Table 3.6. The shortest times are not included since the correlations for η_w and η_x , respectively, are not valid for these short times. The graphs show the differences in temperature rise due to the variation in fire temperature. There is a significant difference in time passed until a certain temperature level is reached depending on which fire temperature curve is used. The effect on the structure due to the increase in temperature and what the difference in fire temperature and wall material means for the structure are not within the scope of this thesis even if the phenomenon spalling is briefly discussed in Section 7.1.

One important effect of the ventilation is that it can increase the *rate* of increase in HRR [68, 83]. This can have dramatic consequences on the outcome of a given incident inside a tunnel. In a research project financed by the Swedish Rescue Service Agency it was concluded that the ventilation could have at least two major effects on the conditions during a fire in a tunnel, i.e. through increasing the rate of increase of HRR and diluting the gases inside the tunnel [84]. One part of the project was to model the evacuation of tunnel occupants. The total effect depends on the evacuation situation in the tunnel, but these effects are important to keep in mind. The first few minutes after ignition of a fire can be crucial to the outcome and therefore, the effect of the ventilation on the rate of increase of the HRR must be considered when designing ventilation etc. for tunnels, not only the maximum HRR. The effect of the ventilation is further discussed in Section 5.2.

The sizing of tunnel ventilation is outside of the scope of this thesis, but within the discussion on the temperature inside a tunnel during a fire it can be of interest to note that Carlotti and Voeltzel showed that the correct estimation of the heating of the walls of the tunnel during a fire can be crucial to the performance of the ventilation system [85]. The effect of the heating of the walls on the velocity in a tunnel was also seen during the Runehamar tunnel [86].

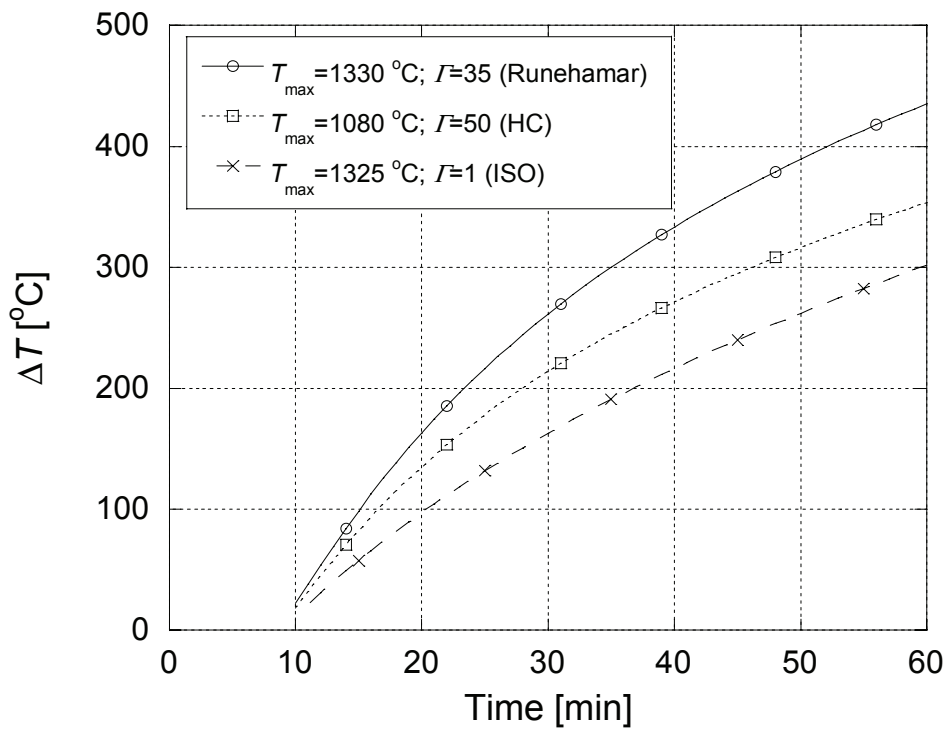


Figure 3.6 Temperature rise at a depth of 0.04 cm in normal-weight concrete exposed to three different fire temperature curves described by Eq. (3.5).

4 Flame length and fire spread in a tunnel

Rew and Deaves identified five different types of mechanism for fire spread between wagons in a rail tunnel [87]:

1. Flame impingement
2. Flame spread (i.e. flame spread across a surface)
3. Remote ignition/'flashover'. Here they discussed spread from one wagon to another due to flashover. (In the rest of this section, remote ignition means ignition by radiation.)
4. Fuel transfer. This includes both spread by burning liquid and by burning debris ('fire brands') transported downstream of the fire.
5. Explosion.

The extended flame along the ceiling in a tunnel is an important factor to consider when studying fire spread in a tunnel. It will influence both mechanism 1 and mechanism 3, above. It can also increase the flame spread along a surface (mechanism 2). Therefore, this section starts with a description of how to estimate the flame length during a tunnel fire.

For unconfined fires there exist a number of relationships for the flame height and different properties of the plume [88-90]. One of the most common relationships for the flame height is the one suggested by Heskestad [91]:

$$h_f/D = -1.02 + 15.6N^{1/5} \quad (4.1)$$

where $N = \left[\frac{c_p T_0}{g \rho_0^2 (\Delta h_c / r)^3} \right] \frac{\dot{Q}^2}{D^5}$, c_p is the specific heat capacity of air, T_0 and ρ_0 are the ambient temperature and density, respectively, g is the acceleration of gravity, Δh_c is the heat of combustion per unit mass, r is the stoichiometric mass ratio of air to volatiles, \dot{Q} is the total HRR, and D is the diameter of the fire source.

This is often written as

$$h_f = -1.02D + 0.235\dot{Q}^{2/5} \quad (4.2)$$

where values for air and typical values for liquid fuels have been used [90].

There are two problems with this equation when applied to fires in tunnels. Firstly, it was developed for free burning fires, without the interference of a ceiling. Correlations that take the influence of the ceiling into account are discussed below. Secondly, the types of fires described by Eq. (4.1) do not include deep-seated fires (e.g. wood cribs, pallets, etc.) [92]. However, Heskestad showed that deep-seated fires are reasonably well represented if the flame height is calculated from the base of the combustion region and if the diameter used in the formula is defined as [47]:

$D = \left(\frac{4\dot{Q}}{\pi\dot{Q}''} \right)^{1/2}$ where \dot{Q}'' is the maximum heat release rate of the fire divided by the plan area of the fire (not the total exposed area of fuel).

Zukoski suggested a relationship based on the non-dimensional heat release rate, \dot{Q}^* , [93]:

$$\frac{h_f}{D} = 3.3(\dot{Q}^*)^{2/5} \quad (4.3)$$

for $1 < \dot{Q}^* < 40$ where

$$\dot{Q}^* = \frac{\dot{Q}}{\rho_0 c_{p,0} T_0 \sqrt{g} D D^2} \quad (4.4)$$

and D is the burner diameter.

For the Runehamar tests, \dot{Q}^* can be calculated as:

$$\dot{Q}^* = \frac{\dot{Q}}{39300}$$

if $D = D_H$ based on the horizontal cross-section of the fuel set-up (2.6 m × 10.5 m). This means that $\dot{Q}^* < 5.1$ for the Runehamar tests.

McCaffrey summarized different flame height relationships based on \dot{Q}^* [89]. In this summary one can also find another version of Heskestad's formula (Eq. (4.2)) written in a form with \dot{Q}^* assuming $\Delta h_c/r = 3185$ kJ/kg air (ethane):

$$\frac{h_f}{D} = 3.7\dot{Q}^{*2/5} - 1.02 \quad (4.5)$$

He also described the difficulty in identifying the *average* flame height. The variation of the flame height is affected by the puffing phenomenon described below. This phenomenon also affects the entrainment.

Fires in tunnels are not unconfined. The influence of the ceiling and the walls is substantial. Babrauskas studied flames under a ceiling and tried to estimate flame lengths by comparing the entrainment in a ceiling jet with the entrainment in a free burning flame [94]. If h_f is flame height for the free burning flame and h_r is the extension of the flame beneath the ceiling (radially), Babrauskas showed that $h_r/(h_f - H_f)$ ranged from 1.2 to 2.0 for cases $0.5 < H_f/h_f < 0.85$. This means that the fires studied were much smaller (in relative measures) than those primarily discussed in

this thesis. Babrauskas also discussed plumes from a fire in a corridor and his calculations for a chosen example showed the ratio $L_f/(h_f - H_f)$ to be approximately 2 (1.81), but the value was very dependent on the width of the corridor and if the width was decreased from 3 m to 2 m, the value increased to 2.94. Again the relationship between the free burning flame height and the height of the ceiling was relatively small. The flame length, L_f , is in this thesis defined as the distance from the cross-section in the centre of the fire (i.e. corresponding to h_f in the work by Babrauskas and L_r in the work by Heskestad and Hamada), see Figure 4.1.

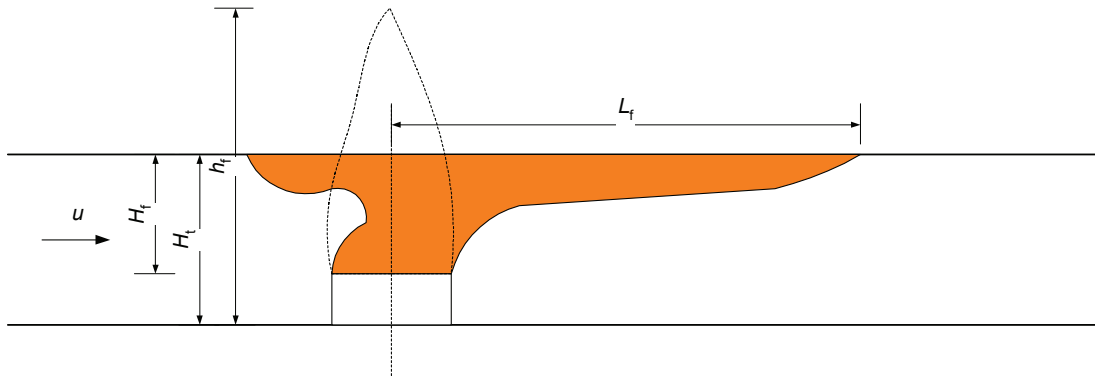


Figure 4.1 Definition of parameters used in the flame length correlations.

A similar investigation with a propane burner, by Heskestad and Hamada, found that $L_f/(h_f - H_f)$ varied between 0.88 and 1.05 with an average of 0.95 [95].

Alpert derived a correlation for maximum ceiling jet temperatures based on fire experiments where the fire sizes ranged from 668 kW to 98 MW [96, 97]. The tests were performed beneath a ceiling where the ceiling height varied between 4.6 m and 15.5 m. Alpert's correlation is a function of heat release rate, \dot{Q} , radial position, r , and height of ceiling above the fuel, H_f :

$$T_{\max} - T_0 = \frac{5.38(\dot{Q}/r)^{2/3}}{H_f} \quad (4.6)$$

It is worth noting that different temperatures at the flame tip have been assumed by different authors. Sugawa *et al.* used a flame tip temperature of 250 °C (defined by the highest position of the temperature contour line) [98]. Oka used the temperature of 350 °C, defining the boundary between intermittent and plume region [99]. Heskestad suggested an excess temperature of 500 °C above ambient at the mean flame height of purely buoyant diffusion flames [90]. Heselden used the value of 580 °C, corresponding to a critical distance for ignition in a tunnel [14]. A similar value (600 °C) was used by Rew and Deaves [87], based on the work by Heselden. In Paper VII it was shown that a flame length based on the value 600 °C approximately corresponds to the distance of fire spread. The value 600 °C will also be used below.

A relationship such as the one in Eq. (4.6) can be used to estimate the flame length if a certain temperature is assumed at the flame tip (see Paper VII). This will be discussed further below, but let us begin with a case more closely associated with a tunnel, i.e. a beamed ceiling. If the beams are deep enough to channel the ceiling jet, the flow of the hot gases appears to be similar to that found in a tunnel, with the significant difference of forced ventilation often used in tunnels. Delichatsios analysed the flow beneath a beamed ceiling, both theoretically and experimentally and derived the following expression for the temperature rise, ΔT , for the case when $h_b/H = 1/5$ and $x > L_b$ [100]:

$$\frac{\Delta T}{\Delta T_0} = 0.29(H/L_b)^{1/3} \exp[-0.20(x/H)(L_b/H)^{1/3}] \quad (4.7)$$

where ΔT_0 is the temperature rise near the ceiling above the fire, H is the height of the ceiling above the fire source, h_b is the beam depth, L_b is half the width between the beams, and x is the horizontal distance from the centre of the fire. Delichatsios showed in his analysis that the main process for the decrease in temperature along the ceiling is the heat transfer to the ceiling. The cooling due to entrainment is not important to the same extent. If Eq (4.7) is used to estimate the flame length it can be rewritten as:

$$x = -5H_f \left(\frac{2H_f}{W} \right)^{1/3} \ln \left[\frac{\Delta T \left(\frac{W}{2H_f} \right)^{1/3}}{0.29\Delta T_0} \right] \quad (4.8)$$

where W is the width of the tunnel ($= 2L_b$). It was investigated whether this equation could be used to estimate the flame length by putting $x=L_f$, $\Delta T = 590$ (600-10) and $\Delta T_0 = 1290$ (1300-10). The problem is, however, that the whole expression becomes negative if the logarithmic expression is greater than zero. This means that certain restrictions must be assigned to the logarithmic expression for the whole expression to give sensible (although not necessarily correct) results:

$$\frac{0.29\Delta T_0}{\Delta T} > \left(\frac{W}{2H_f} \right)^{1/3} \quad (4.9)$$

Using this expression for the values of the temperatures given above results in the condition that $W < 0.51 H_f$. Even if the value of H_f can be discussed, neither of the possible values gives a width of the tunnel near the one in the Runehamar tests. It is, therefore, obvious that the equation (4.8) was developed for a different situation than that in the large-scale tunnel tests in the Runehamar tunnel.

One other difficulty in using Eq. (4.8) for a tunnel, especially with forced ventilation, can be to accurately define ΔT_0 , both in magnitude and position. Preferably, this should be related to the heat release rate to be comparable to the

other methods. One such model is suggested by Motevalli, who described the maximum temperature rise as a function of the non-dimensional HRR (based on the convective HRR and the height) [101, 102]. Using this correlation, however, overestimates the temperatures significantly compared to the temperatures reached during the Runehamar tests (see Papers I and VII). The reason can be the very small fire sources (0.75 kW and 2 kW) compared to the heights (1 m) used when deriving the correlation. There is obviously a large difference in \dot{Q}^* between the two cases.

Newman and Tewarson developed a model for the average temperature in ducts [103]. They provided a model for the convective heat flow downstream of a fire. From this, the average temperature can be calculated. Heat losses are calculated for convection and radiation, respectively, using:

$$\dot{Q}_{l,c} = h_x A_w (T_{avg} - T_w) \quad (4.10)$$

$$\dot{Q}_{l,r} = \bar{F}_{ws} A_w \sigma (\epsilon_g T_{avg}^4 - \epsilon_w T_w^4) \quad (4.11)$$

where

$$h_x = 0.026 [Re]^{-0.2} \left\{ 1 + \left[\frac{D_{Ht}}{x} \right]^{0.7} \right\} \rho_0 c_0 u_0 \quad (4.12)$$

is the average convective heat transfer coefficient to the walls over a distance x , based on work by McAdams [104]. The area, A_w , is the total tunnel surface area (here named ‘walls’ even if this also includes the ceiling and road surface) from the fire to the distance x , \bar{F}_{ws} is the view factor between the walls and the fire source, σ is the Stefan-Boltzmann constant, and ϵ_g and ϵ_w are the emissivity of the gas and walls, respectively. The Reynolds number, Re , is based on the hydraulic diameter of the tunnel, D_{Ht} . If the same assumptions are used as Newman and Tewarson, i.e. $T_w = T_0$, $\bar{F}_{ws} = 1$, and $\epsilon_g = \epsilon_w = 1$, the following equation can be derived:

$$T_{avg} = T_0 + \frac{1}{\rho_0 c_{p,0} u_0 A_{t0} + h_x A_w} \left[\dot{Q}_{tot} - A_w \sigma (T_{avg}^4 - T_0^4) \right] \quad (4.13)$$

A modification of this equation was used in Paper VII (with two different cross-sectional areas and wall temperatures) to calculate the variation in cross-sectional temperature along the tunnel. This showed that with an assumed temperature of 500 °C, the equation estimated the distance of fire spread from the seat of the fire quite well. The temperature of 500 °C corresponds to a radiative heat flux of 20 kW/m², which is often taken as the temperature when many materials ignite. As a comparison, 30 kW/m² corresponds to 580 °C (*c.f.* the discussion on the flame tip temperature above).

Based on the results of experiments in different scales, Oka *et al.* drew the conclusion that with natural ventilation in the tunnel, the flame length was about the same as the free burning flame length when the flame did not touch the ceiling [99, 105]. If the flame touched the ceiling it became somewhat longer than in the free burning case. Under conditions of forced ventilation when the flame tip does not reach the ceiling, the flame was shorter in the model tunnel than in the free burning case (without wind). When the flame touched the ceiling under the influence of forced ventilation, the flame length became longer in the model tunnel than in a free burning case subjected to wind.

It is known from Rew and Deaves that the flame length in tunnels is dependent on the longitudinal velocity [87]. When studying the EUREKA test data they ended up with the following correlation:

$$L_f = 20 \left(\frac{\dot{Q}}{120000} \right) \left(\frac{u}{10} \right)^{-0.4} \quad (4.14)$$

This relationship also indicates that the flame length decreases with increasing velocity. The reason for this feature is that increased velocity leads to increasing entrainment, which in turn leads to a shorter flame length.

In Paper VII the flame lengths estimated from the Runehammar test results are presented and discussed. In this paper a correlation based on the HRR and the air velocity was developed

$$L_f = \frac{1370 \cdot \dot{Q}^{0.8} u^{-0.4}}{(T_{fl} - T_0)^{3/2} H_t^{3/2}} \quad (4.15)$$

If the effect of velocity was not included the correlation constant in Eq (4.15) was calculated to be 941 instead of 1370. In Figure 4.2, three of the different correlations for the flame length discussed in this section (i.e. Alpert, Rew and Deaves, and Lönnermark and Ingason (Paper VII)) are compared to (normalized with) the experimental flame length from the Runehammar test series and presented as function of the HRR. In the correlation by Alpert a value for H_f of 0.5 m has been used. In the graph the flame length given by a certain correlation for a particular HRR has been divided by the corresponding experimental value. Each such ratio is presented as function of the HRR.

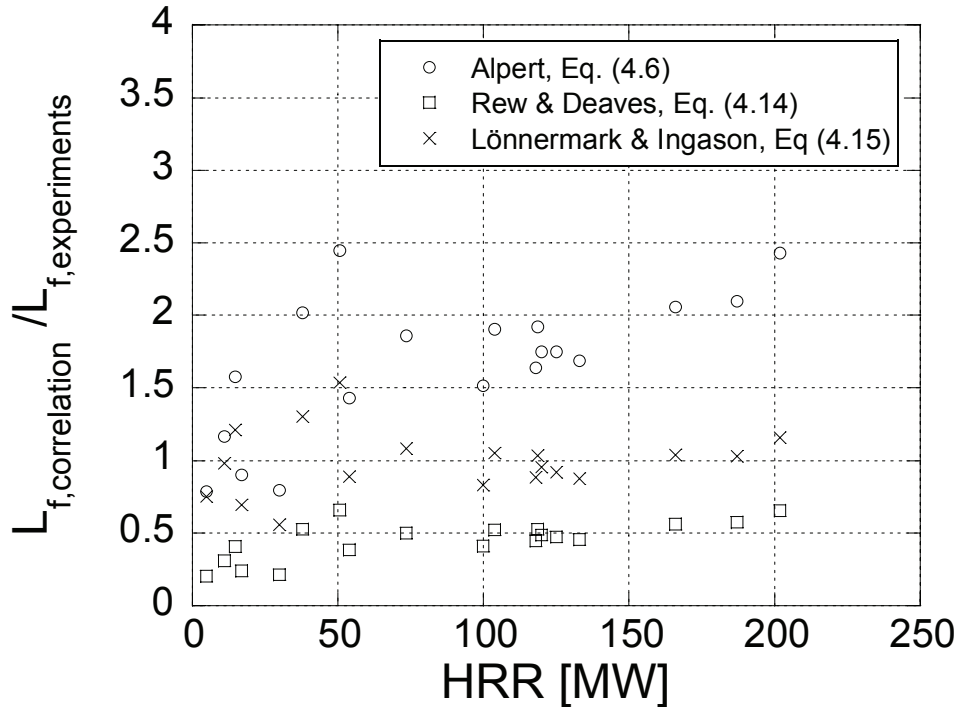


Figure 4.2 Comparison of different correlations for the flame length, normalized relative to the estimated flame length from the Runehamar test (Paper VII).

An absolute correlation with experiments corresponds to a straight horizontal line equal to one. As can be seen from Figure 4.2, the correlation by Alpert overestimates the flame length, while the correlation by Rew and Deaves underestimates the flame length. The reason for Alpert's over-estimation, besides not being developed for tunnels, could be the sensitivity of the model to the height of the ceiling above the fuel. For a 3D burning fuel this height is not well defined. It could be argued that the height, H_f , in Alpert's correlation could be defined from the base of the fuel, but the exponent 1.5 means that there will be a ratio of approximately 22 between the case of using $H_f = 0.5$ m and $H_f = 3.9$ m. Best correlation with the experiment shows the correlation from Paper VII. The explanation for this result is, of course, that it was derived from the same experiments. For all three correlations there is a scatter in the results for low HRRs.

As mentioned above, several authors have related the extension of a flame under a ceiling, in a corridor or in a tunnel to the unconfined flame height. The work by Heskestad and Hamada showed that $L_f/(h_f - H_f)$ ranged from 0.88 to 1.05, with an average of 0.95. In the graph in Figure 4.3 a value of 0.95 has been used. For the correlation based on the work by Heskestad and Babrauskas, h_f has been calculated from Heskestad's relationship and $L_f/(h_f - H_f)$ was assumed to be 2. In both correlations based on the work of Heskestad, the height H_f was taken to be the height

between the base of the fuel and the ceiling. The reason for this choice was based on the work by Heskestad on three dimensional fires [47].

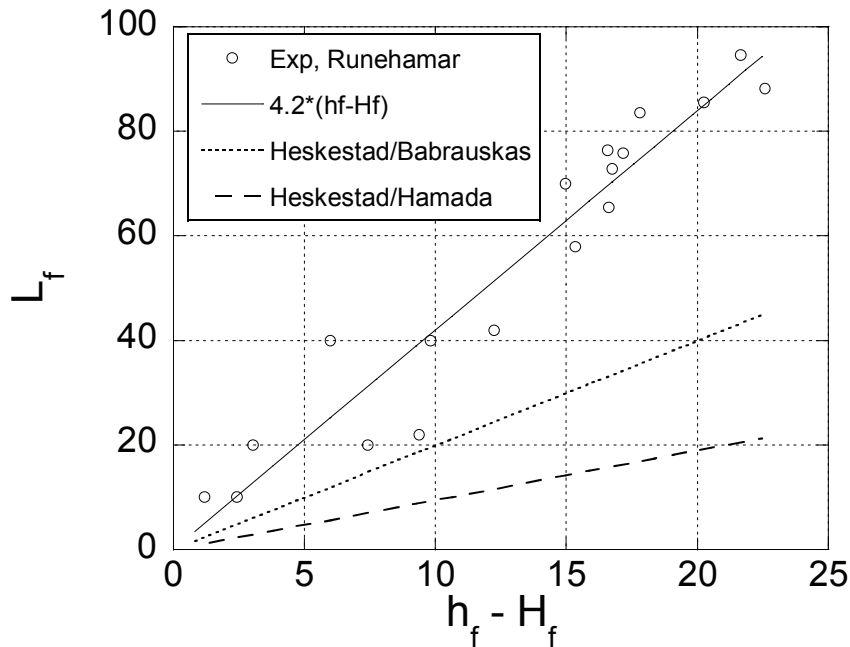


Figure 4.3 Flame length as function of the cut-off height ($h_f - H_f$). Results from the Runehammar tests are compared to three different correlations.

It can be seen from Figure 4.3 that a coefficient close to 4 (4.2) corresponds well with the experimental data, i.e. four times the cut-off height gives the flame length, L_f , inside the tunnel.

It should be noted that most of the correlations have not included any dependency of the width of the tunnel. It can be assumed that this parameter is important for the flame length and needs to be included in future studies. As was discussed above, Babrauskas showed that the ratio $L_f / (h_f - H_t)$ increased from 2 to 3 when the width of the corridor increased from 2 m to 3 m.

One of the few models specifically developed for fire spread in tunnels is the one developed by Beard [106-110]. The model (FIRE-SPRINT) was created to model the fire spread from a burning HGV to a second HGV. There has been a continuous development of the model through different versions as summarised below (if nothing is mentioned the next version of the model has the same assumptions as the one before):

FIRE-SPRINT A1[106]: It was assumed that the fire does not extend over or around the target vehicle, but is retained near the region of the initially burning vehicle (no flames extend downstream of the initial fire). A flow of air of ambient temperature exists in the tunnel due to forced ventilation. No smoke is assumed to move upstream. No radiative heat transfer occurs from the fire to the gases, but radiative feedback exists on the fire from the gases.

FIRE-SPRINT A2[107]: A flame is assumed to extend in the upper part of the tunnel, also above the target, but there is a region above the target with no flame (between the target and the flame). It is assumed that no direct radiative heat transfer occurs between the downstream flame and the target.

FIRE-SPRINT A3 [108]: As in FIRE-SPRINT A2, but with a thicker flame in the region between the fire and the target. Thermal radiation is assumed to exist between the downstream flame section and the top of the target object.

FIRE-SPRINT B1 [109]: Flame impingement onto the target is assumed to exist (a persistent flame impingement is assumed).

The models have been used to estimate the fire spread by calculating the limits of stability of the system (correlated with a jump in the temperature) by means of non-linear dynamics, and investigating how these limits depend on the heat release rate, the air flow velocity and the distance between the fire and the target. In each of the above mentioned cases the limit for HRR to reach unstable condition (fire spread) has decreased, which is in line with what can be expected. For a case with 6.45 m distance between the fire and the target and an air velocity of 2 m/s, the critical value of the heat release rate was calculated to be 55.2 MW, 45.3 MW, 38.6 MW, and 14 MW, respectively, for the four different model versions.

The differences in results obtained with the different versions show both the impact different processes can have on the results, and the importance of large-scale fire tests to validate both models used and assumptions made. There are also cases when flame impingement onto the target (e.g. another vehicle) does not exist, which means that knowledge about the actual situation is needed to make the correct assumptions (i.e. in order to choose the correct version of the fire spread model). In Paper VII a few different aspects of this issue are presented and discussed, both regarding flame length and fire spread. These are discussed below.

Kurioka *et al.* studied the flame tilt and temperature in the near field of a fire (gas burner and pool fires) in tunnels of different scales [111]. Another well instrumented test series was performed by Apte *et al.* in a 130 m long tunnel using pool fires with aviation fuel [112]. These two latter test series can give some insight into the flame behaviour even if the fire sizes and flame lengths were limited. A test series with a more realistic geometrical set-up, although still in reduced scale and using liquid fuel (one test with wood cribs), were performed by Bettis *et al.* [113]. The tunnel was 366 m long and had a cross-sectional area of 5.6 m². The fire sizes ranged from 1 MW up to 19 MW. The test set-up simulated parts of a train with HGVs of the type used in the Channel tunnel. The results from this work include, for example, details of temperatures and velocities around the test set-up.

To shed some light on the issue regarding whether flame impingement is probable during a certain fire situation or not, Carvel *et al.* collected experimental information from the literature and used Bayes' Theorem to calculate the probability of impingement [114]. Bayes' Theorem is suitable due to the possibility to perform probability studies with little information and its ability to improve the accuracy of the estimated probability by complementing the analysis with new information. The basic equation for Bayes' Theorem can be written as:

$$P(\text{imp}|E) = \frac{L(E|\text{imp})P(\text{imp})}{L(E|\text{imp})P(\text{imp}) + L(E|\overline{\text{imp}})P(\overline{\text{imp}})} \quad (4.16)$$

where $P(\text{imp}|E)$ is the probability of impingement with regard to the new evidence, E , $L(E|\text{imp})$ is the likelihood of the evidence assuming that impingement occurs, $P(\text{imp})$ is the probability of impingement, $P(\overline{\text{imp}})$ is the probability of non-impingement, and $L(E|\overline{\text{imp}})$ is the likelihood of the evidence assuming that impingement does not occur [114].

The authors scale the experimental results and draw the conclusion that the flames from a majority (“a large portion”) of HGV fires will impinge on another HGV up to 20 m downstream of the fire. For a car fire (assumed to have a HRR less than 8 MW) it is unlikely that the flame will impinge on another vehicle more than 5 m downstream. In both cases the results are assumed to be valid for air velocities between 1 m/s and 4 m/s. Even if the analyses are based on a limited amount of experimental data and these data are rather small scale, the approach is interesting.

In Paper VII observations of fire spread are presented and discussed. Different types of targets were used: large targets with the same type of commodity as used in each of the full scale tests and smaller wooden and plastic targets placed on the ground at different distances from the seat of the fire. The plastic targets were affected approximately up to the flame length (which correlates well with Heselden’s assumption of 580 °C corresponding to a critical distance for ignition) while the fire spread to the pieces of wood occurred up to a distance of about (or somewhat more than) 70 % of the flame length. For the 202 MW fire in test T1 this corresponds to fire spread distances of 95 m for plastic targets and 70 m for wooden targets. This corresponds to spontaneous ignition due to radiation dominated fire spread from the upper layer to the road surface. With a higher target, e.g. a vehicle with a cargo, the fire might spread even further distances between the initial fire and the target since convective heating and high temperature in the upper layer influence the target to a larger extent. Also direct impingement of flames onto the target can occur. The radiation will, however, still be an important factor for the fire spread.

The fire spread to the large target was observed on video in test T3. This information together with measurements of temperature and radiation was used to estimate the time of fire spread in the tests T1 and T2 (see Paper VII). When the fire spread to the large target (20 to 22 m downstream of the centre of the fire), the heat release rate was in the range of 20 MW to 40 MW. This was obtained in a longitudinal flow of about 2 to 3 m/s.

The fire spread results presented in Paper VII can be compared to the observations from the fire in the Fréjus tunnel in June 2005. The fire started in the engine of an HGV loaded with tyres. The fire then spread to a HGV loaded with cheese 100 m away. An HGV with scrap metal another 100 m away was also ignited. A fourth HGV, 450 m from the initial fire was ignited, but this was extinguished before the tank containing toxic glue was ruptured [115]. These observations correlate well with the results from the Runehamar tests. It shows the long distances this type of fire can spread and, once again emphasizes the importance of HGVs on the outcome of tunnel fires.

A tool more commonly used these days is CFD (computational fluid dynamics) modelling, particularly for smoke movement calculations and investigations of the critical velocity, but also for studies of the fire spread in tunnels. CFD codes are in many cases general in their application, often with a certain application or development towards fires. In recent years some of these codes have been specially developed for tunnels. The CFD codes represent a complex tool where the usefulness often needs to be verified against experimental data for each new type of scenario. The variation can relate to choice of method, submodels, values of parameters, type of boundary condition, values of boundary conditions, etc. Therefore, the CFD codes will not be discussed here, but are only mentioned to emphasize the importance of large-scale fire tests of the kind discussed in this thesis. The importance of assessing the use of a fire model (including the fire model itself, the methodology of use, and the user) is thoroughly discussed in a paper by Beard [116]. However, CFD is already an important tool and the development of both the CFD codes and computer capacities will further increase the usefulness. The possibility of varying conditions and different parameters makes CFD an important complement to fire tests.

5 Ventilation

The ventilation is an important parameter defining the conditions of a fire in a tunnel. Therefore, different types of ventilation systems in tunnels are briefly discussed in Section 5.1. The rest of this chapter is focused on three different phenomena observed in connection with tunnel fires: the effect of ventilation on the HRR (Section 5.2), backlayering (Section 5.3), and the pulsations observed in two of the Runehamar tests (Section 5.4). The ventilation is also important for the combustion and the concentration of different gases in the tunnel. This will be discussed in Chapter 6.

5.1 Different types of ventilation

Ventilation in tunnels has become an important issue during designing of equipment found inside a tunnel. During the regular use of a tunnel, toxic emissions from the traffic need to be ventilated away. In short, low traffic tunnels this problem is often solved by “natural” air movements, e.g. due to vehicle movement inside the tunnel, differences in elevation between the portals, temperature differences, or other meteorological effects (e.g. wind). The natural ventilation can create flow from portal to portal, from shaft to shaft, or from portal to shaft. For mechanically ventilated tunnel systems, there exist two main ventilation systems, longitudinal ventilation and transverse ventilation systems. The latter can be subdivided into fully transverse, supply semi-transverse, and exhaust semi-transverse ventilation systems.

A longitudinal ventilation system creates a longitudinal flow inside the tunnel using a limited number of fans or inlets/exhausts. The transverse systems, on the other hand, use a large number of inlets and/or exhausts, uniformly distributed over the tunnel length. Fully transverse ventilation systems mean that air is both supplied and exhausted along the length of the tunnel. Semi-transverse means that either fresh air is supplied to or vitiated air extracted from the tunnel along its full length. A stage between fully and semi-transverse ventilation also exists, called partial transverse ventilation, depending on the ratio between air supplied and extracted. For more information on ventilation in tunnels see references [12, 117].

Extraction of vitiated gases, locally near the fire, has been shown in fire tests to be a successful method to create better conditions inside a tunnel during a fire, both for the evacuating people and for the rescue service. The tests in the Memeorial tunnel showed that both extraction and longitudinal airflow are crucial parameters when removing smoke and heat near a fire [48]. The efficiency of extraction of fire gases near the fire has also been observed by Ingason in model scale tests (results to be published). This strategy of local extraction has become a reality in some modern systems, e.g. in sectioned transverse ventilation system. One good example of this is the new ventilation system in the Mont Blanc tunnel where a combination, of semi-transverse and longitudinal systems, is used [118-121].

5.2 Effects of ventilation on the fire

That the ventilation has an effect on the HRR and fire growth rate has been shown by results from several test series described by different authors. Carvel *et al* used a more systematic approach to these results by using the same type of Bayesian approach as described in Chapter 4 (used by Carvel for flame impingement), to estimate the effect of the ventilation on the growth of the fire and the HRR of the fully developed fire in a single lane tunnel. The probability can be defined using a similar expression to Eq. (4.16), with the two conditions ‘impingement’ and ‘non-impingement’ exchanged for a different hypothesis, and $k=k_i$, where k is the ratio between HRR with and without forced ventilation, respectively. The original work on HGVs led to the conclusion that an air flow of 2 m/s would lead to seven times faster fire growth and four times higher maximum HRR than for natural ventilation. For a ventilation of 10 m/s the corresponding values were estimated to be 22 and 8-9, respectively [122]. For the study, results from the HGV fire test in the Repparfjord tunnel and different wooden crib test were used [46, 78, 113, 123, 124]. Later estimations were made for two-lane tunnels [83] when results from the 2nd Benelux tunnel tests [65] and from the Runehamar tunnel tests were included (see e.g. Paper II). The estimations for a two-lane tunnel were that an air flow of 2 m/s would lead to 3-4 times faster fire growth and 1.5 times higher maximum HRR than for natural ventilation. For a ventilation of 10 m/s the corresponding values were estimated to be 6 and 3, respectively.

The results from the tests with simulated HGVs (36 wood pallets) in the 2nd Benelux tunnel show that the development rate with ventilation was 1.7 to 2 times faster than the fire development without ventilation. The peak heat release rate was 13.5 MW without ventilation, 19 MW with 4-6 m/s ventilation and 16.5 MW with 6 m/s, which corresponds to 1.4 and 1.2 times higher, respectively [60]. Huijben estimated the increase in HRR due to the ventilation to be 35 % [125].

For car fires Carvel *et al.* reported that the increase factor, k , could not be estimated for velocities higher than 1.5 m/s due to lack of experimental data [126]. The authors concluded that at this velocity the ventilation would not have any significant effect on the HRR or the fire growth. When adding some information from the tests in the 2nd Benelux tunnel, including one with an airflow of 6 m/s, Carvel *et al.* draw the conclusion that k for the peak HRR for the new information is equal to or less than one [127]. The same conclusion was drawn by Huijben [125].

When it comes to pool fires, Carvel *et al.* drew the conclusions that for a small or medium sized pool fire, increased ventilation will decrease the HRR [128]. For a large pool fire an increase in ventilation will probably increase the HRR. The limit between these situations is dependent on the tunnel and the ventilation conditions, i.e. whether the fire is well ventilated or under-ventilated. This is further discussed below.

The method used by Carvel *et al.* is interesting due to its ability to estimate probabilities from little information. It can, however, be difficult to find corresponding information for different ventilation velocities, i.e. test series where the ventilation has been varied, keeping all other parameters constant. When comparing different

fire tests and different experimental series one realises that such a comparison can in many cases be very difficult to perform. The reason for this being that the purpose of each study varies from case to case. This means that measurements performed, positions of instruments/probes, calculations performed, assumptions made, presentation of data, etc. vary between the cases. Below some examples of such cases are presented and discussed. The conclusion to be drawn from this is that further experimental studies of the effect of the ventilation on the fire development and HRR are needed to obtain input data for models of these issues.

Model-scale experiments, with methanol pool fires in a tunnel, show that the burning rate decreases with increasing air velocity, at least for the largest pool diameters used (0.2 m and 0.25 m) [41]. For pools with a smaller diameter (0.15 m) the effect is much smaller and for the smallest case (0.1 m), the effect is negligible. The effect can be related to the radiation and the effect of the tunnel on the burning rate. For the smaller pool sizes the differences between burning in open air and burning inside the tunnel are very small and in these cases the effect of the air velocity is very small.

Ingason and Werling performed model scale tests in a 20 m tunnel where kerosene was used as fuel [129]. The effect of longitudinal ventilation was studied and for velocities of 0.5 m/s and 0.75 m/s (corresponding to 1.4 m/s and 2.1 m/s, respectively, in real scale) the mass burning rate per unit fuel area decreased with increasing air velocity. This is due to the decrease in radiation feedback. For higher velocities the mass burning rate per unit fuel area increased with increasing air velocity. The authors explained this effect with increased mixing at the fuel surface.

In Table 5.1, the estimated HRR values from the tests in the Ofenegg tunnel are presented. The HRR values are calculated from the burning rate presented by Haerter [61] using the following equation

$$\dot{Q} = \chi \cdot \dot{V}'' \cdot A_f \cdot \rho \cdot \Delta h_c \quad (5.1)$$

where χ is the combustion efficiency (assumed to be 0.9), \dot{V}'' is the volumetric surface burning rate [$\text{m}^3/(\text{m}^2 \text{ s})$], A_f is the fuel area, and Δh_c is the heat of combustion for petrol (= 43.7 MJ/kg for gasoline according to [130]). From the table it can be seen that the burning rate is decreasing with increasing surface area. This is contrary to previous data, i.e. the surface burning rate increases with area up to a certain limit [131]. In the Ofenegg case the HRR for the surface areas 47.5 and 95 m^2 are about the same for natural ventilation. This is due to the limited ventilation in the tunnel that had one dead end and in the case of natural ventilation, fresh air only from the open portal. One should note that in the calculations, a constant combustion efficiency of 0.9 has been assumed. This value can vary with time and between the tests. Especially in under-ventilated cases the combustion efficiency can be considerably lower [132]. The semi-transverse ventilation decreases the HRR in all cases, while the longitudinal ventilation decreases the HRR for the smallest area and increases the HRR for the case with fire area 47.5 m^2 . The latter can be explained by the case being vitiated without ventilation. In Table 5.1 the estimated air velocity needed for stoichiometric combustion is also included for some of the ventilation conditions in the Ofenegg tunnel test series.

Table 5.1 Estimation of HRR (Eq 5.1) from data from the Ofenegg tunnel tests [61].

Test	Ventilation ^{a)}	\dot{V} ^{b)} [m ³ /s]	v ^{c)} [m/s]	Fuel area [m ²]	Rate of burning ^{d)} [L/(m ² min)]	HRR [MW]	v_c ^{e)} [m/s]
1	N	0	-	6.6	5-6	16-19	0.36-0.43
2	S-T	15	-	6.6	3.7-5	12-16	
2a	L	39	1.7	6.6	3.7-5	12-16	0.13-0.18
5	N	0	-	47.5	1.7-2.1	38-47	0.87-1.08
6	S-T	15	-	47.5	1.5-1.7	34-38	
7a	L	39	1.7	47.5	2.6-3.5	58-79	0.67-0.90
9	N	0	-	95	0.8-0.9	36-40	0.82-0.92
10	S-T	6	-	95	0.7-0.8	31-36	

- a) N = Natural; S-T = Semi-transverse; L = Longitudinal
- b) Air supply ventilation
- c) Longitudinal velocity given by Haerter [61].
- d) Corresponding open air pool fire burning rate is 5-6 L/(m² min)
- e) Velocity needed for the calculated HRR (with $E = 13.1$ MJ/kg O₂); for natural ventilation calculated as fresh air flowing in the lower part of the tunnel (11.5 m²), for longitudinal calculated with full tunnel cross-sectional area, for semi-transverse ventilation no calculation was made due to the difficulty in defining flow region.

The Ofenegg tunnel fire tests show what large differences in conditions can exist for different cases of natural ventilation. In the Ofenegg tests there was a dead end. In other cases other factors can alter the situation, e.g. slope of the tunnel, outside wind, etc.

Liew *et al.* showed by calculations and discussion, how the ventilation can influence the fire spread and smoke movement and thereby the decisions to be made regarding ventilation direction [133]. One of the important questions when it comes to the fire safety strategy in the Eurotunnel is whether a ‘keep going’ philosophy should be used. The conclusion by Liew *et al.* was that the keep going philosophy was acceptable from a fire spread and tunnel damage perspective, but an uncontrolled stop had to be avoided since this otherwise could lead to fatalities.

The HGV test performed within the EUREKA 499 project [54, 123, 134] is often referred to as an example of the effect ventilation can have on the HRR. The measurements clearly show the decrease in heat release rate when the ventilation is turned off during three minutes (13:30 to 16:30). However, during this phase without ventilation, the velocity 100 m upstream of the fire decreases almost to zero (0.1 m/s - 0.2 m/s) [123]. The tunnel was sloping upwards (0.5 % - 1 % [135]) in relation to the ventilation and main flow in the tunnel. This was, however, not enough to prevent some of the gases from flowing backwards. This means that the HRR measurements during this time period are not necessarily as accurate as during the rest of the test, depending on whether some of the gases were delayed in reaching the measuring station. This might also be the reason for a second peak in the HRR (128 MW) higher than the previous peak (121 MW) even if the air flow velocity after the stop of the fan was lower (on average 2.8 m/s) than before the stop (on average 5.5 m/s).

Otherwise there is no significant difference in maximum HRR between the cases with velocities of 5.5 m/s and 2.8 m/s, respectively. The HRR was determined in several different ways, but the ones given by Grant and Drysdale [49] seem to be most reasonable. Their HRR value (a maximum of 128 MW if gas analyses 30 m downstream of the fire are used; a maximum of 121 MW if gas analyses 100 m downstream of the fire are used) is near the maximum value of 119 MW estimated in test T3 in the Runehamar test with similar goods (see Paper II). Grant and Drysdale used assumed values for the net heat of combustion of fuel per mass of produced CO and CO₂, respectively. The assumed values were said to be average values for a representative mix of fuels [49].

In the Repparfjord tunnel, a test with a simulated truck load was also carried out [54]. This test were carried out with natural ventilation and reached much lower maximum HRR (approximately 17 MW [75]) than was the case for the HGV test in the same test series (128 MW). There are, however, two important differences between the tests. The total calorific value was 37 % (87400 MJ compared to 63700 MJ) higher in the HGV tests than in the test with the simulated load. Another important difference is that in the HGV tests, the main commodity used was furniture, while in the simulated load tests densely packed wood cribs was the main component, both weight wise and energy wise. In Section 3.3 it was shown that there exists a relationship between the maximum HRR and the energy content. The overall trend is the same for the tests in the Runehamar tunnel (see Paper II). The HRR was, however, higher in test T2 (mattresses and wood pallets) than in test T3 (furniture), which indicates that the total calorific value is not alone determining the peak HRR.

The geometry of the fuel is very important and as the geometry varies, the effect of the ventilation on the HRR can also vary. It should also be mentioned that the total calorific value in test T3 was higher than both the tests in the Repparfjord tunnel discussed above. The reason for the relatively low HRR in the furniture tests in Runehamar was discussed above and is probably due to the fact that much of the cellulosic material used (e.g. cupboard doors) were packed in a very compact way. The explicit effects of the ventilation in these tests are difficult to assess, since no similar test of the same size was performed without ventilation. However, free burning tests under SP's industry calorimeter were performed with the same commodities as used in test T1, T2, and T4, respectively [136]. From these pre-tests Ingason estimated the expected HRR in the large-scale tests in the Runehamar tunnel before performance of the tests [137]. In Table 5.2 estimated and measured peak HRRs are compared. If all available material is included (i.e. the target is included), the ratio of the measured peak HRR and the estimated peak HRR range from 0.81 to 0.93.

During the test series in the Repparfjord tunnel several tests with wood cribs were performed. A comparison between two of these tests, one without and one with ventilation (on average 2.2 m/s [54]), clearly shows the influence of ventilation. In the first case the maximum HRR was approximately 9 MW, while in the second case the maximum HRR was approximately 27 MW [75], i.e. three times higher with ventilation. Ingason, however, performed an energy analysis, which showed that the HRR in the second case was probably considerably overestimated. Ingason pointed out that a probable reason for the discrepancy was an assumption regarding the O₂ concentration below the lowest measurement point. An estimation of the HRR from

the measured mass loss rate gives a value between 11 MW and 12 MW (using a heat of combustion of 17 MJ/kg). The mass loss signal is not available for the whole tests, but the signal that is available does not show the rapid increase as calculated from the gas analyses. Still, there was a higher HRR in the case with ventilation, even if the factor was only approximately 1.5. Another aspect of the comparison of these tests is the fact that the 3D effect of the burning of wood cribs is significant. The reaction to ventilation in such a case can be quite different to a case with fuel where mainly the outer surfaces are burning.

This is an illustration of how important it is to take different aspects of the set-up and the performance of tests into account when comparing effects of the ventilation. The effect of ventilation can be very dependent on the starting conditions; an under-ventilated fire is more affected than an already well-ventilated fire. This will be discussed further in the section on the combustion and the conditions in the tunnel below (see also Paper III). The availability of oxygen is not important only for the gaseous flaming combustion. It has also been shown that the presence of oxygen near the surface of some polymers (e.g. Polyethene and polypropene) significantly increases the decomposition rate [138]. Most of the experiments indicating these results were performed in laboratory scale (candles), and it is uncertain how important this effect is in a large-scale fire.

Table 5.2 Estimated peak HRR for the Runehamar tests based on laboratory tests ([136, 137] and Paper II).

Test	Estimated peak HRR excl. target [MW]	Estimated peak HRR incl. target [MW]	Measured peak HRR [MW]	Measured HRR/ Estimated HRR excl. target	Measured HRR/ Estimated HRR incl. target
T1	186	217	202	1.09	0.93
T2	167	195	157	0.94	0.81
T4	79	95	66	0.84	- ^{a)}

a) No large target was used in test T4.

There is still a need for further experimental studies of HRR from different types of fires in tunnels. However, the experimental results available are increasing and these should be used to assess the correctness of the models used to date. When doing such assessments it is important to carefully identify the purposes of the tests and discuss differences between different tests and different test series. Furthermore, there is always a degree of uncertainty involved in experimental studies (as is the case for modelling). This became especially obvious in the tests in the Repparfjord tunnel where the estimates of the HRR from the HGV tests varied significantly between the research groups [54]. However, such shortcomings can often be both identified and explained if the results are carefully checked (see e.g. Paper II and reference [75]).

Carvel has developed a fire model, CERBERUS, that besides the effect of the ventilation on the HRR also includes the fire spread model by Beard described above, and the influence of the tunnel geometry on the HRR [139]. There are, however, still some validation studies that need to be performed. Carvel *et al.*

discusses a tunnel fire in a HGV loaded with furniture. In a situation with ventilation giving an air speed of 1 m/s, the heat release rate is estimated to be between 9 MW (10th percentile) and 88 MW (90th %) with a 50th percentile value of 31 MW [140]. For an air speed of 3 m/s or 10 m/s the corresponding values are estimated to be 17 MW, 210 MW, 62 MW and 60 MW, 630 MW (597 MW in the text), 195 MW, respectively. For the 10 m/s case the calculation with CERBERUS A1.1 shows that this fire would not spread to another vehicle 8 m or more away from the original vehicle. These are very extreme results and can be questioned. It should be said that in this version of CERBERUS, the impingement was not included; it has later been included in the fire spread model (see Chapter 4). However, with the sizes of fires mentioned here, the radiation is very high and the flames are long and the fire should spread longer than 8 m. Clearly, there is a need for validation of such models.

5.3 Backlayering

Even if longitudinal flow exists in the tunnel, a backflow of fire gases can travel against the ventilation flow under certain conditions of ventilation flow and heat release rate. This phenomenon is called backlayering and is an important feature of tunnel fires since it can be important for the safety of occupants upstream of the fire.

Thomas was the first to present a relationship for the critical velocity needed to prevent the backflow of smoke from a fire in a tunnel [141]. By comparing buoyancy head and the velocity head he proposed the following equation:

$$u_{cr} = k \left(\frac{g\dot{Q}H_t}{c_p T \rho_o A} \right)^{1/3} \quad (5.2)$$

where A is the cross-sectional area of the tunnel, H_t is the height of the tunnel and T is the temperature of the hot layer. The value of the constant k was not determined by Thomas, but he assumed that the value was of the order of unity. One problem in using Eq. (5.2) is to define a temperature representative of the hot layer.

Based on the work by Thomas, de Ris used the dimensionless number, $\Delta\rho gH/(\rho_o u^2)$ [142] to define critical conditions for backflow. Backflow can be avoided if this expression is less than one. Originally, H is the duct height assuming no stratification. In the case of the Runehamar tests, where stratification occurred, if H is assumed to be 1 m and the density ratio, $\Delta\rho/\rho_o$, is assumed to be 0.75, the critical velocity becomes 2.7 m.

Heselden presented an expression (based on work by Hinkley [143]), similar to the one presented by Thomas [141], for the velocity of the smoke layer [14]:

$$u_{cr} = cK \left(\frac{g\dot{Q}_{sl}T}{c_p \rho_o T_o^2 W} \right)^{1/3} \quad (5.3)$$

where c and K are constants (assumed to be 0.8 and 1, respectively, based on experiments), \dot{Q}_{sl} and T , are the rate of flow of heat in the smoke layer and the temperature of the smoke layer, respectively. To prevent backlayering, in principle a ventilation velocity higher than the velocity given by Eq. (5.3) is needed for a horizontal tunnel. For a downhill sloping tunnel a higher velocity is needed.

Using a limit on the critical Richardson, Ri , number of 4.5, Danziger and Kennedy modelled critical velocities with the following expression [144]:

$$u_{cr} = \left(\frac{g\dot{Q}_c H_t}{4.5c_p \rho_0 A T} \right)^{1/3} \quad (5.4)$$

$$\text{where } T = \frac{\dot{Q}_c}{\rho_0 c_p A u} + T_0$$

A similar correlation, but with a different factor, was developed by Saito *et al.* [41]:

$$u_{cr} = 1.26 \left(\frac{g\dot{Q}H_t}{c_p \rho_0 A T_0} \right)^{1/3} \quad (5.5)$$

The difference between the convective HRR and total HRR is not discussed in the references discussed above. In most cases a reference is made to the heat flow in the hot layer or an explicit equation is given for the HRR, but not in all cases. In the work by Saito *et al.* the calculation of the HRR is not described, but it can be assumed that it is calculated from the mass loss rate.

Guelzim *et al.* developed a computer model, based on conservation equations for a pseudo two-dimensional case, to model the backlayering [145]. The model slightly overestimates the length of the backlayer when compared with small-scale experiments. The agreement is, however, fairly good. Both the experiments and the model show that the backflow length is a strong function of the air velocity.

The expressions discussed above with the exponent 1/3 were developed using dimensional arguments (Froude number preservation), and are only valid in cases when the flames do not reach the ceiling, i.e. for relatively small fires. For cases where the flame heights exceed the height of the tunnel, the critical velocity has a much weaker dependence on the heat release rate [146]. Oka and Atkinson showed, both with experiments and with physical reasoning, that the critical velocity can be taken as independent of the HRR for large fires. They derived a correlation based on the non-dimensional HRR (Eq. (4.4) with D representing the height of the tunnel) and a non-dimensional critical velocity:

$$u_{cr}^* = \frac{u_{cr}}{\sqrt{gH_t}} \quad (5.6)$$

The critical velocity was then represented by two different expressions according to:

$$u_{cr}^* = 0.35(0.124)^{-1/3} (\dot{Q}^*)^{1/3} \text{ for } \dot{Q}^* < 0.24 \quad (5.7)$$

and

$$u_{cr}^* = 0.35 \text{ for } \dot{Q}^* > 0.124$$

For the Runehamar tests this would mean that for HRR above approximately 12 MW the critical velocity is constant and approximately 2.5 m/s. Although Oka and Atkinson did not specify whether the total or convective heat release rate was used in this analysis, Atkinson and Wu indicate that it was the convective HRR [147].

Oka and Atkinson also showed that the critical velocity is lower for a fire occupying a larger proportion of the width of the tunnel and is increased by raising the fire (burner in their case) above the floor level (closer to the ceiling). If the space beneath the fire was blocked, a decrease in the critical velocity was observed. This means that the constant (0.35) can vary for different types of set-up (width, level above the floor, and blockage) and a span from 0.22 to 0.38 was given by Oka and Atkinson. If the fire is on the floor and there is no significant blockage, the value of $u_{cr,max}^*$ varies from approximately 0.35 (for a fire much narrower than the tunnel) to 0.31 (for a fire of the same width as the tunnel) [146]. Also blockages (e.g. vehicles) upstream of the fire decrease the critical velocity [148].

A somewhat different approach was taken by Kunsch who used equations for a plume rising (from a point source) deflected at the ceiling and combined this with equations for the back flow and ended up with the following expressions [149]:

$$u_{cr}^* = C_3 \sqrt{C_1 \Delta T_0^*} \frac{\sqrt{1 + (1 - C_2/C_1) \Delta T_0^* \dot{Q}^{*2/3}}}{1 + \Delta T_0^* \dot{Q}^{*2/3}} \dot{Q}^{*1/3} \quad (5.8)$$

where

$$u_{cr}^* = \frac{u_{cr}}{\sqrt{gH_t}},$$

$$C_1 = \frac{1 - 0.1(H_t/W)}{1 + 0.1(H_t/W)} \left[1 + 0.1 \left(\frac{H_t}{W} \right) - 0.015 \left(\frac{H_t}{W} \right)^2 \right] \cong 1 - 0.1 \left(\frac{H_t}{W} \right),$$

$$C_2 = \frac{1 - 0.1(H_t/W)}{1 + 0.1(H_t/W)} 0.574 \left(1 - 0.20 \frac{H_t}{W} \right),$$

$C_3 = 0.613$, and

ΔT_0^* is a dimensionless constant with a value equal to 6.13 and W is the width of the tunnel. The dimensionless HRR, $\dot{Q}^{*1/3}$, is based on the height of the tunnel, H_t .

The above relationships were, however, derived for horizontal tunnels. For tunnels with a downhill slope, the critical velocity is higher compared to horizontal tunnels

(with other conditions kept the same). Atkinson and Wu studied the effect of the tunnel slope on the critical velocity [147]. The effect of the slope (for slopes between 0° and 10°) on the critical velocity found by Atkinson and Wu can be expressed as:

$$u_{cr}(\psi) = u_{cr}(0)[1 + 0.014 \cdot \psi] \quad (5.9)$$

where $u_{cr}(0)$ is the critical velocity for corresponding horizontal tunnel and ψ is the slope of the tunnel expressed in degrees. Corresponding expressions based on the maximum non-dimensional critical velocity for a certain type of set-up ($u_{cr,max}^*$) include:

$$u_{cr} = \sqrt{gH_t} \cdot u_{cr,max}^* (\dot{Q}^*/0.12)^{1/3} \cdot [1 + 0.014 \cdot \psi] \text{ for } \dot{Q}^* < 0.12 \quad (5.10)$$

and

$$u_{cr} = \sqrt{gH_t} \cdot u_{cr,max}^* \cdot [1 + 0.014 \cdot \psi] \text{ for } \dot{Q}^* > 0.12$$

(Note that in the paper by Atkinson and Wu the denominator is 1.2 and not 0.12 within the first parenthesis in Eq. (5.10). However, the denominator must be 0.12 to express a continuous function).

The slope factor suggested by Atkinson and Wu is much lower than the one presented by Danziger and Kennedy [144], which can be approximately expressed:

$$u_{cr}(\psi) = u_{cr}(0)[1 + 0.034 \cdot \psi - 0.0011 \cdot \psi^2] \quad (5.11)$$

for $\psi < 10\%$.

The grade factor used in NFPA 502 (presented graphically) is approximately $K_g = 1 + 0.025 \cdot \psi$, where ψ is the downhill slope in %. The relation used in NFPA 502 for the critical velocity without slope is very similar to the one presented by Danziger and Kennedy.

Wu and Bakar showed that the critical velocity was affected by the width of the tunnel for the same tunnel height and derived, from experiments, a similar relation to those above, but based on the hydraulic diameter, D_H , instead of the tunnel height [150]:

$$u_{cr}^* = 0.4(\dot{Q}^*/0.20)^{1/3} \text{ for } \dot{Q}^* \leq 0.20 \quad (5.12)$$

and

$$u_{cr}^* = 0.40 \text{ for } \dot{Q}^* > 0.20$$

where

$$u_{cr}^* = \frac{u_{cr}}{\sqrt{gD_H}} \quad (5.13)$$

and \dot{Q}^* is also based on D_H .

With this correlation the critical velocity for the Runehamar tests becomes constant 3.3 m/s above approximately 29 MW (convective). These values were calculated for the rock tunnel. If the dimensions of the inner protective tunnel are used the constant critical velocity becomes 3.0 m/s above 18 MW. These values should then be corrected for the slope of the tunnel (1 %).

The Memorial Tunnel Fire Ventilation Test Program (MTFVTP) showed that jet fans are effective in controlling the direction of the smoke, even for large fires [48]. For a range in heat release rates of 10 MW to 100 MW, the test results suggest that an air velocity between 2.54 m/s and 2.95 m/s is sufficient to prevent backlayering.

In Figure 5.1 critical velocities according to Eq. (5.2) [141], Eq. (5.3) [14], Eq. (5.4) [144], Eq. (5.5) [41], Eq. (5.6) & (5.7) [146], Eq. (5.8) [149] and Eq. (5.12) & (5.13) [150] are presented. As mentioned above it is difficult to define a temperature representative for the hot layer. In the equations suggested by Thomas and Heselden, respectively, the same bulk temperature relationship as was given by Danziger and Kennedy (see Eq. (5.4)), has been used.

There was a 1 % downhill slope at the position of the fire and this was considered by multiplying the results from the correlations with a slope factor based on Eq. (5.9). It has been assumed that all the correlations are based on convective HRR. For comparison, the correlation by Saito *et al.* has been calculated also with total HRR. Four experimental values from the Runehamar test series are included. The HRR and velocity at the time when the smoke layer passes the position 15 m upstream of the centre of the fire set-up is plotted for each test. The scale for the HRR in the graph corresponds to total HRR. For the relationships using convective HRR, a factor of 0.7 (corresponding to 30 % radiation heat transfer) has been used in the calculations.

The Runehamar values seem to fall between the two horizontal constant values lines. The value, including correction for the slope, is 2.5 m/s based on the work by Oka and Atkinson and 3.0-3.1 m/s based on the work by Kunsch or Wu and Bakar. This correlates well with the results from the Memorial tunnel tests and might also confirm the existence of a super-critical velocity (an asymptotic value of the critical velocity for high HRR) that has been suggested by several authors. The results from the Runehamar tests seem to correlate well with these results. Best correlation seems to be with the relationship suggested by Kunsch. The experimental results cannot, however, be taken as validation since there are few data points and the velocity was not systematically varied. One should also keep in mind that the HRR in the Runehamar tests were transient and that no real steady state conditions were reached. The effect of the slope according to Eq (5.9) in this comparison is relatively small. More information on the time resolved results from the temperature measurements upstream of the fire are given in Paper I.

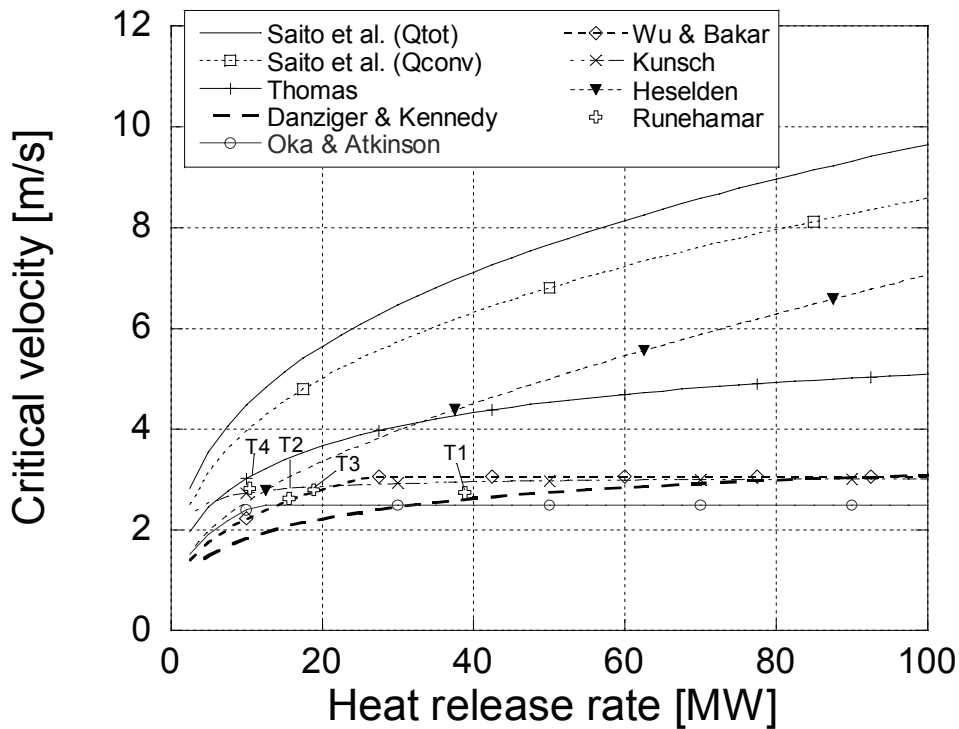


Figure 5.1 Critical velocities as function of total HRR according to four different relations. The values of the parameters in the correlations are based on the conditions in the Runehammar tunnel. All correlations are multiplied with a slope factor according to Eq (5.9). The HRR and velocity at the time when the smoke reached 15 m upstream of the fire in the four Runehammar tests are included for comparison.

The buoyancy factor, B , recognized in several of the equations described above can be expressed as [151]:

$$B = \left(\frac{g\dot{Q}_c H}{\rho_0 c_p A T_o} \right)^{1/3} \tag{5.14}$$

Grant *et al.* presented the function of critical velocity for different relationships and experimental data using the buoyancy factor. The critical velocity increases with increasing tunnel height. The critical velocity is also linearly dependent on B for a wider range of B when the height of the tunnel increases [149].

Heselden discusses the effect of the radiation from the smoke gases on bare skin for the people being inside a tunnel during a tunnel fire [14]. He refers to a value of 2 kW/m^2 being the criterion for causing unbearable pain after one minute. He converted this into a smoke layer temperature of $160 \text{ }^\circ\text{C}$ by assuming a blackbody radiator and a configuration factor of 1. Even with these assumption kept in mind it illustrates the effect the temperature of the smoke layer can have on the people in the tunnel and the importance of controlling the smoke flow. In the Runehammar tests, temperatures of $200 \text{ }^\circ\text{C}$ were reached 40 m upstream of the fire (see Paper I). This was with a longitudinal flow, even if the flow was not large enough to prevent backlayering.

In recent years a new term, “confinement velocity”, has been used [152-154]. While the critical velocity is the lowest velocity needed upstream of the fire to prevent the existence of backlayering, the confinement velocity is the lowest velocity needed to stop an existing backlayering at a certain position, i.e. prevent further spreading upstream. The reason for using such a velocity is the attempt to control backlayering at the same time as stratification is preserve. The capacity of the ventilation system is also an issue. This is therefore closely linked to the design of ventilation systems. Since that is not a focal point of this thesis, the issue is not further discussed here.

5.4 Pulsations

During two of the large-scale fire tests conducted in the Runehamar tunnel in Norway and discussed in this thesis, regular pulsations were observed during the most intense part of the fire (see Paper V and Paper VI). Pulsations with two different periods, 4 s and 18 s, respectively, were observed when the HRR was higher than a certain level (between 125 MW and 135 MW). In this section, the properties and explanations of these pulsations are presented and discussed. However, first some other pulsation phenomena observed in connection with different kinds of fires are presented.

Pulsating phenomena can be observed in different fire situations. Two of the more common are the interplay of buoyancy and fluid dynamics resulting in pulsating flames (vortex shedding) sometimes referred to as “puffing”, most obvious in connection with large pool fires, and the “breathing” phenomena that can arise in a fire in a room or another confined space when the relationship between the flow of pyrolysis gases and available oxygen is not stable.

McCaffrey analysed the frequency of the puffing from a 0.3 m square natural gas burner [155]. He found the frequency to be 3 Hz. Later several authors have investigated, described, and summarized the phenomenon [156-159]. Cetegen and Ahmed observed puffing also with isothermal helium plumes, which suggests that the puffing phenomenon is associated with the instability of buoyant flow [156]. The puffing frequency seems to be independent of the fuel type, but proportional to $1/\sqrt{D}$. The results further suggest that the frequency increases with increasing fuel velocity (decreasing Richardson number). This effect seems to become more apparent for smaller D . The intensity of the fluctuations appears to be affected by the local heat release rate.

Weckman and Sobiesak suggest that the pulsating flames from pool fires are a result of instabilities in the fluid dynamics rather than the local availability of fuel and air [158]. This is supported by the work by Hamins *et al.* [159]. It does, however, affect the entrainment of air and mixing of air and fuel. The pulsations due to vortex shedding has been summarized by Malalssekera [157] and will be further discussed below.

The second feature, breathing, arises when the fire in an enclosure becomes ventilation controlled. There exists a positive pressure inside the enclosure preventing air to enter the combustion zone. This leads to a decrease in the combustion rate and in

the temperature inside the enclosure. The following decrease in relative pressure makes it possible for fresh air to reach the pyrolysis gases resulting in an increase in the combustion rate again. This phenomenon was first described by Takeda and Akita [39] and has later been studied by Kim *et al.* [160]. They showed that the oscillation period is a function of the ventilation factor ($A\sqrt{H}$) in a region of unstable combustion (the combustion could not be sustained). In the region of stable combustion, the oscillation period was between 1 s and 1.5 s and did not depend on the ventilation factor. Utiskul *et al.* have later shown that the limiting oxygen concentration for the different regions decreases with increasing temperature [161].

If a vent is suddenly opened to an oxygen depleted compartment this process can be dramatic and result in what is called a backdraft (see e.g. [162, 163]), which can be very dangerous for fire fighters being engulfed in the exiting flames from the enclosure, but it can also result in the mentioned breathing condition with alternating inflow of air and outflow of combustion gases. The size and position of the ventilation area are, naturally, important factors. Breathing was observed in some of the tests in the ISO 9705 room with reduced opening area within the TOXFIRE project even if the frequencies related to the breathing was not evaluated [132].

Another type of pulsation was observed by Prétrel *et al.* during fire experiments in confined enclosures with forced ventilation [164, 165]. In most of the tests the oscillations ($f \approx 0.1$ Hz) seems to start when the vessel, inside which a pool fire was situated, reaching a situation of oxygen starvation. However, there is also a well-ventilated example with a long period of oscillations in the pressure ($f \approx 0.2$ Hz). The authors discussed mainly two plausible explanations: flame intermittency (*c.f.* the case for pool fire above) and Helmholtz resonator. They also discussed the phenomenon of alternating combustion conditions inside a naturally ventilated compartment (*c.f.* the phenomenon breathing discussed above) where periods of high intensity combustion (resulting in oxygen depletion) were periodically followed by periods of low-intensity combustion (resulting in fresh air flowing into the compartment). Neither theory fully explained the observations, and they might be a combination of factors. The Helmholtz resonator has been used to study thermoacoustic instabilities within the combustion field [166, 167]. The thermoacoustic instabilities will be the theme of the remainder of this section.

Combustion instabilities or pulsating flames are not new phenomenon. Byron Higgins was the first to have noted the type of combustion instability that usually is called a “singing flame” [168]. The discovery was made in 1777, but it was first in 1802 that he described the discovery in a letter to Nicholson’s Journal and was later further described by other authors [169-171]. The first pulsating flames studied were with hydrogen and several explanations involved the production and condensation of water vapour, but Faraday observed this phenomena both under conditions too hot for the condensation of water vapour and using carbon monoxide, which does not form water vapour when burned [172].

Other explanations include repeated detonations, decrease in pressure in the tube due to the draft, and velocities close to the critical velocity for the transition between streamline flow and turbulent flow. These latter explanation lead to the assumption that the maintenance of vibrations cannot occur without draft, and therefore cannot

occur in a horizontal pipe [172]. It has, however, been shown that this is not the case. Indeed, draft is not necessary for the maintenance of an oscillating flame although it does have an effect [170].

The best known explanation of the observed oscillations was given by Lord Rayleigh in 1878. He stated:

“...If heat is given to the air at the moment of greatest condensation, or taken from it at the greatest rarefaction, the vibration is encouraged. On the other hand if heat is given at the moment of greatest rarefaction, or abstracted at the moment of greatest condensation, the vibration is discouraged...” [173].

This is referred to as Rayleigh’s criterion and is still taken as valid today even if it is extended in the sense that the regions of oscillation are considerably broader than those described by Rayleigh’s criterion [170].

The vibrations in an air tube can be initiated by some kind of disturbance. In the laboratory a small puff of air may be enough. In the large-scale, wind might have this initiating effect. Often, there is no obvious external reason for the start of the oscillations [172]. Vortex shedding can be a reason for the production of oscillations and periodic heat release rate (the periodic heat release rate observed during the tests presented in this Paper V and VI were, as discussed in the papers, mainly related to pulsations in the pressure measurements and not to the actual heat release rate). The vortex shedding frequency can either coincide (approximately) with the second natural mode of the system or be large enough to force the system to follow the vortex shedding frequency or interact with the acoustic system in such a way that the vortex shedding is forced to attain the acoustic frequency [174, 175].

The vortex shedding phenomenon has been widely studied when it comes to pool fires. In the review of pulsation of flames and pool fire performed by Malalasekera *et al.* [157], the authors give a relationship between the Strouhal number, St , and the Froude number, Fr , in the form:

$$St = \alpha \cdot Fr^\beta \quad (5.15)$$

with the best fit for many experiments (burner diameter from 0.0074 m to 2.2 m) giving $\alpha = 0.52$ and $\beta = -0.505$, which means that

$$f = 0.52 \cdot \frac{U}{D} \left[\frac{gD}{U^2} \right]^{0.505} \quad (5.16)$$

The influence of the fuel velocity, U , is very limited and is therefore neglected in the analyses. Thus, the formula becomes similar to the one used in several cases in the literature:

$$f = a \cdot D^b \quad (5.17)$$

where the best fit for the same experiments as above gives $a = 1.68$ and $b = -0.5$. These values are similar to those given by McCaffrey ($a = 1.6$ and $b = -0.5$) for fires with diameters between 2 m and 50 m [157]. Beyler presented a summary of the constant a from many different investigators and the values for the constant fall between 0.85 and 1.90 [88]. The highest values reported are based on square fires where the edge length has been used for D . If the values presented by Malalasekera or McCaffrey are used together with the dimensions of the set-up in the Runehamar fire tests, the frequency becomes 1 Hz if the width (2.6 m) is used and 0.5 Hz if the length (10.5 m) of the HGV mock-up is used. This corresponds to a period between 1 and 2 seconds, i.e. somewhat shorter than the measured period, but as mentioned it can still affect the oscillations by interacting with the acoustic system.

Schadow and Gutmark presented a review of combustion instabilities related to vortex shedding in dump combustors [176]. They reported that vortex interactions can occur in the shear layer of a jet and that this can be characterized by a number of instability frequencies related to different vortex sizes. If a combustor flow is dominated by vortex flow in the flameholding region it can result in a periodic heat release. The authors concluded that in all cases the instability was associated with the formation of large-scale vortices in the mixing layer. This was coupled with the acoustic pressure and excited strong oscillations. The periodic heat release reaches its maximum when the vortices brakes down to small scale turbulence.

Oscillating combustion is used in modern applications such as pulse combustors, and these have been shown to have advantages including high heat transfer rate, high combustion efficiency and low emissions of NO_x in particular, but also CO [167, 174, 177-180]. Oscillations have also been studied as they appear as unwanted instabilities or combustion driven oscillations (CDO). Combustion instabilities can occur in a wide variety of combustion system, e.g. residential oil-fired heaters, industrial burners, blast furnaces, rockets, jet aeroengines, etc.

Theoretical analysis of thermoacoustic instability in combustion chambers has been presented in the literature by several authors. Culick analysed the non-linear behaviour of acoustic waves [181, 182]. His special interests were the non-linear growth and limiting amplitudes of the waves. He also included surface combustion in the analyses. Comparisons between linear and nonlinear theories show that the linear theory can describe the frequency and the mode shape well [183]. To describe the amplitude of the oscillations and to model the combustion rate in a correct way, nonlinear theory is needed. In premixed combustion stabilized with a flame holder, it has been shown that significant oscillations in the heat release rate exist [183-185]. These studies all concern premixed combustion. For non-premixed combustion, the situation is different and the heat release rate is not necessarily unsteady [186]. The importance of the combustion in the premixed case is also illustrated by the existence of a critical fuel-air ratio above which self-excited oscillations occur [187]. The amplitude of the pressure oscillation increases with increasing fuel-air ratio (equivalence ratio) [188].

One reason for developing the type of models mentioned above has been to be able to control the oscillations, due to the risk of structural damage caused by the oscilla-

tions, but also to develop clean, quite, efficient, and highly performing combustors [189-199].

One type of pulse combustor that can be of special interest when comparing with the pulsations in the tunnel is the Rijke type pulse combustor or the Rijke tube. Rijke found in 1859 that if a piece of gauze was placed in the lower half of a wide vertical tube and heated either by a Bunsen flame or an electric current, a musical vibration started [200]. In the former case the sound disappeared after a few minutes, while in the case with the current the sound could be maintained indefinitely [168, 171]. The heat released from the gauze generates a periodic pulsation by the flow up in the tube. Rijke found that the maximum effect was achieved when the gauze was positioned one fourth of the length of the tube from its lower end. It is, however, possible to maintain oscillations also at other positions depending on the size of the flame [172]. Small flames must be inserted further than larger flames, into an air tube before they oscillate. The position and the size of the flame affects the pitch of the flame, and the pitches rise when the flame is moved further up/into the air tube [170, 172]. It has also been found that the frequency of the fundamental and the first harmonic can exist on the same time. Small flames have, on these occasions, been observed between the larger flames [170]. The physics of the Rijke tube has been analysed and described, both experimentally and theoretically, by several authors in the literature [201-213].

Thermoacoustic instabilities in relation to distributed combustion (still premixed) was presented by Finlinson et al. [214], who used a modified Rijke burner to study the effect of frequency, flame position, tube length, inlet gas composition, and energy balance on the acoustic growth rate. The temperature proved to be important and the acoustic driving forces depended on the acoustic mode shapes in relation to the flame and distribution of energy.

The mentioned phenomena are usually called thermoacoustic instabilities. The pulsations during the Runehamar tests were not acoustic in that sense that they were audible (the oscillation periods were too long). The excitation and behaviour of the oscillations seem, however, to be very similar and therefore it can be of interest to study these thermoacoustic instabilities in more detail.

Matveev presented a thorough analysis of the thermoacoustic instabilities in the Rijke tube, both experimentally and theoretically [215]. He showed the importance of the characteristics of the heat transfer from a heat source to the flow. The position for the heat source most favourable for exciting the thermoacoustic instability is near one fourth of the tube length from the upstream end of the tube. Actually, to excite the first acoustic mode, the heat source needs to be somewhere in the upstream half of the tube. Most studies on the Rijke tube are related to the first mode and the vast majority of the studies have been performed with the heat source one fourth of the length of the tube, from the upstream end. However, even higher acoustic modes can be excited, but then the favourable regions for the heat source are different. The energy levels needed to excite the higher modes are also higher than for the fundamental mode.

The main reason for the thermoacoustic instability is a component of the heat release that oscillates in phase with the pressure perturbation (*c.f.* the Rayleigh's criterion

above), i.e. a phase difference less than 90°. Since the heat transfer rate for several scenarios has been shown to be a function of the velocity perturbations, with a certain time delay due to the inertia in the heat transfer process, it is possible for a situation to occur where the Rayleigh's criterion is fulfilled, i.e.:

$$\int_{\tau} p'(t) \dot{Q}'(t) dt > 0 \quad (5.18)$$

The stability of a specific excitation mode is determined by the net difference between the energy input to the mode and the acoustic losses. An important part of the process is the energy transfer to the flow, which can be described by a heat transfer function, Tr :

$$\frac{\dot{Q}'(t)}{\dot{Q}} = Tr \frac{u'(t)}{\bar{u}} \quad (5.19)$$

The absolute value, $|Tr|$, and the phase, φ , of the energy transfer function are of special interest and are discussed further below.

The form of the heat transfer functions depends on the system studied. Dowling presented a heat transfer function for a case of premixed combustion behind a bluff-body flame holder [183], based on a work by Bloxsidge *et al.* [185]:

$$Tr = \frac{1}{1 + i\omega\tau_1} e^{-i\omega\tau_2} \quad (5.20)$$

where

$\tau_1 = 2\pi r_B (1 - \alpha) / \bar{u}$, $\tau_2 \propto (L - b) / \bar{u}$, r_B is the radius of the flame holder, α is the blockage ratio of the flame holder, L is the length of duct, and b is the distance between the choked inlet and the flame holder. This relationship seemed to give too high amplitudes at high frequencies and therefore the following equation was developed [183]:

$$Tr = \frac{1}{(1 + i\omega\tau_1)(1 + i\omega\tau_3)} e^{-i\omega\tau_2} \quad (5.21)$$

where

$\tau_1 = 5r_B (1 - \alpha) / \bar{u}$, $\tau_2 = 0.4(L - b) / \bar{u}$, and $\tau_3 = r_B (1 - \alpha) / \bar{u}$. A non-linear theory can estimate the limit cycle, amplitudes and spectra. The non-linearities arise due to the relationship between the heat release rate and velocity fluctuations at the flame holder. The authors noticed that if the fuel-air ratio was increased, the damping factor decreased, the flame became less stable, and the amplitude gradually increased. Dowling later developed this model and gave expressions for τ_1 and τ_3 as functions of the radius of the flame holder, the radius of the tube, the flame speed, and the gas flow velocity [187]. The time delays involved in thermoacoustic instabilities can be

associated with different factors, e.g. the convection time for the fuel to reach the flame zone, combustion kinetics, turbulent mixing, and the inertia of the combustor [216].

The structure of the transfer functions are similar to the functions arrived at in automatic control engineering and the problem and systems can be represented by different parts connected by loops (see Figure 5.2). This has been used in efforts to control the oscillations [190, 191].

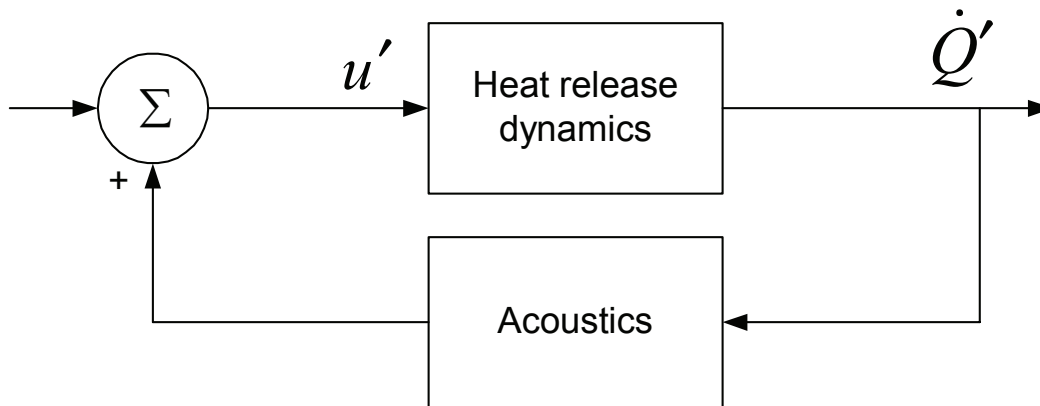


Figure 5.2 Schematic of a feedback loop representation of the thermoacoustic instability in a (premixed) combustion system (after Fleifil *et al.* [191]).

None of the heat transfer functions described above corresponds to a system representative of the tunnel fire situation; either the geometry or the heat release process (or both) differ in a significant way. However, all of the transfer functions include the velocity, indicating that the convective heat transfer is an important part. One explanation can be that the fractional change in velocity is much larger than the fractional change in pressure and temperature. This explains the dependence on the mass flow rate (see Figure 5.3)

Since the ventilation in the Runehamar tests was not varied (except for the decrease in velocity during the most intense part of the fire), no heat transfer function has been developed for the tunnel case; but this could be an important area of research in the future. It is, however, recognized that the rather constant level of heat release rate needed to start the oscillation in the Runehamar tests (see Paper V and Paper VI), is in accordance with the behaviour suggested by the heat transfer functions, i.e., the transferred energy needs to overcome the acoustic losses (radiation at the tube ends and losses at the walls).

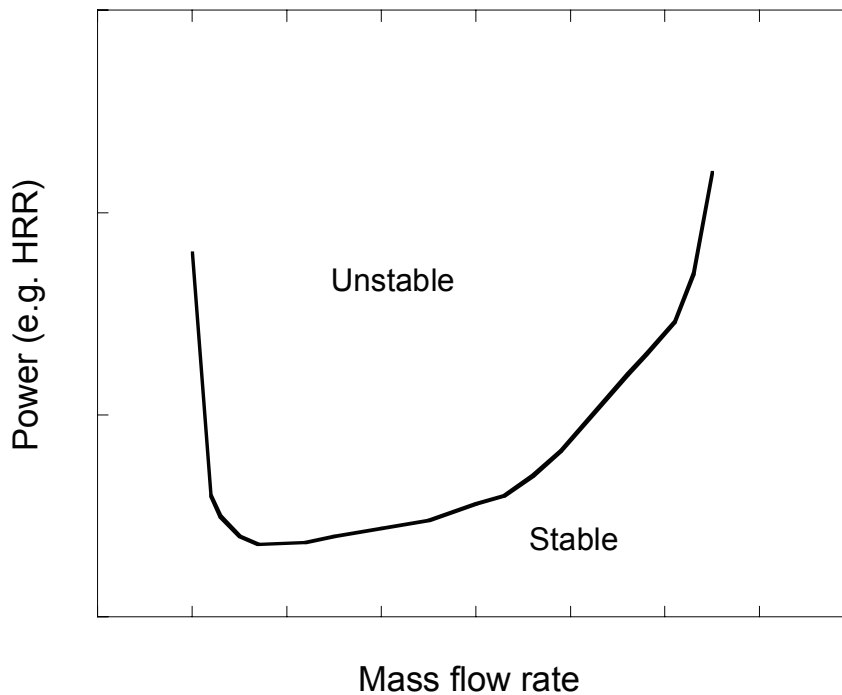


Figure 5.3 Example of stability limit (after Matveev [215]).

In Figure 5.3 an example of a stability limit is given. The stability limit indicates in what region of mass flow rate and power (in the power-mass flow rate graph), the system becomes unstable. As can be seen in the figure, in this example (heated wire in an air flow in a Rijke tube) there is a lower and an upper limit outside which the system always seems to be stable, independent of the power. Qualitatively the lower limit has been explained in that oscillations have not been observed for flow rates lower than what is necessary to maintain a turbulent air flow in the tube [201].

The figure should be seen as an example of the shape of the stability limit and Matveev showed that the shape depends on the position of the heat source in the tube, which affects which mode is excited. Furthermore, higher power is needed to excite higher harmonics. This can be explained by the heat transfer function. In the function used by Matveev, developed for flow around a heated wire and described by Kwon and Lee [205], the function is zero when the mean flow rate is zero and for higher mean flow rates the phase shift is such that the thermoacoustic instability is not encouraged. This gives rise to curves of the shape presented in Figure 5.3. Similarly, the transfer function given by Kwon and Lee is dependent on the frequency. Therefore, the heat transfer function has different values for the different modes. Considering both the thermoacoustic energy added to a certain mode, n , and the acoustic losses (sound radiation from the open ends and losses due to the acoustic boundary layer), a value for the critical power needed for transition to instability can be calculated [215, 217]:

$$\dot{Q}_{cr,n} = \frac{\dot{m}(\pi c P L \sqrt{\omega_n} (\sqrt{\nu} + (\gamma - 1)\sqrt{\alpha}) + \sqrt{2} \omega_n^2 A^2)}{\sqrt{2}(\gamma - 1)\pi |Tr_n| A \sin(\varphi_n) \sin(2k_n x_h)} \quad (5.22)$$

where c is the speed of sound, P is the perimeter of the cross section, L is the length of the tube, ν is the kinematic viscosity, α is the thermal diffusivity, A is the cross-sectional area, γ is the specific heat ratio, $k_n = \omega_n/c$ is the wave number, and x_h is the position of the heat source (measured from the tube inlet). The phase shift, φ_n , is less than $\pi/2$ and therefore the sign of the expression is defined by $\sin(2k_n x_h)$ and this thereby defines the regions where instability is favoured. In Figure 5.4, the regions for heat addition favourable for the first three acoustic modes are shown.

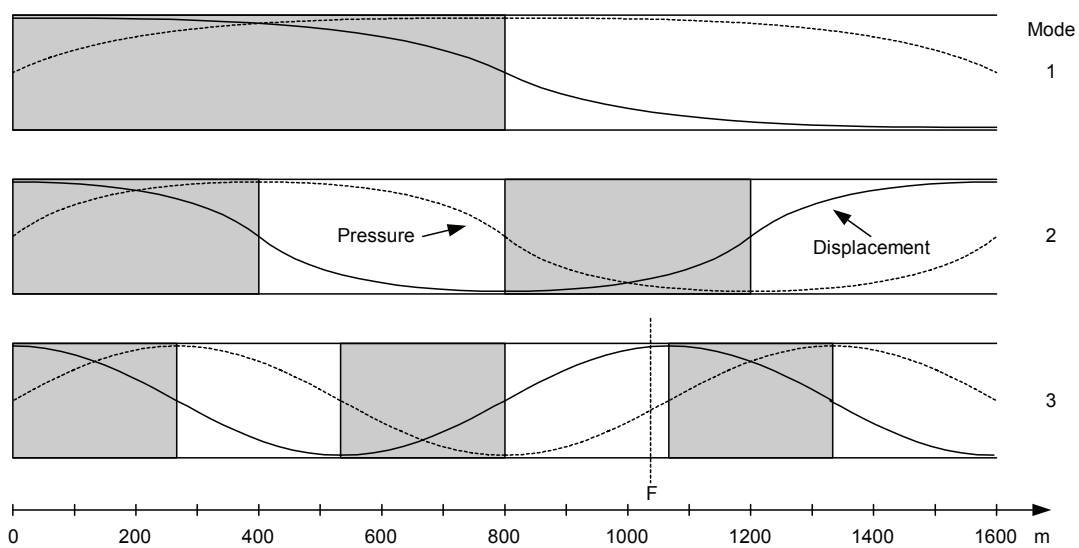


Figure 5.4 The figures represent the amplitude for the first three modes of oscillations in a tube (the top one is the fundamental). The length scale of the Runehamar tunnel is included for comparison. The vertical dashed line (F) represents the position of the centre of the fire during the tests in the Runehamar tunnel. The shadowed areas indicate regions favourable for instability for each mode.

There are a number of factors and conditions in the Runehamar tests that differ from the original conditions for which Equation (5.22) was developed. The main differences are the different mechanism of heat release (intense fire compared to controlled electrical heating), the distributed area of heat release rate, non-uniformities over the cross-sectional area (regarding the temperature, heat release, and the geometrical obstruction of the flow), backlayering resulting in upstream heating of the gases, the tunnel not being a smooth, straight, and horizontal pipe, etc. Several of these conditions also vary with time since the fuel is consumed and both the mass and the volume of the set-up decrease with time. It is still, however, interesting to compare the conclusions drawn from Eq. (5.22) with the results in the Runehamar tests, presented in Paper V and VI.

In the first two fire tests, T1 and T2, a pulsation inside the tunnel was experienced during a time period when the HRR was higher than approximately 125-135 MW

(see Paper V). This created a pulsating flow situation at the measuring station, where the measurements showed that the maximum velocity was pulsating in the range of 3 m/s to 4.2 m/s down to a minimum in the range of 1.5 m/s to 3 m/s.

The periods of the different pulsations during the fire tests are summarized in Table 5.3. For the upstream measurements during T1 and both upstream and downstream measurements during T2, one can notice a short oscillation period between 4 and 5 seconds (median very close to 4 s) and a longer period around 18 s.

Table 5.3 Periods of the oscillations registered during T1 and T2 in the Runehammar tunnel.

Oscillation ^a	Average period [s]	Median period [s]
T1 upstream short	4.84	4.02
T1 upstream long	18.33	18.06
T1 downstream ^b	-	-
T2 upstream short	4.47	4.08
T2 upstream long	17.72	17.64
T2 downstream short	4.49	4.08
T2 downstream long	17.57	17.4

^a Observe that the period of the long oscillations is measured from one maximum to the next and is actually half the modulation period (see Paper V).

^b The sampling period was longer in this case and is therefore left out of the analyses.

Two different methods have been used to explain the observed periods of oscillations: an acoustic approach (see Paper V) and a frequency analysis based on an impedance approach (see Paper VI).

In the acoustic approach the shorter oscillation period was shown to be close to the first two harmonics (4.74 and 3.16, respectively) of a tube of the same length as the tunnel. The longer period was explained as a beat phenomenon. Using the periods of the second and the third mode (4.75 s and 3.16 s, respectively) would give $\bar{T} = 3.8$ s and $T_b = 9.4$ s. The average period is close to the observed one, while the period of the beat is further away. However, a small change in the original waves can give a significant change in the resulting period due to the difference in the denominator. If the observed periods are assumed to be $\bar{T} = 4$ s and $T_b = 18$ s, then one can calculate the periods of the original waves to be 4.5 s and 3.6 s, respectively. Also the characteristics of the time resolved signal indicated a beat phenomenon. The details are given in Paper V.

In order to obtain more detailed information about the phenomenon, a frequency response analysis of a tunnel system, represented by impedances, has been performed. The different parts of the tunnel were assigned impedances and equations developed for unsteady flow were used to study the tunnel as a system in more detail than was done in the acoustic analysis. The equations are used together with a frequency response analysis where it is assumed that a forced vibration takes place in the tunnel, even if the excitation source of the vibration is unknown. The analysis follows the impedance approach described by Wylie and Streeter [218]. Three differ-

rent cases were analysed: I) constant inlet pressure and small disturbance at the fire; II) constant outlet pressure and small disturbance at the fire; and III) constant inlet pressure and small disturbance at the outlet. All cases showed resonance peaks, with different periods for the different cases. Most similar to the experimental results were the cases with constant pressure at the inlet. The case with disturbance at the tunnel outlet gave results very close to those registered during the fire tests (see Paper VI).

The oscillations start when the heat release rate increases above a certain value (between 125 and 135 MW). This situation has not been modelled quantitatively, but is similar to the condition shown in Figure 5.3 with a stability limit dependent on the heat release rate (heat transfer rate) and the mass flow rate. This supports the suggestion that the pulsations can be regarded as thermoacoustic instabilities. This can be explained also by Figure 5.4 where it can be seen that the seat of the fire was almost in the centre of the region favourable for excitation of the second mode of oscillation. The seat of the fire was also close to the region favourable for excitation of the third mode of oscillation. Keeping in mind the long flames and extended region of combustion it could be possible to make the third mode unstable.

The frequency of the oscillation can be affected if the heat input is distributed over a region and cannot be considered to be concentrated [186]. However, this effect is not significant if the flow rate or the mean temperature ratios (between temperature after and before heat input) is low.

The temperatures along the tunnel were measured during the tests and a model of the distribution of the average temperature over a cross-section along the tunnel has been presented (Paper VII). More temperature measurements would, however, be needed near the fire to fully describe the conditions there. The assumption of uniform conditions over the cross-section is not valid. The parameter most difficult to derive is, however, the transfer function for heat in the system. This is a complex function of the velocity and frequency, and includes information on the thermal inertia and therefore the information on the amplitude and phase needed to determine the stability boundaries of the system when different parameters are varied, e.g. the mass flow rate. Despite this, it is believed that the results and discussion presented in this section provide insight into the pulsations and important factors controlling them.

6 Gas concentrations in the tunnel

The reason for fatalities in fires is most often due to inhalation of fire gases. In several of the catastrophic fires presented in Table 2.1, people were found dead in their cars. Increased temperature can, however, affect both the physical health and the capacity to escape. Among the fire effluents, carbon monoxide (CO) is seen to be the most important component responsible for causing fatalities, even if the effect of hydrogen cyanide (HCN) has been much discussed during recent years [219-222]. In a comprehensive review, Nelson showed that even if high blood concentrations of HCN were found in fire victims, most fatalities can be explained by the CO concentration [223]. Therefore, the influence of ventilation in Section 6.2 will focus on CO and the CO/CO₂ ratio. In Section 6.3, however, HCN will be included in the analyses. Furthermore, carbon dioxide (CO₂) has an important affect, both by being toxic at high levels, but mostly by increasing the uptake of other fire gases, e.g. CO, due to increasing the breathing rate. This is also discussed in Section 6.3.

Even if fire gases do not always lead to fatalities, sublethal effects, e.g. incapacitation, reduced egress speed, reduced motor capability, decreased mental acuity, and visual obscuration are also important [224]. Further, many effluents can cause long-term or chronic effects, which is of particular importance for fire fighters and rescue personal.

In the design of tunnel ventilation, even the ventilation of gases (e.g. CO) in a non-fire situation is an important issue. For a description of the procedure see for example reference [144].

Another issue becoming increasingly important in the context of fire emissions is the effect on the environment and emissions which may pose potentially long-term hazards to health. Some of these issues will be discussed in Section 6.1 even if they have not typically been considered to be central issues for fires in tunnels.

6.1 Emissions from fires

There are a number of reports and papers on the issue of fires and the environment. Some of them present summaries of emissions from common materials or types of fires [225-227], while others focus on emissions from fires in a more general sense or present results from single fires that have had a large impact on the environment [228-230].

The analysis of the smoke gases from an automobile fire showed that emissions with a potentially negative impact on the environment, or humans, are produced in significant concentrations (see Paper IV). Three separate, full scale fire tests were performed under SP's industry calorimeter: a fire ignited and developed in the engine compartment; a fire ignited inside the vehicle that was extinguished in the early stages; and a similar fire ignited inside the vehicle that was allowed to spread until the entire vehicle was involved in the fire. Both fire gases and run-off water were analysed.

The emissions included HCl, SO₂, VOCs (e.g. benzene), PAHs, and PCDDs/PCDFs. Sources of chlorine in the vehicle for production of HCl and PCDDs/PCDFs included, most probably: upholstering materials, dash board components and electrical wirings, as indicated from the small-scale experiments conducted on selected materials from an automobile similar to that used for the full scale automobile fire.

Aldehydes and isocyanates were also found in the smoke gases, both compounds with well-documented short-term and long-term effects on humans. Other toxic compounds included: HCN and SO₂. These compounds have a direct effect on people and are of concern for rescue personal and others exposed to smoke from vehicle fires. The health effects, especially time to incapacitating dose for some of the gases, are further discussed in Section 6.3.

The particles emitted from the fire had a particle size distribution with a high number of particles with a diameter below 1 µm. Such small particles can be transported far from the location of the fire and are respirable, implying that the bodies defence system against particles (in the nose and throat) cannot provide adequate protection. Analysis of the content of the fire-generated particles revealed that these contained high concentrations of zinc, lead, and chlorine.

Analysis of extinguishing water showed that this was severely contaminated, containing elevated levels of both organic compounds and metals. Comparison with data from other vehicle fires found in the literature showed that contamination of lead, copper, zinc, and antimony appear to be significant in water run-off from these types of fires.

Within the EUREKA project EU499 (FIRETUN) [54] the release of PCDD/Fs and PAHs were analysed in connection with some of the tests: an old car (1974), a new car (1988), a German subway carriage, and a Deutsche bahn wagon with a steel body and a modern InterCityExpress (ICE) interior [231]. The release into the tunnel was estimated by using 1 m² passive collectors (cotton and steel, respectively) and active sampling at different positions along the tunnel. In addition, the fire residue was analysed. In Table 6.1 the releases of PCDD/F and PAH into the tunnel from the different vehicle fires are summarized. To better compare the results with results from other tests the values have been normalized relative to the energy content of each vehicle. The results show that the PCDD/F from the subway carriage and the ICE-wagon are similar and that these results are approximately one order of magnitude larger than those from the cars. Corresponding values obtained in the car fires reported in Paper IV were 0.023 mg I-TEQ/GJ (0.0868 mg I-TEQ in total) for PCDD/F and 31.3 g/GJ (119 g in total) for PAH, i.e. almost an order of magnitude higher than for the cars reported by Wichmann. Apart from actual differences in production between the tests, there are two other possible explanations for the differences. There might be a higher collection efficiency in the tests performed beneath the industry calorimeter. There is also a difference in how the total energy was calculated. In the case of the EUREKA tests, the energy content was estimated from the composition of the fuel load, while in the test presented in Paper IV the total energy was calculated from the heat release measurements. This latter difference is, however, relatively small. A comparison with the integrated values available for the subway carriage and the ICE-wagon [75] show that the estimated total energy content is

approximately 10 % higher than the integrated HRR value for the subway carriage and approximately 30 % higher for the ICE-wagon .

Table 6.1 Emissions of PCDD/F and PAH from vehicle fires in a tunnel and PCDD/F found in the fire residue [231]. The values are divided by the energy content.

Vehicle	Q_{tot}	Fire residue PCDD/F		Tunnel PCDD/F		Tunnel PAH	
		mg I-TEQ	mg I-TEQ/GJ	mg I-TEQ	mg I-TEQ/GJ	g	g/GJ
Old car	6	0.012	0.002	0.032	0.0053	13	2.2
New car	9	0.008	0.00089	0.044	0.0049	27	3.0
Subway carriage	41	0.54	0.013	2.0	0.049	NA	NA
ICE-wagon	77	1.1	0.014	9.2	0.12	NA	NA

The effect of the ventilation on the production of various chemical compounds is presented in Paper III. How this is related to the conditions in a tunnel, and to results from tests performed in tunnels, is discussed in the next section.

6.2 Influence of ventilation on the gas composition

The ventilation is an important means to affect, and hopefully improve, the conditions in a tunnel. Longitudinal ventilation can improve the conditions upstream of the fire significantly, making it possible for the rescue service to reach the fire. It is, however, important to remember that the situation downstream of the fire can be exacerbated by the ventilation. In Norway, at least at some places, the ventilation is used as a part of the fire fighting tactics where in case of fire the ventilation is used in a pre-defined direction [232]. Two reasons in particular are given for this methodology: first, the fire fighters know in advance the ventilation direction in the tunnel and thereby what portal to attack the fire from, and second, the conditions downstream of the fire are assumed to be of no danger to people being in this part of the tunnel, due to dilution of the fire gases. This strategy is partly based on the results from the experiments with two passenger cars in the Byfjord tunnel in 1998 and the Bømlafjord tunnel in 2000. These results showed that downstream of the car fires, the concentrations of CO and NO_x were not life threatening [233].

In a Swedish study concerning the heat release rate from tunnel fires, the ability of the rescue service to rescue people from the tunnel and to attack the fire, and the possibility for people to escape from a tunnel fire showed that the two main effects of longitudinal ventilation on the conditions during a tunnel fire is an increase of the growth rate of the fire and an increased dilution of the gases [84].

A parameter commonly used to describe the ventilation conditions during a fire is the equivalence ratio, ϕ , defined as:

$$\phi = \frac{\dot{m}_{fuel} / \dot{m}_{oxygen}}{(\dot{m}_{fuel} / \dot{m}_{oxygen})_{stoich.}} \quad \begin{array}{ll} \phi = 1 & \text{stoichiometric combustion} \\ \phi < 1 & \text{well ventilated combustion} \\ \phi > 1 & \text{under-ventilated combustion} \end{array} \quad (6.1)$$

where \dot{m}_{fuel} is the mass loss rate of the fuel and \dot{m}_{oxygen} is the mass flow rate of oxygen and the subscript “stoich.” refers to these values under stoichiometric conditions. Thus, in Eq (6.1), ϕ is defined as the quotient of the actual fuel/oxygen ratio and the stoichiometric fuel/oxygen ratio.

Different terms are used for the different ventilation conditions that can be attained in a fire situation. The situation when more air (oxygen) is available than is needed for stoichiometric combustion is referred to as over-ventilated, well ventilated, fuel-lean, or fuel-controlled. If insufficient air is available for stoichiometric combustion the situation is termed under-ventilated, vitiated, fuel-rich, or ventilation-controlled. In this thesis the terms well ventilated and under-ventilated, respectively, are mainly used and are related to the whole system. Even under well ventilated conditions the geometric conditions and flow pattern can be such that fresh air does not reach the combustion zone. Such a situation is here referred to as vitiated or locally under-ventilated.

In cases where the spatial variation either can be assumed to be small or when it is difficult to resolve the variations, the overall combustion process is often studied instead. In such cases ϕ can be defined in a more general sense using the equivalence ratio for the total combustion process. This is usually referred to as the global equivalence ratio, GER. Originally, this was defined as the ratio of the mass of gas in the upper layer in an enclosure derived from the fuel divided by that introduced from air, normalized by the stoichiometric ratio [234]. Beyler, who was the first to correlate the species concentrations in the upper layer with the equivalence ratio, used a variant called the plume equivalence ratio defined as the ratio of the fuel volatilization rate to the air entrainment rate, normalized by the stoichiometric fuel to air ratio [235-237]. In the work presented in Paper III, the definition of the GER is the ratio between the mass loss rate of the fuel and the mass flow of oxygen entering the combustion room normalised by the stoichiometric ratio.

In order to measure the GER in the two different test room in Paper III, a device called “the phi meter” [36, 238], was constructed. The essential parts of the phi meter are the combustor, into which the fire gases and additional pure oxygen are introduced, and the O₂ analyser. Complete combustion of the fire gases is achieved in the combustor by the high temperature (1000 °C was used in these specific tests) and by using a platinum catalyst and additional oxygen. The readings on the O₂ analyser are compared with background measurements without fire gases through the phi meter. A simple computation gives the equivalence ratio. The instrumentation and the calculations needed to conduct the measurements of the equivalence ratio are described in detail in Paper III.

There are not many cases reported on measured under-ventilation in tunnel fires. Most reported cases can probably be said to be either fuel controlled or ventilation

controlled (e.g. see [5]). The latter correspond to a case where limited ventilation leads to a decrease (or control) in the fire size, but if the temperature is high a continuous mass loss can lead to under-ventilated combustion. Among the large-scale fire test series, the one in the Ofenegg tunnel is an obvious example of the effect of the ventilation (see Section 5.2), but that case was also rather special due to the blockage in one end of the tunnel.

Ingason performed fire tests in a model tunnel (1.08 m × 1.2 m × 10.96 m) to study the effect of the ventilation on the fire behaviour [42, 43]. Under-ventilated conditions were of special interest and both natural ventilated and forced ventilated scenarios were studied. In the first case the fire size and the size of the inlet opening were varied, while in the latter case the fire size and the flow rate of incoming air were varied. The author describes the difficulty in achieving under-ventilated condition. The transition to such conditions is highly dependent on the temperature and the thermal feed-back to the fuel. This was also seen in the test series described by Lönnemark *et al.* [132], where a case with 0.5 m² chlorobenzene (test CB3) gave a very slow developing fire inside a room. The fire reached high temperatures and under-ventilated conditions first after approximately 35 min. Increasing the pool size to 0.8 m² (test CB4) gave a significantly different fire development with much higher temperatures and under-ventilated conditions after approximately 6 minutes. This illustrates the importance of the fire size. In a tunnel with ventilation, the flame tilt also influences the thermal feed back and thereby the mass loss rate.

In the test series presented by Ingason some of the tests, however, became under-ventilated. Gas composition (CO, CO₂, and O₂) was analyzed at three different heights (0.15 m, 0.5 m, and 0.9 m below the ceiling), 4.5 m downstream of the centre of the fire, which was situated 1.5 m from the tunnel entrance. In most of the tests the $\Delta\text{CO}/\Delta\text{CO}_2$ -ratios were rather similar at the different sampling heights. The ratio was, however, often somewhat higher in the highest position (0.15 m below the ceiling) during some period of the tests. In a few cases the $\Delta\text{CO}/\Delta\text{CO}_2$ -ratio was highest in the lowest position (e.g. in test 2 and test 8). In Figure 6.1 the $\Delta\text{CO}/\Delta\text{CO}_2$ -ratios for heptane pool fires are presented as a function of the equivalence ratio. The values were chosen to be representative values for the position with the highest $\Delta\text{CO}/\Delta\text{CO}_2$ -ratio at the selected time. Note that Ingason used an equivalence ratio based on the air to fuel ratio, while throughout this section all equivalence ratios (including those presented in Figure 6.1) are based on fuel to air ratios. Two different cases are represented in the figure: natural ventilation and forced ventilation. The values of the $\Delta\text{CO}/\Delta\text{CO}_2$ -ratios were determined at the time when the mass loss rate was at its maximum for each test. For the natural ventilation an exponential curve fit is included. It fits the data points very well, but due to the limited number of points it should be seen as an illustration.

The points for the forced ventilation show a pattern different from the natural ventilation case. All cases are well ventilated, but the point at $\phi = 0.89$ shows features of under-ventilation. This could have two possible explanations. There are studies that indicate that the CO production starts to increase well below $\phi = 1$, at $\phi \approx 0.6$ (see e.g. [234, 235]). Another explanation could be the flow pattern around the fire during forced ventilation. The experimental results, especially the O₂-measurements, show a significant gradient with height, which indicates that even if the

tunnel is well ventilated it could be locally under-ventilated in the combustion zone. The three-dimensional flow typically found close to the fire in a tunnel was illustrated by Ingason, showing the main ways for the flows of different density [239].

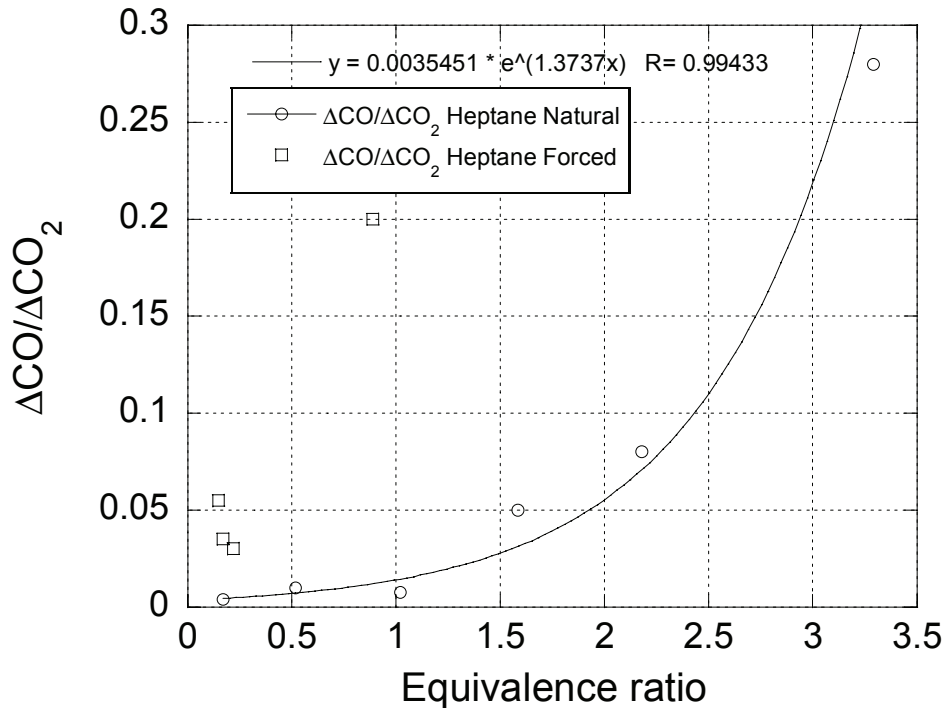


Figure 6.1 $\Delta\text{CO}/\Delta\text{CO}_2$ -ratio as function of equivalence ratio for heptane pool fires performed by Ingason [42, 43]. The results are given both for natural ventilation and for forced ventilation. Included for illustration is an exponential curve fit of the natural ventilation data. It is, however, based on only six data points.

The results from the experiments with xylene and methanol are summarized in Table 6.2. Compared to the experiments with heptane pool fires presented in Figure 6.1, xylene results in high values and methanol in low values of $\Delta\text{CO}/\Delta\text{CO}_2$ -ratios. This is in line with the results of Beyler showing that oxygenated hydrocarbons produce small amounts of CO (expressed as yield) at low equivalence ratios [235]. Aromatics (Beyler used toluene) on the other hand, produce a rather constant CO yield independent on the equivalence ratio; only a small increase was reported. This means that aromatics at low equivalence ratios produce relatively high CO yields and at high equivalence ratios produce relatively low CO yields. The variation in $\Delta\text{CO}/\Delta\text{CO}_2$ -ratio with equivalence ratio presented in Table 6.2 might be explained by a decrease in CO_2 production.

Table 6.2 $\Delta\text{CO}/\Delta\text{CO}_2$ -ratio as function of equivalence ratio for xylene and methanol pool fires performed by Ingason [42, 43].

Fuel	Ventilation	Fire size [m ²]	Opening [m ²]	ϕ	$\Delta\text{CO}/\Delta\text{CO}_2$
Xylene	Natural	0.3 × 0.3	0.3 × 0.3	0.37	0.20 (0.38) ^{a)}
Xylene	Natural	0.3 × 0.3	0.15 × 0.15	1.01	0.30 (0.41) ^{a)}
Xylene	Natural	0.3 × 0.3	0.1 × 0.1	1.94	0.36 (0.43) ^{a)}
Xylene	Natural	0.3 × 0.3	0.2 × 0.2	0.70	0.23 (0.31) ^{a)}
Xylene	Forced	0.3 × 0.3	0.2 ($\phi=0.5\text{m}$)	0.15	0.15 (0.26) ^{a)}
Methanol	Natural	0.4 × 0.4	0.6 × 0.6	0.04	0.003-0.035 ^{b)}
Methanol	Forced	0.4 × 0.4	0.2 ($\phi=0.5\text{m}$)	0.02	-0.01 – 0.02 ^{b)}

- a) The $\Delta\text{CO}/\Delta\text{CO}_2$ -ratio was highest in the beginning of the result period reported and then decreased; the maximum value (within parenthesis) is not used (see discussion of Figure 6.3) but instead something closer to a steady state value.
- b) The $\Delta\text{CO}/\Delta\text{CO}_2$ -ratio is varying significantly; therefore a range is given (including all the three heights).

Lönnermark *et al.* performed under-ventilated fire experiments in an enclosure (the ISO 5705 room: 2.4 m × 3.6 m × 2.4 m), where the size of the opening was varied [132]. Five different fuels were used: Polypropene, Nylon 66, Tetramethylthiuram monosulfid, 3-Chloro-4 nitro-benzoic acid, and Chlorobenzene. In Paper III results are given for CO and other components in the fire gases, and their dependence on the equivalence ratio. For comparison with the results from model scale tunnel tests presented in Figure 6.1, CO/CO₂-ratios have been calculated from tests in the enclosure fires [132]. Note that here absolute concentrations have been used and not changes from background values as in the case presented by Ingason.

In Figure 6.2 CO/CO₂-ratios for polypropene, Nylon 66, and chlorobenzene pool fires (polypropene and Nylon 66 were solid polymers in form of pellets) are presented as function of the equivalence ratio. For all three materials, results are presented for measurements both in the opening from the enclosure and in the exhaust duct connected to the hood collecting the fire gases. For illustration an exponential curve-fit for the results from the opening for polypropene is included. This fit seems to be qualitatively representative for the other cases also, even if there are differences between the materials.

The effect of combustion outside the opening during under-ventilated conditions can be seen for Nylon 66. This effect is also obvious for chlorobenzene. For heptane the CO/CO₂-ratio are rather similar in the opening and duct for most values of the equivalence ratios reported. From the figure it can be seen that when passing from well ventilated to under-ventilated conditions (passing the point $\phi = 1$), the CO/CO₂-ratios increases above approximately 0.05. This is comparable to the natural ventilated tests with heptane in the model scale tunnel performed by Ingason (see Figure 6.1). For the cases with forced ventilation the differences are larger. The explanations for this, besides differences between materials, were discussed above.

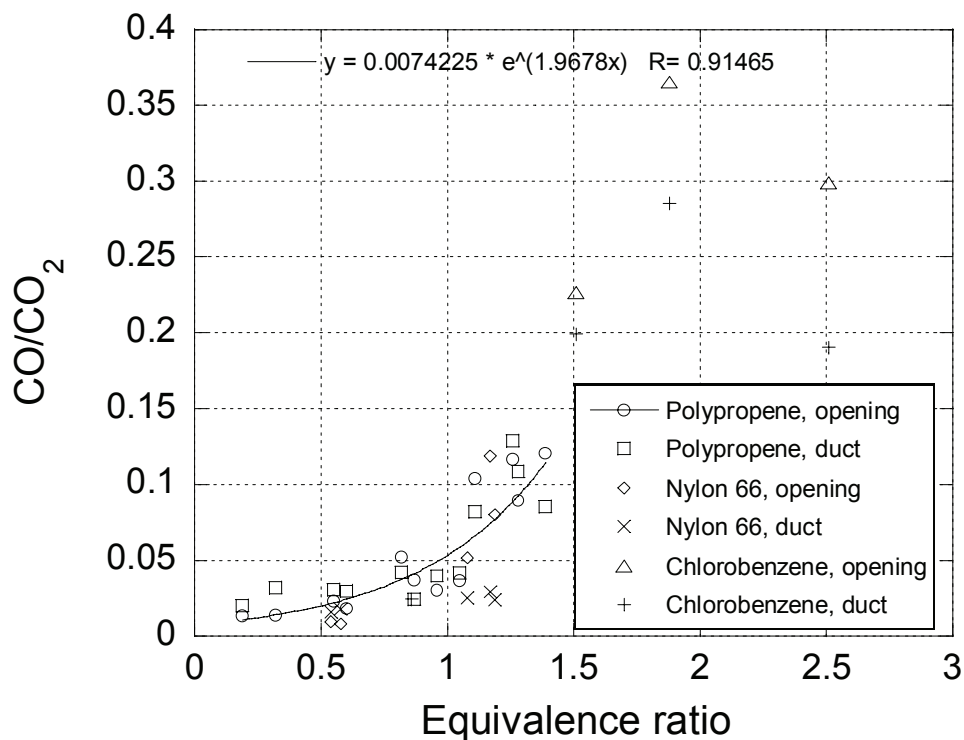


Figure 6.2 CO/CO₂-ratio as function of equivalence ratio for polypropene, Nylon 66, and chlorobenzene. For all three materials, results are given for measurements in the opening of the enclosure and in the exhaust duct connected to the hood collecting the fire gases. An exponential curve fit is included for polypropene (opening).

Grant and Drysdale presented analyses of CO and CO₂ for the EUREKA project EU499 (FIRETUN). The heat release rate calculations based on these measurements were presented above. The calculated CO/CO₂-ratios show that high values (maximum 0.2 30 m downstream of the fire and 0.13 100 m downstream of the fire) are obtained during the initial phase before the HRR starts to increase rapidly, i.e. when the fire spreads to the trailer. During the most intense part of the fire the CO/CO₂-ratios 100 m downstream stay below 0.02. At 100 m downstream of the fire the CO/CO₂-ratio are also approximately 0.02 or lower, but a clear increase during the period when the ventilation was switched off can be seen. The maximum value given is 0.05, but the peak value during this time period could be higher since values are missing for a few minutes. Comparing these results with those presented in Figure 6.1 and Figure 6.2 indicates under-ventilated combustion during this time period, which is understandable due to low ventilation during a period of high temperatures and probably high mass loss rates.

Similar results were found in the four Runehamar tests, i.e. high CO/CO₂-ratios during the initial phase of the fire and low values during the intense fire and the decay period (see Figure 6.3). The gas analyses (CO and CO₂) were performed at two different heights (2.9 m and 5.1 m respectively above the road surface), 458 m from the centre of the fire. Analyses of O₂ were also performed in these positions and at the height 0.7 m (see Paper II for detailed description of the measurement set-up and analysers). It can be seen from Figure 6.3 (in comparison with Figure 6.2)

that all the tests seem well ventilated. The high values at the beginning of the tests can be explained by incomplete combustion. The temperature in the combustion zone may have affected the results. It is known from fire experiments in compartments that both the residence time and the temperature in the upper layer are important factors for the production of CO [240]. Even for well ventilated conditions, high CO concentrations can be measured if the temperature is below approximately 800 K. The situation looks similar to the one called pre-flaming combustion described by Tsuchiya and discussed below [241]. The highest values (not shown in the figure) are also dependent on the absolute relationship between the CO and CO₂ analyses. A small difference in response time or time to reach a concentration above the detection limit, significantly affects the initial values. To better be able to compare the CO/CO₂-ratios with the HRR and the temperature measurements near the fire, the time scales in Figure 6.3 were corrected for the transport time between the fire and the measurement station. This transport time varies with the HRR and the procedure to calculate this is described in Paper II. The estimated transport time varies between 1.5 and 2.5 min depending on the HRR.

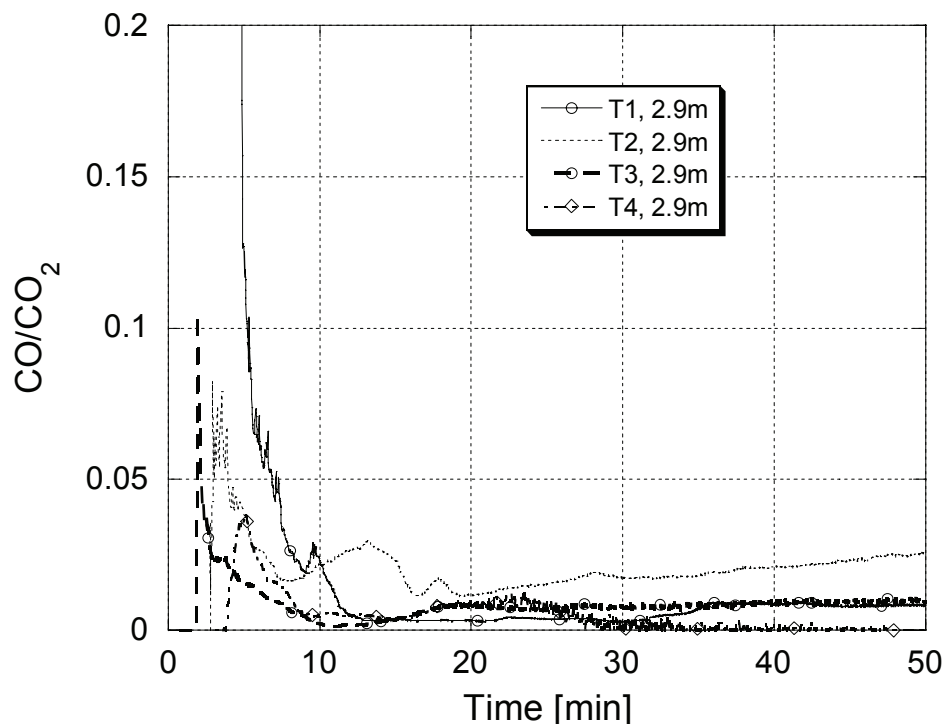


Figure 6.3 CO/CO₂-ratio as function of time for the Runehamar tests. The gas analyses were performed at 458 m from the centre of the fire, 2.9 m above the road surface.

The results from the Runehamar tests look similar to those reported by Bettis *et al.* [113] where the tests were well ventilated, apart from a short period during one of the tests. The CO/CO₂ ratios ranged, in most cases, from 0.005 to 0.025. In a few cases there was a higher value (0.05 - >0.1) in the beginning of the test followed by a continuous decrease. A steady state value as high as 0.05-0.06 was reported in only one test (Test 6). The fire was partly sheltered due to the set-up and this can have affected the local ventilation conditions.

During ventilated conditions in a tunnel, the situation at the fuel can be ventilation controlled or locally under-ventilated if the fuel set-up is such that the air flow does not reach the vaporized or pyrolyzed fuel. This was discussed in Section 5.2 and was also mentioned in relation to the initial period of fires discussed above. In Section 5.2 the effect of the local availability of oxygen on the decomposition rate was also briefly discussed.

Tewarson performed an extensive work on collecting data on yield of CO and CO₂, respectively, for different materials, and on how these yields depend on the equivalence ratio [35]. From the result he developed relationships of the ratio of actual yield to well-ventilated yield as function of equivalence ratio. Combining his results gives the following equation:

$$\frac{X_{CO}}{X_{CO_2}} = \frac{44 \left[1 + \frac{\beta}{\exp(2.5\phi^{-\xi})} \right] y_{CO,wv}}{28 \left[1 - \frac{1}{\exp((\phi/2.15)^{-1.2})} \right] y_{CO_2,wv}} \quad (6.2)$$

where y is the yield [g/g], β and ξ are correlation coefficients, and the index wv corresponds to well ventilated conditions. The values of the different parameters are given for four selected materials in Table 6.3. The CO/CO₂ ratio as a function of ϕ based on Eq. (6.2) is given for three materials in Figure 6.4. Polypropene was not included since it is almost identical to polyethylene. The curves diverge from each other, but for all three fuels the CO/CO₂ ratio at $\phi = 1$ is between 0.03 and 0.05

Table 6.3 Yields of CO and CO₂ during well ventilated conditions and values of correlation coefficients in Eq. (6.2) given for four materials [35].

Material	$y_{CO,wv}$ [g/g]	$y_{CO_2,wv}$ [g/g]	β	ξ
Polyethylene (PE)	0.024	2.76	10	2.8
Polypropene (PP)	0.024	2.79	10	2.8
Polystyrene (PS)	0.060	2.33	2	2.5
Wood	0.005	1.33	44	3.5

Different fuels utilize available oxygen at high equivalence ratios to very different extents. Beyler reported residual oxygen in exhaust gases from a hood system simulating the upper layer in a two-layer situation at $\phi > 1.2$ for different types of fuels [235]. These results are summarized in Table 6.4. There is a wide range in residual oxygen for the different fuels, from 0.1 % (methanol and ethanol) to 8.0 % (toluene). These values can be compared to the minimum oxygen concentration measured in each test in the Runehamar tunnel: 6.4 %, 8.6 %, 11.7 %, and 15.9 % for T1, T2, T3, and T4, respectively (values corrected for estimated H₂O concentration; see also Table 6.7).

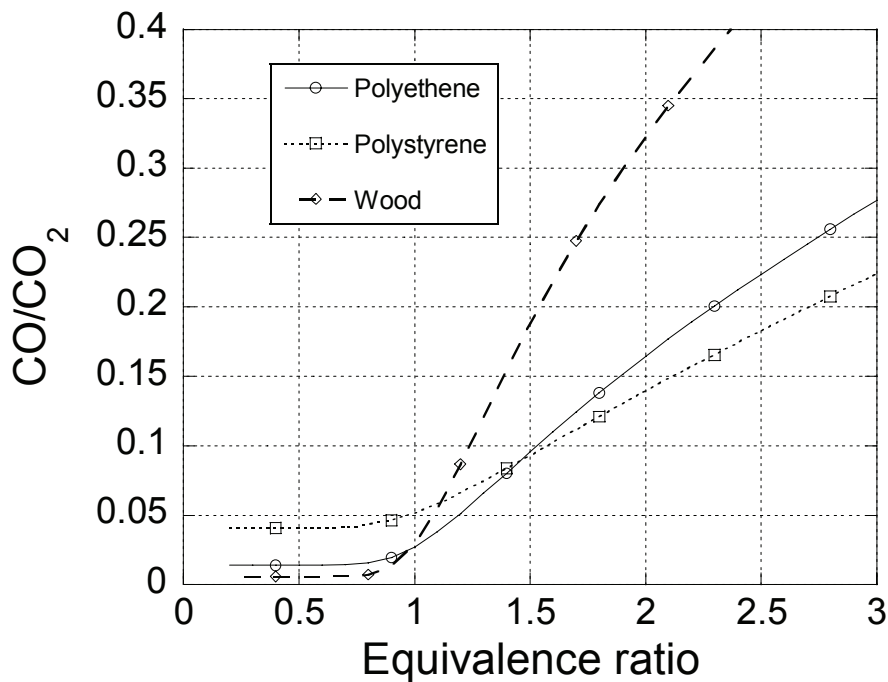


Figure 6.4 CO/CO₂ ratio for polyethene, polystyrene, and wood as a function of ϕ , based on the work by Tewarson (Eq. (6.2)) [35].

Table 6.4 Residual oxygen for combustion of different fuels at $\phi > 1.2$ [235].

Fuel	Chemical formula	Residual O ₂ [%]
Propane	C ₃ H ₈	0.5
Propene	C ₃ H ₆	2.0
Hexanes	C ₆ H ₁₄	3.0
Toluene	C ₇ H ₈	8.0
Methanol	CH ₃ OH	0.1
Ethanol	C ₂ H ₅ OH	0.1
Isopropanol	C ₃ H ₇ OH	2.0
Acetone	C ₃ H ₆ O	0.7

The CO/CO₂-ratio depends on the mode of combustion. For combustion of wood the combustion can be divided into three stages: 1) pre-flaming pyrolysis, 2) flaming combustion, and 3) char combustion or glowing [241]. Tsuchiya presented mean values of CO/CO₂-ratios for the three phases of combustion for plywood: 0.9 (pyrolysis), 0.0035 (flaming combustion), and 0.25 (glowing), respectively. In the discussion above, the mode of combustion has been considered to be flaming in all cases. There is an abrupt transition from pre-flaming pyrolysis to flaming combustion. Tsuchiya showed that this transition occurred when the O₂ concentration was higher than a certain value that depends on the incident heat flux according to:

$$C_{O_2} = 19.4 - 0.19 \cdot \dot{Q}'' \quad (6.3)$$

where C_{O_2} is the concentration of O_2 (in %) and \dot{Q}'' is the incident heat flux (in kW/m^2).

Modes other than flaming combustion will not be discussed further here. Tsuchiya also presented CO/CO₂-ratios for liquids and non-charring plastics under different levels of incident radiation in the cone calorimeter. Some selected materials of particular interest for the discussion in this section are presented in Table 6.5.

There are large differences between the different types of fuels. When ranking fuels according to their produced CO/CO₂-ratio (from low to high) they can be listed as alcohols and oxygen containing fuels, hydrocarbons, and finally aromatics. This order is valid for well ventilated conditions. For under-ventilated condition the ranking is reversed [235, 242].

Table 6.5 CO/CO₂-ratios for selected liquids and non-charforming plastics combusted in normal air in the cone calorimeter [241].

Material	Radiation [kW/m^2]	CO/CO ₂
Methanol	5	0.0002
Ethanol	5	0.0004
n-Heptane	5	0.010
Benzene	5	0.065
Xylene	5	0.056
Polypropene	30	0.024
Polypropene	50	0.025
Polystyrene	25	0.046
Polystyrene	40	0.051

6.3 Toxicity

In Sections 6.1 and 6.2, the importance of CO in determining the hazard posed by a fire, and the difference in production of CO in different situations, was discussed. In this section the effect on humans of CO and other important combustion gases will be quantified using the results from the Runehamar tests as an example.

A group of important gases in connection with a fire are the asphyxiant gases. These gases mainly affect the central nervous system and cause brain tissue hypoxia. The main gases within the asphyxiant group are CO and hydrogen cyanide (HCN), although low oxygen concentrations and high CO₂ concentrations will also be considered since these can have asphyxiant effects. The toxic effect of CO is due to its combination with haemoglobin in the blood to form carboxyhaemoglobin (COHb). In Table 6.6 health effects at different COHb concentrations in the blood are summarized.

The toxicity of CO and its relationship to COHb and effects on the oxygen-carrying blood capacity is well-known, but CO can have other adverse affects, e.g. interruption of energy production of cells, interference of oxygen delivery, and other cellular activities [223]. These latter effects are not as well understood or widely discussed as the binding of CO producing COHb, resulting both in the haemoglobin not being

able to transport as much oxygen and the oxygen being more tightly bonded to the haemoglobin. The values in Table 6.6 should be seen as examples and not as exact limits. A concentration of 50 % COHb is often taken as a threshold for lethality; Purser reports a range of 50 % to 70 % [222]. Nelson, however, reports that a larger variety can be expected and that the actual limit depends on the situation. A lower level and longer exposure can result in effects on the cellular processes and this can lead to fatalities at lower levels of COHb than if a person is subjected to shorter and higher exposures.

Table 6.6 Summary of health effects at different COHb levels [243].

COHb level [%]	Effect
10	Asymptomatic or headache
20	Dizziness, nausea, and dyspnea
30	Visual disturbance
40	Confusion and syncope
50	Seizures and coma
≥ 60	Cardiopulmonary dysfunction and death

While CO decreases the possibilities for the blood to take up, carry, and deliver oxygen to the tissues, HCN decreases the ability to use the oxygen delivered to the tissues [222]. The dynamics of HCN in the human body is, however, poorly understood and blood cyanide is not analysed as routinely as COHb. This is partly due to difficulties associated with the measurement of HCN in the blood of a fire victim and the decay of HCN levels in the blood after mortality. To date there is no standardised method to determine the concentration of HCN in the blood of fire victims, although work is underway within ISO TC92/SC3 to develop such a standard.

Low oxygen concentrations can cause hypoxia effects similar to those caused by CO and HCN. CO₂ affects the time to incapacitation in two ways. At low concentrations, CO₂ stimulates breathing, i.e. increases the breathing rate (RMV). This increases the uptake of other toxic gases. At high concentrations (above approximately 5 %) CO₂ becomes an asphyxiant. Its asphyxiant effect is, however, not additive to the effects of CO and HCN.

Irritant gases are important when determining the possibility for people to escape from a fire. These gases can be both inorganic (e.g. hydrogen chloride (HCl)) and organic (e.g. acrolein). The main effect is irritation of mucous membranes, e.g., in the eyes, upper respiratory tract, and to some extent the lungs. Another effect is that the gases can cause oedema and inflammation in the lungs, leading to death 6 to 24 hours after exposure [222]. No irritant gases were analysed during the Runehamar tests. Therefore, these gases are not discussed further here.

The smoke contains particles hazardous to health. The decreased visibility due to the smoke also influences the walking speed of the people trying to escape from a fire in a tunnel. Neither of these effects is discussed further in this thesis.

The focus in the following discussion will be the time to incapacitation (or partial incapacitation). The calculations are based on the expressions given by Purser [222]:

$$F_{I_{CO},n} = \frac{3.317 \cdot 10^{-5} \cdot Y_{CO,n}^{1.036} \cdot RMV \cdot (t_n - t_{n-1})}{I} \quad (6.4)$$

where F_I is the fraction of an incapacitating dose, $Y_{CO,n}$ is the concentration of CO (in ppm) during the time step, RMV is the breathing rate (25 L/min for light activity), $t_n - t_{n-1}$ is the length of the time step (min), and I is the COHb concentration at incapacitation (30 % for light activity).

$$F_{I_{CN},n} = \frac{t_n - t_{n-1}}{\exp(5.396 - 0.023Y_{HCN,n})} \quad (6.5)$$

where $Y_{HCN,n}$ is the concentration of HCN (in ppm) during the time step.

$$F_{I_{O_2},n} = \frac{t_n - t_{n-1}}{\exp(8.13 - 0.54(20.9 - C_{O_2,n}))} \quad (6.6)$$

where $C_{O_2,n}$ is the concentration of O₂ (in %) during the time step.

The fraction of an incapacitating dose for all asphyxiant gases (excluding effects of irritants), F_{IN} , can then be written (for a certain time step):

$$F_{IN,n} = (F_{I_{CO},n} + F_{I_{CN},n}) \cdot V_{CO_2,n} + F_{I_{O_2},n} \quad (6.7)$$

where

$$V_{CO_2,n} = \frac{\exp(0.1903C_{CO_2,n} + 2.0004)}{RMV_r} \quad (6.8)$$

is the multiplying factor for the enhanced uptake of asphyxiant gases (other than CO₂) due to induced hyperventilation, $C_{CO_2,n}$ is the concentration of CO₂ (in %) during the time step, and RMV_r is the resting RMV (7.1 L/min is used). The total fraction of an incapacitating dose is calculated as the sum

$$FI(t = t_N) = \sum_{n=2}^N F_{IN,n} \quad (6.9)$$

Since the asphyxiant effect of CO₂ is not additive to the effects of the other gases it is not included in Eq (6.7). However, the fraction of an incapacitating dose of CO₂ can be calculated separately as

$$F_{I_{CO_2},n} = \frac{t_n - t_{n-1}}{\exp(6.1623 - 0.5189C_{CO_2,n})} \quad (6.10)$$

In Figure 6.5 fractions of an incapacitating dose based on results from the Runehamar tests using the equations above are presented. The gas analyses were performed using an Uras 3G HCN gas analyser at the measurements station, 458 m from the centre of the fire. The measurement station is described in Paper II. Since some of the measurements are only available at the height 2.9 m above the road, all gas concentrations has been evaluated as this height. This is higher than the height representative for a person in the tunnel, but this choice was made to be able to compare the different contributions to the fraction of an incapacitating dose.

The HCN analyses are described by Brandt [244]. The HCN concentrations are affected with some uncertainties. The HCN concentration is, for example, below zero during different time periods in the tests T1, T3, and T4 (only positive values have been used in the calculations). Therefore, the total fraction of an incapacitating dose is given both with and without the effect of HCN. In Figure 6.5 the individual contributions of O₂ and CO, respectively, are presented separately. In the figure the fraction of an incapacitating dose due to the asphyxiant effect of CO₂ (Eq (6.10)) is also included. This effect is not additive to the effect of the other gases and is not included in the total fraction of an incapacitating dose. In Table 6.7 the extreme values of CO, CO₂, HCN, O₂, and *T*, respectively, are given for each of the Runehamar tests. Further details on the gas analyses performed in the tests in the Runehamar tunnel are planned to be published separately.

Table 6.7 Peak values for CO, CO₂, HCN, and *T* and minimum values for O₂ in the Runehamar tests. All values correspond to a position 2.9 m above the road, 458 m from the centre of the fire.

	T1	T2	T3	T4
CO _{max} [ppm]	1810	2430	491	741
CO _{2,max} [%]	11.7	9.2	6.7	3.9
HCN _{max} [ppm]	298	218	66	94
O _{2,min} [%]	6.4	8.6	11.7	15.9
<i>T</i> _{max} [°C]	137	97	79	76

In all cases the HCN concentration significantly affects the time to incapacitation ($F_1 = 1$), even if the effect is largest in test T1 and T2. In these tests, incapacitation is quickly reached (within a few minutes from the start of the increase). In all four tests, significant amounts of HCN were produced. HCN is formed in a fire during combustion of nitrogen-containing materials. In the Runehamar test series, the polyurethane mattresses in test T2 are the most obvious nitrogen source (analyses show 4.6 % (by weight) nitrogen). Further, the fuel was placed on particle boards in all the tests. The nitrogen content of these boards were not analysed, but a nitrogen content of the order of a few percent has been reported in other cases [245, 246]. Wood also contains nitrogen, but to a lower extent, 0.1 % to 0.2 % (by weight) [245, 247, 248]. The formation of HCN is affected by the combustion conditions. High

temperatures and under-ventilated or vitiated condition favour the formation of HCN [219, 249, 250].

Even without HCN included, incapacitating dose is reached fairly quickly, approximately five minutes after the start of the increase. It should be noted that the transport time is not subtracted, i.e. the time in the graphs is the time at the measurement station after ignition. For test T3 and T4 incapacitating dose was not reach for the time period studied. This does not mean that a person in the tunnel would not be affected. Purser suggests a value of $0.1F_1$ to ensure safe escape.

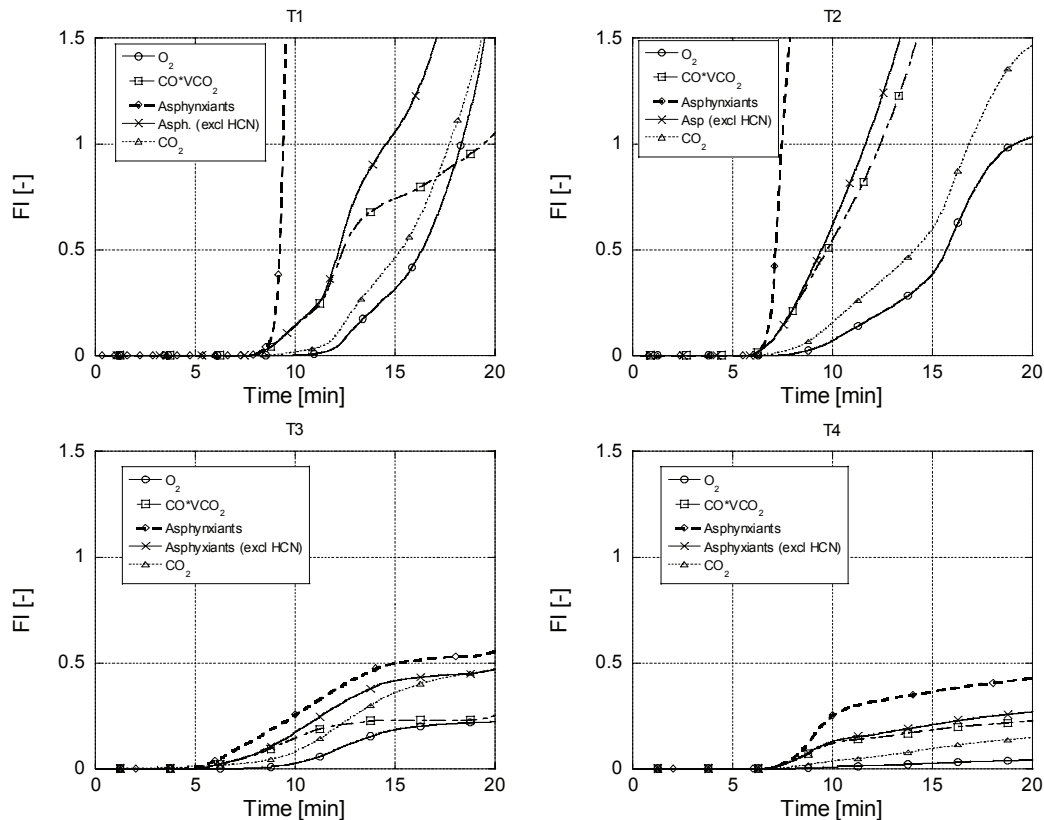


Figure 6.5 Fraction of an incapacitating dose for asphyxiant gases analysed during the four tests in the Runehamar tunnel.

So far the discussion has regarded the gas composition. However, the temperature (heat exposure) also affects an escaping occupant. The heat exposure can cause both incapacitation and death due to hyperthermia.

The tenability limit for radiant heat flux on skin is, according to Purser, approximately 2.5 kW/m^2 [222]. This level was never reached at the measurement station. For convective heat, Purser presents a relationship that is the same as the one for a unclothed or lightly clothed person according to ISO/TS 13571:2002 [251]:

$$F_{I_{conv_L},n} = \frac{t_n - t_{n-1}}{5 \cdot 10^7 T^{-3.4}} \quad (6.11)$$

where T is the gas temperature ($^{\circ}\text{C}$). In the ISO standard there is also an expression for exposure of convective heat for a fully clothed person:

$$F_{I_{conv_F},n} = \frac{t_n - t_{n-1}}{4.1 \cdot 10^8 T^{-3.61}} \quad (6.12)$$

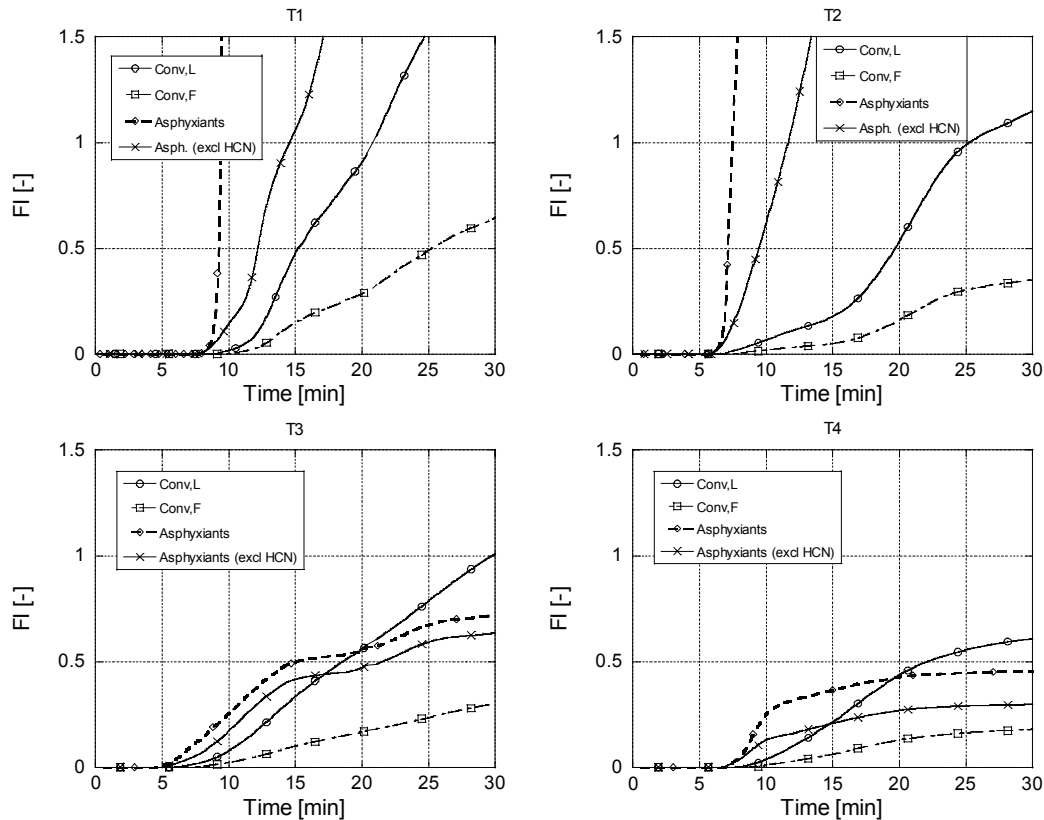


Figure 6.6 Fraction of an incapacitating dose for convective heat exposure compared with asphyxiant gases for the four tests in the Runehamar tunnel.

The fraction of an incapacitating dose for heat exposure based on the Runehamar tests is compared with the results for asphyxiant gases in Figure 6.6. Incapacitating dose for a lightly clothed person is reached in test T1 to T3, but the time to this situation differs. In T1 the curve is similar to that for asphyxiant gases without HCN, but lags somewhat. In T2 the convection curve is far behind the one for asphyxiant gases. In test T3 the curve for convective heat exposure passes the asphyxiant curves. In the case with a fully clothed person the level of incapacitating dose is never reached in the cases discussed. It should be remembered that the calculations presented here are based on measurements performed 458 m from the seat of the fire. The effect of the heat exposure will increase closer to the fire. In the work presented by Ingason *et al.* it was shown that in most cases (scenarios) the temperature and radiation quickly increases above critical values for the occupants in the tunnel [84]. Another conclusion from the same work was that the calculations showed a critical value of 75 MW above which it can be difficult for the occupants in the tunnel to reach the escape routes and survive the fire. If no evacuation is stated, only the

smallest fire (8 MW) can be survived. During a bus fire (25 MW) critical levels can be reached after long exposition times and for larger fires the critical values are relatively rapidly reached. The occupants in the cases of no evacuation were assumed to be either 70 m or 150 m from the fire.

The results given in this section should be seen as an example of the influence of gas composition and heat on the fraction of an incapacitating dose. The conditions in a specific situation during a fire in a tunnel are very complex and several parameters, e.g. the degree of activity of the occupants, affect the results. It should also be noted that age and different kinds of impairment (e.g. disease and physical conditions) significantly affects the critical COHb level (COHb levels found in victims) [223]. The results do confirm, however, the importance of the first minutes during a tunnel fire for the ability of the occupants in the tunnel to escape the incident.

7 Application of the results

In this section the importance and application of some of the results described in this thesis are briefly discussed. An overview of a few areas within the field of fires in tunnels is given. The reader should keep in mind that these discussions are not exhaustive and shall be seen as examples of how to use the results for different applications or further studies.

7.1 Effects on the tunnel structure

In the Sections 2.2.2 and 3.3 the temperature in a tunnel during different types of fires was discussed. The temperature is important for several different processes in the tunnel, e.g. the safety and evacuation of people (see Section 6.3), fire spread (see Section 4), the possibility of the rescue service to manage the incident, etc. One process that has gained much interest lately is the spalling of concrete, i.e. the almost explosive disintegration of concrete when exposed to high temperatures. The findings in Paper I are of interest when defining what heat load (temperature-time curve) the tunnel structure may be exposed to.

Spalling and the effects on tunnel linings have been proven to be important results of fires in tunnels (see Table 2.1). The effects of spalling of rocks was also seen during the tests in the Runehamar tunnel, where rocks fell down from the ceiling both upstream and downstream of the fire [252]. The rocks falling down upstream of the fire emphasizes the importance of the backlayering in determining the risk to tunnel occupants of the developing fire incident. Downstream of the fire in the Runehamar tunnel the road was covered with debris almost all the way to the measurement station 458 m from the centre of the fire.

Much research is presently underway to improve our understanding of the spalling behaviour of the modern high performance and self-compacting concrete. For further details on the subject of spalling see for example references [253-256].

7.2 Rescue operations

The measurements presented above show that after an initial delay the increase in HRR and temperature is fast and the actions undertaken during this initial fire growth are crucial for the outcome of the fire. It is difficult to extinguish an intense fire. The high temperature and radiation associated with an intense fire prevent the fire-fighters from coming close enough to the seat of the fire to be able to extinguish it. Tests performed with fire-fighters in protective clothing [257] show that they feel pain after approximately five minutes when exposed to a radiation of 5 kW/m^2 . For the fire-fighters to withstand radiation during a longer time period and to be able to carry out hard labour, the radiation level must be even lower. This can be compared with the results from the Runehamar tests where the radiation upstream of the fire was well above 5 kW/m^2 , 10 m from the fire for the tests T1 to T3 (see Figure 7.1). At a distance of 20 m from the fire the radiation was 2 kW/m^2 to 3 kW/m^2 in these tests (see Table 7.1). It is presently not known if fire-fighters would be able to effectively fight a large fire from this distance. If the fire is not extinguished during the time period when the fire is still small, it may not be able to be extinguished until the

fire has decreased in intensity after its peak – long after egress is an issue for occupants. The often long distances to the seat of the fire also pose problems for the fire fighters and if they are to reach the fire much personnel and equipment are often needed.

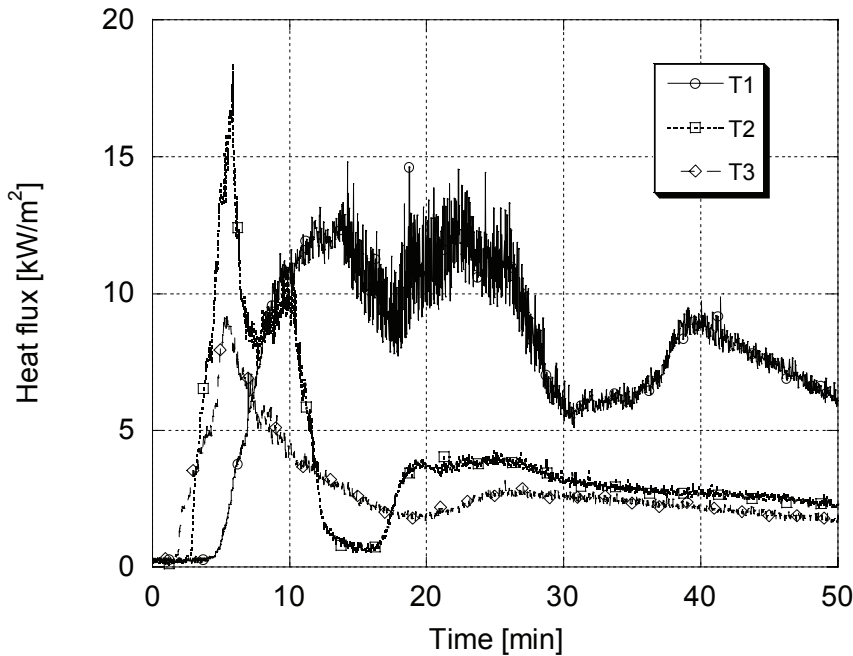


Figure 7.1 Radiation 10 m from the upstream end of the HGV set-up in the Runehammar tests (T1 to T3).

Table 7.1 Peak radiation values upstream of the HGV fires in the Runehammar tunnel [252, 258]. The distances are measured from the upstream end of the HGV set-up.

Test id	Radiation 5 m upstream of the fire [kW/m ²]	Radiation 10 m upstream of the fire [kW/m ²]	Radiation 20 m upstream of the fire [kW/m ²]
T1	80	14	2
T2	35	18	3
T3	20	9	2
T4	40	10	4 (15 m)

Ingason *et al.* drew the conclusion that even a relatively small fire of 25 MW can pose problems for fire fighters, depending on where the fire is situated and whether the extinguishment operation needs to be preceded by a BA operation (BA = breathing apparatus) [84]. For fires of sizes 75 MW or higher the radiation will be so high that the extinguishment work has to be performed at least 15 m to 20 m from the fire. This means that a high water flow rate and much equipment are needed. A general conclusion was also that current methods used in BA operations are not suitable for fires in tunnels and new methods should be developed.

Since in many situations it will be difficult to extinguish the fire during the initial phase or even to reach the tunnel in time, it is very important that people react quickly and start the evacuation prior to fire brigade intervention. However, typical human behaviour is to sit and wait in the car to get more information or for the queue to start to move [259]. This waiting can result in people not reaching the escape routes, shelters or other safe havens. After the fire in the Mont Blanc tunnel some victims were found sitting in their cars with their seat-belts on.

The high temperatures presented in Paper I and Paper VII together with the long flames from large tunnel fires and low visibility makes it almost impossible to attack a fire from the downstream side. Ventilation can be an effective tool in making the conditions upstream of the fire tenable. This tool must, however, be used with caution since the conditions downstream of the fire can be made more severe by the ventilation and people trying to escape can be trapped in the flames or fire gases. In connection with the ventilation it is also important to consider different phenomena, *e.g.* backlayering, an increase of the fire intensity and fire spread, etc. Pulsations of the kind observed in two of the tests in the Runehamar tunnel (see Section 5.4 and Papers V and VI) have not been reported from any real large-scale fire in a tunnel, but under certain conditions such pulsations could occur.

7.3 Sprinkler and other water-based extinguishment systems

The construction and exact use of sprinkler and other water-based extinguishment systems have not been focused on in this thesis. However, the results in Paper VII show that there is a significant risk of fire spread to a vehicle far from a burning HGV. This has also been seen in real fires, *e.g.* in the recent fire in the Fréjus tunnel.

In Japan water extinguishment systems are widely used in tunnels and testing has been performed to design and support this use [260, 261]. Similarly in Australia, the use of fire suppression systems in tunnels is widespread. In Europe, however, there has been a reluctance to use sprinkler in tunnels. This reluctance is based on a fear of increasing the hazard in the tunnel, *e.g.* destroying the smoke stratification and thereby decreasing the visibility, spreading liquid fuel over a larger area and thereby spreading the fire, the risk for explosion, the production of steam affecting the people inside the tunnel, etc. The large installation costs have also played an important role.

This reluctance to consider the installation of extinguishment system has also affected the willingness to fund research within this field and until only a few years ago much of the experience was based on tests performed in 1965 [55]. However, in recent years more interest has been paid to the benefits of extinguishment systems [262]. Large-scale testing has also been performed [60]. In 2004, a large test series with extinguishment test was performed within the UPTUN project. The results of this test series are still to be published.

One argument against sprinkler systems is that they cannot reach the seat of the fire and therefore not extinguish the fire. However, by reducing the gas temperature and the radiation one also dramatically decreases the risk for fire spread, which can mean

the difference between a manageable fire and a catastrophic fire. This area, therefore, needs further attention and studies.

8 Conclusions

The recent catastrophic fires and the experimental results from tunnel fire tests presented and discussed in this thesis have shown the high temperatures and heat release rates that can be reached during such fires, and the effect these can have, both on the safety of people, and on the structure of the tunnels. Experience from real fires has shown that HGVs pose special risks when they are involved in fires in tunnels. The tests in the Runehammar tunnel show that even non-hazardous goods can give rise to high HRRs, considerably higher than cited in tunnel design guidelines. This also places a focus on the fire load and fire behaviour of the vehicles involved in fires in tunnels. A correlation between the total energy content and the maximum HRR has been presented for passenger cars and HGVs, but the validation of this correlation requires further investigation.

Another important issue is the rapid increase in temperature and heat release rate after an initial development period, e.g. after fire spread from the vehicle to the cargo in an HGV. This means that there is only a short period of time for the occupants in a tunnel to begin evacuation and find a safe haven. Further, the toxicity calculations corroborate this conclusion. It is a question of minutes available for egress. This means that occupants need to be quickly aware of the fire and be able to evacuate by themselves, since the rescue services seldom are able to reach a tunnel fire in the short time frame available.

It has also been shown in the Runehammar tests that a fire in an HGV can spread a long distance downstream, of the order of 100 m. This is approximately the same maximum flame length that was estimated in the Runehammar tests based on temperature measurements. These results comply very well with what was experienced in the fire in the Fréjus tunnel in June 2005, where the fire spread over 100 m between vehicles. Based on the test results and real incidents one must also emphasize the importance of the operation during the first five to ten minutes of the fire. The actions of the people inside the tunnel and the rescue personnel during this time period can be crucial to the outcome.

Results presented in the literature has shown that the ventilation significantly affects the heat release rate and the conditions in a tunnel during a fire, but it is often difficult to determine the ventilation conditions related to a certain case or a specific increase in the HRR. The combustion conditions need to be taken into account when studying the effect of the ventilation on the increase in HRR and the maximum HRR. This needs to be studied further.

Ventilation can be an important tool for the rescue service since evacuation of smoke improves the operation conditions (e.g. visibility, heat exposure, etc.). However, it can also make the conditions inside the tunnel more severe by increasing the intensity of the fire, by spreading the fire, or by trapping the occupants in the tunnel in smoke and flames. Rescue operations and the use of fans should, therefore, be carefully planned in advance based on different types of fires scenarios. One aim of this thesis has been to present data and information that can be used when describing such scenarios and developing action plans.

The radiation level upstream of a fire in a tunnel can be significant, both due to direct radiation from the flames and due to backlayering. This severely complicates an extinguishment operation since the firefighters must try to extinguish the fire from a distance. The backlayering appears when the air velocity is below a critical velocity. In the Runehamar tests the air velocity decreased during the most intense period of the fire. Calculations have shown that the main factor influencing this decrease was the thermal resistance due to the slope of the tunnel.

Pulsations were observed in two of the Runehamar tests, during the most intense part of the fire (when the HRR was above 125 MW to 135 MW). This phenomenon has never previously been discussed or observed when considering road or rail tunnel safety. The reasons for the pulsations have been discussed in this thesis and explanations for the observed periods of the pulsations (4 s and 18 s, respectively) were given based two different method: an acoustic approach and a frequency analysis based on an impedance approach. Both methods show that the observed periods are results of the tunnel as a system. The conditions for instability are mainly determined by the position of the fire in the tunnel, the HRR, and the air flow rate through the tunnel. These pulsations appeared in real scale fire experiments in a tunnel. This means that there is a risk that this kind of pulsations can occur also in real fires in tunnels. Such a situation could pose an extra threat to the people inside the tunnel, especially the rescue personal trying to reach the fire from the upstream side.

Work with safety in tunnels is an ongoing process in many countries, on different levels, and within different engineering fields. Even if research in recent years has improved our knowledge on fires in tunnels and tunnel safety, there is still a need for more knowledge. Some areas where more information is needed, related to the work presented in this thesis, are presented in the next section.

9 Future work

Two of the most important parameters in connection with a fire in a tunnel are the heat release rate and the temperature. These parameters are affected by the fuel, the geometry of the fuel, the geometry of the tunnel, the ventilation, etc. These effects have been observed in different studies, but there exist very few studies where the relationship between these parameters is studied extensively, i.e. systematically varied keeping other parameters constant. Such a study is planned, with model scale tests planned in the beginning of 2006.

The effect of the ventilation on the development and maximum size of a fire in a tunnel is of particular interest. To better assess the effect of the ventilation, response to specific conditions, i.e. whether the conditions are well ventilated or under-ventilated, needs to be defined. A method of relating the change in HRR as a function of the change in air velocity needs to be developed.

During two of the tests in the Runehamar test series presented in this thesis, long-period pulsations were observed. Plausible explanations were given in Paper V and Paper VI and the results have been compared with the findings from other field, *e.g.* combustion, in more detail in this thesis. This work shows two important parameters. One is the transfer function for the transfer of heat from the process to the flow field and the oscillations. The other is the stability limit, which determines within what regions in the HRR – mass flow rate graph the system becomes unstable and where it is stable. Most studies on the transfer function and the stability limit have been performed either with premixed combustion or with electrically heated wires inside a tube. To better understand this phenomena these parameters, therefore, need to be studied under conditions similar to those prevailing during fires in tunnels, and the significance of this phenomenon for egress and fire-fighting needs to be established.

10 References

1. Carvel, R. O. and Marlair, G., "A history of fire incidents in tunnels". In *The handbook of Tunnel Fire Safety* (A. N. Beard and R. O. Carvel, Eds.), Thomas Telford Publishing, 3-41, London, UK, 2005.
2. "Fire and Smoke Control in Road Tunnels", PIARC, 05.05B-1999, 1999.
3. Andersen, T. and Paaske, B. J., "Railroad and Metro Tunnel Accidents", Det Norske Veritas (DNV), http://home.no.net/lotsberg/artiklar/andersen/en_table_1.html.
4. Thamm, B., "The new EU directive on road tunnel safety", Proceedings of the International Symposium on Catastrophic Tunnel Fires, SP Report 2004:05, 19-30, Borås, Sweden, 20-21 November, 2003.
5. Ingason, H., "Fire Development in Catastrophic Tunnel Fires (CTF)", International Symposium on Catastrophic Tunnel Fires (CTF), 31-47, Borås, Sweden, 20-21 November, 2003.
6. Bettelini, M., Neuenschwander, H., Henke, A., Gagliardi, M., and Steiner, W., "The Fire in the St Gotthard Tunnel of October 24, 2001", International Symposium on Catastrophic Tunnel Fires (CTF), 49-68, Borås, Sweden, 20-21 November, 2003.
7. "Closure of the Fréjus tunnel: Europe must ensure that the Alps can be crossed more safely and in a less polluting way", IP/05/690, Brussels, Belgium, 2005.
8. "Directive 2004/54/EC of the European Parliament and of the Council of 29 April 2004 on minimum safety requirements for tunnels in the Trans-European Road Network", In *Official Journal of the European Union*, 2004.
9. Høj, N. P., "Guidelines for Fire Safe Design Compared Fire Safety Features for Road Tunnels", 1st International Symposium on Safe & Reliable Tunnels, 127-138, Prague, Czech Republic, 4-6 February, 2004.
10. Zuber, P., "Compared Safety Features for Rail Tunnels", 1st International Symposium on Safe & Reliable Tunnels, 139-148, Prague, Czech Republic, 4-6 February, 2004.
11. Gabay, D., "Compared Fire Safety Features for Metro Tunnels", 1st International Symposium on Safe & Reliable Tunnels, 149-156, Prague, Czech Republic, 4-6 February, 2004.
12. Bendelius, A., "Tunnel ventilation - state of the art". In *The Handbook of Tunnel Fire Safety* (A. N. Beard and R. O. Carvel, Eds.), Thomas Telford Publishing, 127-143, London, UK, 2005.
13. Heselden, A., "Studies of fire and smoke behavior relevant to tunnels", 2nd Int Symp on Aerodynamics and Ventilation of Vehicle Tunnels, J1-1 -- J1-18, Cambridge, UK, 23-25 March, 1976.
14. Heselden, A. J. M., "Studies of fire and smoke behaviour relevant to tunnels", Building Research Establishment, CP 66/78, Borehamwood, UK, 1978.
15. NFPA 502, "Standard for Road Tunnels, Bridges, and other Limited Access Highways", 2004 ed., National Fire Protection Association, 2004.

16. Bendelius, A. and Brinckerhoff, P., "The Latest PIARC Road Tunnel Fire and Smoke Control Publications", In *Joint Issue ITA/PIARC of Route-Roads on Fire Safety in Tunnels*, 2004.
17. Lacroix, D., "New French Recommendations for Fire Ventilation in Road Tunnels", 9th International Conference on Aerodynamics and Ventilation of Vehicle Tunnels, Aosta Valley, Italy, 6-8 October, 1997.
18. NFPA 502, "Road Tunnels, Bridges, and Other Limited Access Highways", 2001 ed., National Fire Protection Association, 2001.
19. Lacroix, D., "Guidelines for Fire Safe Design: Synthesis and Current Harmonisation Processes", 1st International Symposium on Safe & Reliable Tunnels, 107-115, Prague, Czech Republic, 4-6 February, 2004.
20. prEN 45545-2, "Railway application - Fire protection on railway vehicle - Part 2: Requirement for fire behaviour of materials and components", 2004-02, CEN/CENELEC/TC, 2004.
21. NFPA 130, "Standard for Fixed Guideway Transit and Passenger Rail Systems", 2003 ed., 7 August, National Fire Protection Association, 2003.
22. Brousse, B., "Comparison of Fire Safety Problems for the Various Transport Modes in Tunnels", 1st International Symposium on Safe & Reliable Tunnels, 117-126, Prague, Czech Republic, 4-6 February, 2004.
23. ISO 834-1, "Fire-resistance tests - Elements of building construction - Part 1: General requirements", First ed., 1999-09-15, International Organization for Standardization, 1999.
24. EN 1363-2, "Fire resistance tests - Part 2: Alternative and additional procedures", First ed., 1999-09-24, European Committee for Standardization, 1999.
25. "Richtlinien für Ausstattung und Betrieb von Tunneln (RABT)", Ausgabe 1985 ed., Forschungsgesellschaft für Straßen- und Verkehrswesen, 1985.
26. "Beproeving van het gedrag bij verhitting van twee isolatiematerialen ter bescherming van tunnels bij brand", Instituut TNO voor Bouwmaterialen en Bouwconstructies, B-79-391, Delft, The Netherlands, 1979.
27. "Rapport betreffende de beproeving van het gedrag van twee isolatiematerialen ter bescherming van tunnels tegen brand", Instituut TNO voor Bouwmaterialen en Bouwconstructies, Rapport B-80-33, Delft, The Netherlands, 1980.
28. "Systems and Equipment for Fire and Smoke Control in Road Tunnels", PIARC Committee on Road Tunnel Operation (C-5), Working group No. 6, To be published.
29. Lacroix, D. and Haack, A., "PIARC Design Criteria for Resistance to Fire for Road Tunnel Structures", In *Joint Issue ITA/PIARC of Route-Roads on Fire Safety in Tunnels*, 2004.
30. Russell, H. A., "ITA Guidelines for Structural Fire Resistance of Road Tunnels", In *Joint Issue ITA/PIARC of Route-Roads on Fire Safety in Tunnels*, 2004.
31. "ATB Tunnel 2004", Vägverket (The Swedish Road Administration), Publikation 2004:124, Borlänge, Sweden (in Swedish), 2004.

32. Babrauskas, V. and Peacock, R. D., "Heat Release Rate: The Single Most Important Variable in Fire Hazard", *Fire Safety Journal*, **18**, 255-272, 1992.
33. Huggett, C., "Estimation of Rate of Heat Release by Means of Oxygen Consumption Measurements", *Fire and Materials*, **4**, 2, 61-65, 1980.
34. Parker, W. J., "Calculations of the Heat Release Rate by Oxygen Consumption for Various Applications", National Bureau of Standards, NBSIR 81-2427, Gaithersburg, USA, 1982.
35. Tewarson, A., "Generation of Heat and Chemical Compounds in Fires". In *The SFPE Handbook of Fire Protection Engineering* (P. J. DiNenno, D. Drysdale, C. L. Beyler, W. D. Walton, R. L. P. Custer, J. R. Hall, and J. M. Watts, Eds.), National Fire Protection Association, 3-82 -- 3-161, Quincy, MA, USA, 2002.
36. Lönnemark, A. and Babrauskas, V., "TOXFIRE - Fire Characteristics and Smoke Gas Analyses in Under-ventilated Large-scale Combustion Experiments: Theoretical Background and Calculations", SP Swedish National Testing and Research Institute, SP REPORT 1996:49, Borås, Sweden, 1997.
37. Drysdale, D., *An Introduction to Fire Dynamics*, John Wiley & Sons, 1992.
38. Casale, E. and Marlair, G., "Heptane Fire Tests with Forced Ventilation", Proceedings of the International Conference on Fires in Tunnels, 36-50, Borås, Sweden, 10-11 October, 1994.
39. Takeda, H. and Akita, K., "Critical Phenomenon in Compartment Fires with Liquid Fuels", Eighteenth Symposium (International) on Combustion, 519-527, Waterloo, Canada, 17-22 August, 1980.
40. Carvel, R. O., Beard, A. N., and Jowitt, P. W., "How Much do Tunnels Enhance the Heat Release Rate of Fires", Proc. 4th Int. Conf on Safety in Road and Rail Tunnels, 457-466, Madrid, Spain, 2-6 April, 2001.
41. Saito, N., Yamada, T., Sekizawa, A., Yanai, E., Watanabe, Y., and Miyazaki, S., "Experimental Study on Fire Behavior in a Wind Tunnel with a Reduced Scale Model", Second International Conference on Safety in Road and Rail Tunnels, 303-310, Granada, Spain, 3-6 April, 1995.
42. Ingason, H., "Fire Experiments in a Model Tunnel using Pool Fires - Experimental Data", SP Swedish National Testing and Research Institute, SP AR 1995:52, Borås, Sweden, 1995.
43. Ingason, H., "Effects of Ventilation on Heat Release Rate of Pool Fires in a Model Tunnel", SP Swedish National Testing and Research Institute, SP REPORT 1995:55, Borås, Sweden, 1995.
44. Carvel, R. O., Beard, A. N., and Jowitt, P. W., "How Does the Shape of a Tunnel Affect the Heat Release Rate of a Fire?" Proc. 9th Int. Fire Science & Engineering Conf. (Interflam 2001), 1355-1360, Edinburgh, Scotland, 17-19 September, 2001.
45. Carvel, R. O. and Drysdale, D. D., "The Influence of Tunnel Geometry and Ventilation on the Heat Release Rate of a Fire", *Fire Technology*, **40**, 5-26, 2004.
46. Ingason, H., Nireus, K., and Werling, P., "Fire Tests in a Blasted Rock Tunnel", FOA, Report FOA-R-97-00581-990-SE, Sweden, 1997.

47. Heskestad, G., "Flame Height of Fuel Arrays with Combustion in Depth", *Fire Safety Science - Proceedings of the Fifth International Symposium*, 427-438, Melbourne, Australia, 3-7 March, 1997.
48. "Memorial Tunnel Fire Ventilation Test Program - Test Report", Massachusetts Highway Department and Federal Highway Administration, 1995.
49. Grant, G. B. and Drysdale, D., "Estimating Heat Release Rates from Large-scale Tunnel Fires", *Fire Safety Science - Proceedings of the Fifth International Symposium*, 1213-1224, Melbourne, 1995.
50. Enright, T. and Fleischmann, C., "An Uncertainty Analysis of Calorimetric Techniques", *Poster Notes - 5th International Symposium on Fire Safety Science*, 1332, Melbourne, Australia, 3-7 March, 1997.
51. Enright, P. A. and Fleischmann, C. M., "Uncertainty of Heat Release Rate Calculation of the ISO5660-1 Cone Calorimeter Standard Test Method", *Fire Technology*, **35**, 2, 153-169, 1999.
52. Axelsson, J., Andersson, P., Lönnemark, A., Van Hees, P., and Wetterlund, I., "Uncertainties in Measuring Heat and Smoke Release Rates in the Room/Corner Test and the SBI", SP Swedish National Testing and Research Institute, SP REPORT 2001:04, Borås, Sweden, 2001.
53. Axelsson, J., Andersson, P., Lönnemark, A., Van Hees, P., and Wetterlund, I., "Uncertainty of HRR and SPR Measurements in SBI and Room/corner Test", 9th International Fire Science & Engineering Conference (Interflam 2001), 507-518, Edinburgh, Scotland, 17-19 September, 2001.
54. "Fires in Transport Tunnels: Report on Full-Scale Tests", edited by Studiengesellschaft Stahlanwendung e. V., EUREKA-Project EU499:FIRETUN, Düsseldorf, Germany, 1995.
55. "Schlussbericht der Versuche im Ofenegg Tunnel von 17.5 - 31.5 1965", Kommission für Sicherheitsmassnahmen in Strassentunneln, 1965.
56. Feizlmayr, A., "Research in Austria on tunnel fire, Paper J2, BHRA", 2nd Int Symp on Aerodynamics and Ventilation of Vehicle Tunnels, 19 - 40, Cambridge, UK, 1976.
57. "State of the Road Tunnel Equipment in Japan - Ventilation, Lighting, Safety Equipment", Public Works Research Institute, Technical note, Vol. 61, Japan, 1993.
58. Keski-Rahkonen, O., Holmlund, C., Loikkanen, P., Ludvigsen, H., and Mikkola, E., "Two full scale pilot fire experiments in a tunnel", Technical Research Centre of Finland, Research Reports 453, Espoo, Finland, 1986.
59. Keski-Rahkonen, O., "Tunnel Fire Tests in Finland", *Proceedings of the International Conference on Fires in Tunnels*, 222 -237, Borås, 10 - 11 October 1994, 1994.
60. Lemaire, A., van de Leur, P. H. E., and Kenyon, Y. M., "Safety Proef: TNO Metingen Beneluxtunnel - Meetrapport", TNO, TNO-Rapport 2002-CVB-R05572, 2002.
61. Haerter, A., "Fire Tests in the Ofenegg-Tunnel in 1965", *International Conference on Fires in Tunnels*, SP REPORT 1994:54, 195-214, Borås, Sweden, 10-11 October, 1994.

62. ILF, "Brandversuche in einem Tunnel", Ingenieurgesellschaft Lässer-Feizlmayr; Bundesministerium f. Bauten u. Technik, Strassenforschung, P0244, 1976.
63. Pucher, K., "Fire Tests in the Zwenberg Tunnel (Austria)", International Conference on Fires in Tunnels, 187-194, Borås, Sweden, 1994.
64. Kunikane, Y., Kawabata, N., Ishikawa, T., Takekuni, K., and Shimoda, A., "Thermal Fumes and Smoke Induced by Bus Fire Accident in Large Cross Sectional Tunnel", The fifth JSME-KSME Fluids Engineering Conference, Nagoya, Japan, 17-21 November, 2002.
65. "Project 'Safety Test' - Report on Fire Tests", Directorate-General for Public Works and Water Management, Utrecht, The Netherlands, 2002.
66. Ingason, H. and Lönnemark, A., "Heat Release Rates and Temperatures during Fires in Tunnels", To be submitted.
67. Carvel, R. O. and Marlair, G., "A history of tunnel fire experiments". In *The handbook of tunnel fire safety* (A. N. Beard and R. O. Carvel, Eds.), Thomas Telford Publishing, 201-230, London, 2005.
68. Ingason, H. and Lönnemark, A., "Recent Achievements Regarding Measuring of Time-heat and Time-temperature Development in Tunnels", 1st International Symposium on Safe & Reliable Tunnels, Prague, Czech Republic, 4-6 February, 2004.
69. Mangs, J. and Keski-Rahkonen, O., "Characterization of the Fire Behavior of a Burning Passenger Car. Part I: Car Fire Experiments", *Fire Safety Journal*, **23**, 17-35, 1994.
70. Mangs, J. and Keski-Rahkonen, O., "Characterization of the Fire Behavior of a Burning Passenger Car. Part II: Parametrization of Measured Rate of Heat Release Curves", *Fire Safety Journal*, **23**, 37-49, 1994.
71. Steinert, C., "Smoke and Heat Production in Tunnel Fires", The International Conference on Fires in Tunnels, 123-137, Borås, Sweden, 10-11 October, 1994.
72. Steinert, C., "Experimentelle Untersuchungen zum Abbrand-und Feuerübersprungsverhalten von Personenkraftwagen", *vfdB-Zeitschrift, Forschung, Technik und Management im Brandschutz*, **4**, 163-172, 2000.
73. Shipp, M. and Spearpoint, M., "Measurements of the Severity of Fires Involving Private Motor Vehicles", *Fire and Materials*, **Vol. 19**, 143-151, 1995.
74. Joyeux, D., "Development of Design Rules for Steel Structures Subjected to Natural Fires in Closed Car Parks", Centre Technique Industriel de la Construction Métallique, INC-96/294d-DJ/VG, Saint-Rémy-lès-Chevreuse, France, 1997.
75. Ingason, H., "Heat Release Rate Measurements in Tunnel Fires", International Conference on Fires in Tunnels, 86-103, Borås, Sweden, October 10-11, 1994, 1994.
76. Ingason, H. and Lönnemark, A., "Fire development of Large Vehicles in Road Tunnels", Proceedings of the Fifth International Conference on Tunnel fires, 203-212, London, UK, 25-27 October, 2004.

77. Barber, C., Gardiner, A., and Law, M., "Structural Fire Design of the Øresund Tunnel", Proceedings of the International Conference on Fires in Tunnels, 313-332, Borås, Sweden, 10-11 October, 1994.
78. Ingason, H., Gustavsson, S., and Dahlberg, M., "Heat Release Rate Measurements in Tunnel Fires", SP Swedish National Testing and Research Institute, SP Report 1994:08, Borås, Sweden, 1994.
79. Wickström, U., "Application of the Standard Fire Curve for Expressing Natural Fires for Design Purposes". In *Fire Safety: Science and Engineering, ASTM STP 882* (T. Z. Harmathy, Ed.), American Society for Testing and Materials, 145-159, Philadelphia, USA, 1985.
80. ISO, "Revision of ISO - 1975. Fire resistance tests - Elements of building construction. Part 3 - Guidance on test method and test data application. Third Draft", ISO, ISO TC92/SC2/WG1 N270, 1987.
81. Wickström, U., "Expression for the HC curve based on a sum of exponential functions", Personal communication, Borås, Sweden, 2005.
82. Wickström, U., "Natural Fires for Design of Steel and Concrete Structures - A Swedish Approach", International Symposium on Fire Engineering for Building Structures and Safety, 67-72, Melbourne, Australia, 14-15 November, 1989.
83. Carvel, R. O., Beard, A. N., and Jowitt, P. W., "The Influence of Longitudinal Ventilation and Tunnel Size on HGV Fires in Tunnel", 10th International Fire Science & Engineering Conference (Interflam 2004), 815-820, Edinburgh, Scotland, 5-7 July, 2004.
84. Ingason, H., Bergqvist, A., Lönnemark, A., Frantzych, H., and Hasselrot, K., "Räddningsinsatser i vägtunnlar", Räddningsverket, P21-459/05 (in Swedish), 2005.
85. Carlotti, P. and Voeltzel, A., "The impact of wall heating on longitudinal ventilation", *Tunnel Management International*, 7, 2, 40-46, 2004.
86. Ingason, H. and Lönnemark, A., "Ventilation of the Runehamar tunnel tests", To be submitted.
87. Rew, C. and Deaves, D., "Fire spread and flame length in ventilated tunnels - a model used in Channel tunnel assessments", Proceedings of the International Conference on Tunnel Fires and Escape from Tunnels, 397-406, Lyon, France, 5-7 May, 1999.
88. Beyler, C. L., "Fire Plumes and Ceiling Jets", *Fire Safety Journal*, 11, 53-75, 1986.
89. McCaffrey, B., "Flame height". In *The SFPE Handbook of Fire Protection Engineering* (P. J. DiNenno, Ed.), National Fire Protection Association, 2-1 - 2-8, 1995.
90. Heskestad, G., "Fire Plumes, Flame Height, and Air Entrainment". In *The SFPE Handbook of Fire Protection Engineering* (P. J. DiNenno, Ed.), National Fire Protection Association, 2-1 -- 2-17, Quincy, Massachusetts, USA, 2002.
91. Heskestad, G., "Luminous Heights of Turbulent Diffusion Flames", *Fire Safety Journal*, 5, 103-108, 1983.

92. Heskestad, G., "Dynamics of the Fire Plume", *Phil. Trans. R. Soc. Lond.*, **356**, 2815-2833, 1998.
93. Zukoski, E. E., "Fluid Dynamic Aspects of Room Fires", Proceedings of the First International Symposium on Fire Safety Science, 1-30, Gaithersburg, USA, 7-11 October, 1985.
94. Babrauskas, V., "Flame Lengths under Ceiling", *Fire and Materials*, **4**, 3, 119-126, 1980.
95. Heskestad, G. and Hamada, T., "Ceiling Jets of Strong Fire Plumes", *Fire Safety Journal*, **21**, 69-82, 1993.
96. Alpert, R. L., "Calculation of Response Time of Ceiling- Mounted Fire Detectors", *Fire Technology*, **8**, 3, 181-195, 1972.
97. Alpert, R. L., "Ceiling Jet Flows". In *SFPE Handbook of Fire Protection Engineering* (P. J. DiNenno, Ed.), National Fire Protection Association, 2-18 -- 2-31, Quincy, MA, USA, 2002.
98. Sugawa, O., Satoh, H., and Oka, Y., "Flame Height from Rectangular Fire Sources Considering Mixing Factor", Proceedings of the Third International Symposium on Fire safety Science, 435-444, Edinburgh, Scotland, 8-12 July, 1991.
99. Oka, Y., "Flame Behaviour in a Tunnel", Third International Conference on Safety in Road and Rail Tunnels, 159-168, Nice, France, 9-11 March, 1998.
100. Delichatsios, M. A., "The Flow of Fire Gases under a Beamed Ceiling", *Combustion and Flame*, **43**, 1-10, 1981.
101. Motevalli, V. and Ricciuti, C., "Characterization of the Confined Ceiling Jet in the Presence of an Upper Layer in Transient and Steady-State Conditions", NIST, NIST-GCR-92-613, Gaithersburg, Maryland, USA, 1992.
102. Yuan, Z. P. and Motevalli, V., "Steady State Ceiling Jet Behavior under an Unconfined Ceiling with Beams", *SFPE Bulletin*, September/October, 6-12, 1994.
103. Newman, J. S. and Tewarson, A., "Flame Propagation in Ducts", *Combustion and Flame*, **51**, 347-355, 1983.
104. McAdams, W. H., *Heat Transmission*, 3rd ed., McGraw-Hill, New York, 1954.
105. Kuwana, H., "Scale Effect on Temperature Properties in Tunnel Fire", Third International Conference on Safety in Road and Rail Tunnels, 87-96, Nice, France, 9-11 March, 1998.
106. Beard, A. N., Drysdale, D. D., and Bishop, S. R., "A Non-linear Model of Major Fire Spread in a Tunnel", *Fire Safety Journal*, **24**, 333-357, 1995.
107. Beard, A. N., "A Model for Predicting Fire Spread in Tunnels", *Journal of Fire Sciences*, **15**, July/August, 277-307, 1997.
108. Beard, A. N., "Major Fire Spread in a Tunnel: A Non-linear Model", Fourth International Conference on Safety in Road and Rail Tunnels, 467-476, Madrid, Spain, 2-6 April, 2001.
109. Beard, A. N., "Major Fire Spread in a Tunnel: A Non-linear Model with Flame Impingement", Proceedings of the 5th International Conference on Safety in Road and Rail Tunnels, 511-521, Marseille, France, 6-10 October, 2003.

110. Beard, A. N., "Major Fire Spread in a Tunnel, Assuming Flame Impingement: Effect of Separation and Ventilation Velocity", Fifth International Conference on Tunnel Fires, 317-326, London, UK, 25-27 October, 2004.
111. Kurioka, H., Oka, Y., Satoh, H., and Sugawa, O., "Fire properties in near field of square fire source with longitudinal ventilation in tunnels", *Fire Safety Journal*, **38**, 319-340, 2003.
112. Apte, V. B., Green, A. R., and Kent, J. H., "Pool Fire Plume Flow in a Large-Scale Wind Tunnel", Proceedings of the Third International Symposium on Fire Safety Science, 425-434, Edinburgh, Scotland, 8-12 July, 1991.
113. Bettis, R. J., Jagger, S. F., and Wu, Y., "Interim Validation of Tunnel Fire Consequence Models: Summary of Phase 2 Tests", Health and Safety Executive, IR/L/FR/93/11, Buxton, Derbyshire, UK, 1993.
114. Carvel, R. O., Beard, A. N., and Jowitt, P. W., "The Influence of Longitudinal Ventilation on Fire Spread between HGV Fires in Tunnels", Fifth International Conference on Tunnel Fires, 307-316, London, UK, 25-27 October, 2004.
115. Brinson, A., "Fire in French Tunnel Kills Two", Eurosprinkler, 2005.
116. Beard, A. N., "Requirements for acceptable model use", *Fire Safety Journal*, **40**, 477-484, 2005.
117. Jagger, S. and Grant, G., "Use of tunnel ventilation for fire safety". In *The Handbook of Tunnel Fire Safety* (A. N. Beard and R. O. Carvel, Eds.), Thomas Telford Publishing, 144-183, London, UK, 2005.
118. Guigas, X., Weatherill, A., Trottet, Y., Casale, E., and Houseaux, B., "The New Ventilation Systems of the Mont Blanc Tunnel. Specificities and Performances of the Fire Ventilation", Fourth International Conference on Tunnel Fires, 105-113, Basel Switzerland, 2-4 December, 2002.
119. Brichet, N., Weatherill, A., Crausaz, B., and Casale, E., "The New Ventilation Systems of the Mont Blanc Tunnel Active Smoke Control: From Simulation to Successful Operation", Fourth International Conference on Tunnel Fires, 95-104, Basel Switzerland, 2-4 December, 2002.
120. Casale, E., Brousse, B., Weatherill, A., and Marlier, E., "Full Scale Fire Tests Performed in the Mont Blanc Tunnel - Evaluation of the Efficiency of the Fully Automatic Ventilation Responses", Fourth International Conference on Fires in Tunnels, 313 - 325, Basel, Switzerland, 2-4 December, 2002.
121. Brousse, B. and Voeltzel, A., "Comparison of the Performance of the Smoke Clearing System of the Mont Blanc Tunnel before and after Renovation Works", Proceedings of the Fifth International Conference on Safety in Road and Rail Tunnels, 49-58, Marseille, France, 6-10 October, 2003.
122. Carvel, R. O., Beard, A. N., and Jowitt, P. W., "The Effect of Forced Longitudinal Ventilation on a HGV Fire in a Tunnel", Proceedings of the International Conference on Tunnel Fires and Escape from Tunnels, 191-199, Lyon, France, 5-7 May, 1999.
123. French, S. E., "EUREKA 499 - HGV Fire Test (Nov. 1992) - Summary Report". In *Proceedings of the International Conference on Fires in Tunnels* (E. Ivarson, Ed.), SP Swedish National Testing and Research Institute, 63-85, Borås, Sweden, 1994.

124. Bettis, R. J., Jagger, S. F., and Moodie, K., "Reduced Scale Simulations of Fires in Partially Blocked Tunnels", Proceedings of the International Conference on Fires in Tunnels, 162-186, Borås, Sweden, 10-11 October, 1994.
125. Huijben, J. W., "The Influence of Longitudinal Ventilation on Fire Size and Development", Fourth International Conference on Tunnel Fires, 115-124, Basel Switzerland, 2-4 December, 2002.
126. Carvel, R. O., Beard, A. N., Jowitt, P. W., and Drysdale, D. D., "Variation of Heat Release Rate with Forced Longitudinal Ventilation for Vehicle Fires in Tunnels", *Fire Safety Journal*, **36**, 6, 569-596, 2001.
127. Carvel, R. O., Beard, A. N., and Jowitt, P. W., "The Influence of Longitudinal Ventilation on Fire Size in Tunnel: Update", Fifth International Conference on safety in Road and Rail Tunnels, 431-440, Marseille, France, 6-10 October, 2003.
128. Carvel, R. O., Beard, A. N., and Jowitt, P. W., "A Bayesian Estimation of the Effect of Forced Ventilation on a Pool Fire in a Tunnel", *Civil. Eng. and Env. Syst.*, **18**, 279-302, 2001.
129. Ingason, H. and Werling, P., "Experimental Study of Smoke Evacuation in a Model Tunnel", FOA Defence Research Establishment, FOA-R--99-01267-311--SE, Tumba, Sweden, 1999.
130. Babrauskas, V., "Heat of Combustion and Potential Heat". In *Heat Release in Fires* (V. Babrauskas and S. J. Grayson, Eds.), E & FN Spon, London, UK, 1995.
131. Babrauskas, V., "Burning rates". In *In SFPE Handbook of Fire Protection Engineering* P. J. DiNunno, C. L. Beyler, R. L. P. Custer, P. D. Walton, J. M. Watts, D. D. Drysdale, and J. R. Hall, Eds.), The National Fire Protection Association, USA, 3.1 - 3.15, 1995.
132. Lönnemark, A., Blomqvist, P., Månsson, M., and Persson, H., "TOXFIRE - Fire Characteristics and Smoke Gas Analysis in Under-ventilated Large-scale Combustion Experiments: Tests in the ISO 9705 Room", SP Swedish National Testing and Research Institute, SP REPORT 1996:45, Borås, Sweden, 1997.
133. Liew, S. K. and Deaves, D. M., "Eurotunnel HGV fire on 18th November 1996 - Fire development and effects", Proceedings of the third International Conference on Safety in Road and Rail Tunnels, 29-40, Nice, France, 1998.
134. Malhotra, H. L., "Goods Vehicle Fire Test in a Tunnel", Second international Conference on Safety in Road and Rail Tunnels, 237-244, Granada, Spain, 3-6 April, 1995.
135. Richter, E. and Vauquelin, O., "Description of Measuring Techniques used in the Eureka-project", Proceedings of the International Conference on Fires in Tunnels, 20-35, Borås, Sweden, 10-11 October, 1994.
136. Ingason, H. and Lönnemark, A., "Large-scale Fire Tests in the Runehammar tunnel - Heat Release Rate (HRR)", International Symposium on Catastrophic Tunnel Fires (CTF), SP Report 2004:05, p.81-92, Borås, Sweden, 20-21 November, 2003.
137. Ingason, H., "Estimation of heat release rates in Runehammar tests", SP Swedish National Testing and Research Institute, Borås, Sweden, 2003.

138. Cullis, C. F., "The Involvement of Oxygen in the Primary Decomposition Stage of Polymer Combustion", *Fire Safety Science - Proceedings of the First International Symposium*, 371-380, Gaithersburg, MD, USA, 7-11 October, 1985.
139. Carvel, R. O., Beard, A. N., and Jowitt, P. W., "CERBERUS: A New Model to Estimate Size and Spread for Fires in Tunnels with Longitudinal Ventilation", *Proc. Int. Conf. on Tunnel Safety & Ventilation, New Developments in Tunnel Safety*, 69-76, Graz, Austria, 8-10 April, 2002.
140. Carvel, R. O., Beard, A. N., and Jowitt, P. W., "HGV Fires in Tunnels: How Severe are They and under what Conditions will They Spread", *Fourth International Conference on Tunnel Fires*, 171-177, Basel Switzerland, 2-4 December, 2002.
141. Thomas, P. H., "The Movement of Smoke in Horizontal Passages Against an Air Flow", *Fire Research Station, Fire Research Note No 723*, 1968.
142. de Ris, J., "Duct Fires", *Combustion and Science Technology*, **2**, 239-258, 1970.
143. Hinkley, P. L., "The Flow of Hot Gases Along an Enclosed Shopping Mall - A Tentative Theory", *Fire Research Station, Fire Research Note No 807*, 1970.
144. Danziger, N. H. and Kennedy, W. D., "Longitudinal Ventilation Analysis for the Glenwood Canyon Tunnels", *Fourth International Symposium on the Aerodynamics & Ventilation of Vehicle Tunnels*, 169-186, York, UK, 23-25 March, 1982.
145. Guelzim, A., Souil, J. M., Vantelon, J. P., Son, D. K., Gabay, D., and Dallest, D., "Modelling of a Reverse Layer of Fire-Induced Smoke in a Tunnel", *Proceedings of the Fourth International Symposium on Fire Safety Science*, 277-288, Ottawa, Canada, 13-17 June, 1994.
146. Oka, Y. and Atkinson, G. T., "Control of Smoke Flow in Tunnel Fires", *Fire Safety Journal*, **25**, 305-322, 1995.
147. Atkinson, G. T., and Wu, Y., "Smoke Control in Sloping Tunnels", *Fire Safety Journal*, **27**, 335-341, 1996.
148. Kunikane, Y., Kawabata, N., Okukawa, S., Okubo, K., and Shimoda, A., "Influence of Stationary Vehicles on Backlayering Characteristics of Fire Plume in a Large Cross Section Tunnel", *Proceedings of the Fifth International Conference on Safety in Road and Rail Tunnels*, 599-608, Marseille, France, 6-10 October, 2003.
149. Kunsch, J. P., "Simple Model for Control of Fire Gases in a Ventilated Tunnel", *Fire Safety Journal*, **37**, 67-81, 2002.
150. Wu, Y. and Bakar, M. Z. A., "Control of smoke flow in tunnel fires using longitudinal ventilation systems - a study of the critical velocity", *Fire Safety Journal*, **35**, 363-390, 2000.
151. Grant, G. B., Jagger, S. F., and Lea, C. J., "Fires in tunnels", *Phil. Trans. R. Soc. Lond.*, **356**, 2873-2906, 1998.
152. Casale, E. and Biollay, H., "A Fully Controlled Ventilation Response in the Case of a Tunnel Fire. The 'Confinement' Velocity", *Proceedings of the*

- Fourth International Conference on Safety in Road and Rail Tunnels, 477-485, Madrid, Spain, 2-6 April, 2001.
153. Telle, D., Vauquelin, O., and Biollay, H., "An Experimental Evaluation of the <<Confinement Velocity>>", Fourth International Conference on Tunnel Fires, 161-170, Basel Switzerland, 2-4 December, 2002.
 154. Vauquelin, O. and Telle, D., "Definition and experimental evaluation of the smoke "confinement velocity" in tunnel fires", *Fire Safety Journal*, **40**, 320-330, 2005.
 155. McCaffrey, B. J., "Purely Buoyant Diffusion Flames: Some Experimental Results", National Bureau of Standards, NBSIR 79-1910, Washington, D.C., USA, 1979.
 156. Cetegen, B. M. and Ahmed, T. A., "Experiments on the Periodic Instability of Buoyant Plumes and Pool Fires", *Combustion and Flame*, **93**, 157-184, 1993.
 157. Malalasekera, W. M. G., Versteeg, H. K., and Gilchrist, K., "A Review of Research and an Experimental Study on the Pulsation of Buoyant Diffusion Flames and Pool Fires", *Fire and Materials*, **20**, 261-271, 1996.
 158. Weckman, E. J. and Sobiesiak, A., "The Oscillatory Behaviour, of Medium-scale Pool Fires", Twenty-Second Symposium (International) on Combustion, 1299-1310, 1988.
 159. Hamins, A., Yang, J. C., and Kashiwagi, T., "An Experimental Investigation of the Pulsation Frequency of Flames", Twenty-fourth Symposium (International) on Combustion, 1695-1702, 1992.
 160. Kim, K. I., Ohtani, H., and Uehara, Y., "Experimental Study on Oscillating Behaviour in a Small-Scale Compartment Fire", *Fire Safety Journal*, **20**, 377-384, 1993.
 161. Utiskul, Y., Quintiere, J. G., Rangwala, A. S., Ringwelski, B. A., Wakatsuki, K., and Naruse, T., "Compartment fire phenomena under limited ventilation", *Fire Safety Journal*, **40**, 367-390, 2005.
 162. Fleischmann, C. M., Pagni, P. J., and Williamson, R. B., "Exploatory Back-draft Experiments", *Fire Technology*, **29**, 298-316, 1993.
 163. Gottuk, D. T., Peatross, M. J., Farley, J. P., and Williams, F. W., "The development and mitigation of backdraft: a real-scale shipboard study", *Fire Safety Journal*, **33**, 261-282, 1999.
 164. Prétrel, H. and Such, J. M., "Pressure Variations Induced by Large Scale Pool Fires in Forced-Ventilated Enclosures", 9th International Fire Science & Engineering Conference (Interflam 2001), 1429-1434, Edinburgh, Scotland, 17-19 September, 2001.
 165. Prétrel, H., Mélis, S., Minetian, S., and Querre, P., "Experimental Observations of Pressure Instabilities during a Pool Fire in a Confined and Ventilated Enclosure", 4th Int. Sem. on Fire and Explosion Hazards, Londonderry, Northern Ireland, 8-12 September, 2003.
 166. Tang, Y. M., Waldherr, G., Jagoda, J. I., and Zinn, B. T., "Heat Release Timing in a Nonpremixed Helmholtz Pulse Combustor", *Combustion and Flame*, **100**, 251-261, 1995.

167. Lindholm, A., "Pulsating Combustion - Combustion Characteristics and Reduction of Emissions", In *Department of Heat and Power Engineering*, Lund Institute of Technology, Lund, Sweden, 1999.
168. Tyndall, J., *Sound*, Sixth ed., Longmans, Green, and Co., London, 1895.
169. Higgins, B., "On the Sound Produced by a Current of Hydrogen Gas Passing through a Tube", *Nicholson's Journal of Natural Philosophy*, **50**, 129, 1802.
170. Richardson, E. G., "The Theory of the Singing Flame", *Proc. Phys. Soc. (London)*, **35**, 47-55, 1922.
171. Wood, A., *Acoustics*, Blackie & Son, Glasgow, 1943.
172. Jones, A. T., "Singing Flames", *The Journal of the Acoustical Society of America*, **16**, 4, 254-266, 1945.
173. Rayleigh, J. W. S., "The Explanation of Certain Acoustical Phenomena", *Nature*, July, 319-321, 1878.
174. Putnam, A. A., *Combustion-Driven Oscillations in Industry*, American Elsevier Publishing Company Inc., New York, 1971.
175. Castro, I. P., "Vortex shedding from a ring in oscillatory flow", *Journal of Wind Engineering and Industrial Aerodynamics*, **69-71**, 387-398, 1997.
176. Schadow, K. C. and Gutmark, E., "Combustion Instability Related to Vortex Shedding in Dump Combustors and their Passive Control", *Progress in Energy and Combustion Science*, **18**, 117-132, 1992.
177. Putnam, A. A., Belles, F. E., and Kentfield, J. A. C., "Pulse Combustion", *Progress in Energy and Combustion Science*, **12**, 43-79, 1986.
178. Zinn, B. T., "Pulsating Combustion". In *Advanced Combustion Methods* (F. Weinberg, J., Ed.), Academic Press, 113-181, London, 1986.
179. Keller, J. O., Bramlette, T. T., Barr, P. K., and Alvarez, J. R., "NO_x and CO Emissions from a Pulse Combustor Operating in a Lean Premixed Mode", *Combustion and Flame*, **99**, 460-466, 1994.
180. Lundgren, E., Marksten, U., and Möller, S.-I., "The Enhancement of Heat Transfer in the Tail Pipe of a Pulse Combustor", Proceedings of the 27th Symposium (International) on Combustion, 3215-3220, Boulder, Colorado, USA, 2-7 August, 1998.
181. Culick, F. E. C., "Nonlinear behavior of acoustic waves in combustion chambers - I", *Acta Astronautica*, **3**, 715-734, 1976.
182. Culick, F. E. C., "Nonlinear behavior of acoustic waves in combustion chambers - II", *Acta Astronautica*, **3**, 735-757, 1976.
183. Dowling, A. P., "Nonlinear self-excited oscillations of a ducted flame", *Journal of Fluid Mechanics*, **346**, 271-290, 1997.
184. Langhorne, P. J., "Reheat buzz: an acoustical coupled combustion instability. Part 1. Experiment", *Journal of Fluid Mechanics*, **193**, 417-443, 1988.
185. Bloxsidge, G. J., Dowling, A. P., and Langhorne, P. J., "Reheat buzz: an acoustically coupled combustion instability. part 2. Theory", *Journal of Fluid Mechanics*, **193**, 445-473, 1988.
186. Dowling, A. P., "The Calculation of Thermoacoustic Oscillations", *Journal of Sound and Vibration*, **180**, 4, 557-581, 1995.

187. Dowling, A. P., "A kinematic model of a ducted flame", *Journal of Fluid Mechanics*, **394**, 51-72, 1999.
188. Macquisten, M. A. and Dowling, A. P., "Low-frequency Combustion Oscillations in a Model Afterburner", *Combustion and Flame*, **94**, 253-264, 1993.
189. Culick, F. E. C., "Combustion Instabilities in Liquid-fueled Propulsion Systems - An Overview", AGARD Conference Proceedings 1988:450, 1-1 -- 1-73, 1988.
190. Chu, Y.-C., Dowling, A. P., and Glover, K., "Robust Control of Combustion Oscillations", Proceedings of the 1998 IEEE International Conference on Control Applications, 1165-1169, Trieste, Italy, 1-4 September, 1998.
191. Fleifil, M., Annaswamy, A. M., Ghoniem, A. F., and Ghoniem, Z. A., "Active Control of Thermoacoustic Instability in Combustion Systems", Proceedings of the 4th IEEE Conference on Control Applications, 685-696, Albany, New York, USA, 28-29 September, 1995.
192. Annaswamy, A. M., El Rifai, O. M., Fleifil, M., and Ghoniem, A. F., "A Model-Based Active-Adaptive Controller for Thermoacoustic Instability", Proceedings of the 1997 IEEE International Conference on Control Applications, 842-847, Hartford, CT, USA, 5-7 October, 1997.
193. Rumsey, J. W., Fleifil, M., Annaswamy, A. M., Hathout, J.-P., and Ghoniem, A. F., "The Role of Active Control in Suppressing Thermoacoustic Instability", Proceedings of the American Control Conference, 2697-2702, Albuquerque, New Mexico, USA, June, 1997.
194. Hathout, J.-P., Fleifil, M., Rumsey, J. W., Annaswamy, A. M., and Ghoniem, A. F., "Model-Based Analysis and Design of Active Control of Thermoacoustic Instability", Proceedings of the 1997 IEEE International Conference on Control Applications, 830-835, Hartford, CT, USA, 5-7 October, 1997.
195. Rumsey, J. W., Fleifil, M., Annaswamy, A. M., and Ghoniem, A. F., "Low-order Nonlinear Models of Thermoacoustic Instabilities and Model-based Control", Proceedings of the 1998 IEEE International Conference on Control Applications, 1419-1423, Trieste, Italy, 1-4 September, 1998.
196. Fleifil, M., Annaswamy, A. M., Rumsey, J. W., Kojic, A., and Ghoniem, A. F., "A Physically Based Nonlinear Model of Combustion Instability and Active Control", Proceedings of the 1998 IEEE International Conference on Control Applications, 1185-1189, Trieste, Italy, 1-4 September, 1998.
197. Fleifil, M., Annaswamy, A. M., Hathout, J.-P., and Ghoniem, A. F., "Reduced-Order Dynamic Models for Control of Reactive Fluid-flows", Proceedings of the 38th Conference on Decision & Control, 2857-2862, Phoenix, Arizona, USA, December, 1999.
198. Annaswamy, A. M., Fleifil, M., Rumsey, J. W., Prasanth, R., Hathout, J.-P., and Ghoniem, A. F., "Thermoacoustic Instability: Model-Based Optimal Control Design and Experimental Validation", *IEEE Transactions on Control Systems Technology*, **8**, 6, 905-918, 2000.
199. Paschereit, C. O., Gutmark, E., and Weisenstein, W., "Acoustic Control of Combustion Instabilities and Emissions in a Gas-Turbine Combustor", Proceedings of the 1998 IEEE International Conference on Control Applications, 1175-1179, Trieste, Italy, 1-4 September, 1998.

200. Rijke, P. L., "Notiz über eine neue Art, die in einer an beiden Enden offenen Röhre enthaltene Luft in Schwingungen zu versetzen", *Annalen der Physik und Chemie*, **107**, 339-343, 1859.
201. Neuringer, J. L., and Hudson, G. E., "An Investigation of Sound Vibrations in a Tube Containing a Heat Source", *The Journal of the Acoustical Society of America*, **24**, 6, 667-674, 1952.
202. Carrier, G. F., "The Mechanics of the Rijke Tube", *Quarterly Applied Mathematics*, **12**, 4, 383-395, 1955.
203. Maling Jr, G. C., "Simplified Analysis of the Rijke Phenomenon", *Journal of the Acoustical Society of America*, **35**, 1058-1060, 1963.
204. Feldman Jr, K. T., "Review of the Literature on Rijke Thermoacoustic Phenomena", *Journal of Sound and Vibration*, **7**, 1, 83-89, 1968.
205. Kwon, Y.-P. and Lee, B.-H., "Stability of the Rijke thermoacoustic oscillation", *Journal of the Acoustical Society of America*, **78**, 4, 1414-1420, 1985.
206. Carvalho Jr., J. A., Ferreira, M. A., Bressan, C., and Ferreira, J. L. G., "Definition of Heater Location to Drive Maximum Amplitude Acoustic Oscillations in a Rijke Tube", *Combustion and Flame*, **76**, 17-27, 1989.
207. Heckl, M. A., "Non-linear Acoustic Effects in the Rijke Tube", *Acustica*, **72**, 63-71, 1990.
208. Yoon, H.-G., Peddieson Jr, J., and Purdy, K. R., "Mathematical modeling of a generalized Rijke tube", *International Journal of Engineering Science*, **36**, 1235-1264, 1998.
209. Hantschk, C.-C. and Vortmeyer, D., "Numerical Simulation of Self-excited Thermoacoustic Instabilities in a Rijke Tube", *Journal of Sound and Vibration*, **277**, 3, 511-522, 1999.
210. Yoon, H.-G., Peddieson, J., and Purdy, K. R., "Non-linear response of a generalized Rijke tube", *International Journal of Engineering Science*, **39**, 1707-1723, 2001.
211. Pun, W., "Measurements of Thermo-Acoustic Coupling", California Institute of Technology, Pasadena, California, USA, 2001.
212. Agostino, F., Baldini, G., Bittanti, S., Poncia, G., Prandoni, W., and Scarpellini, M., "Nonlinear Identification of Thermoacoustic Instabilities with Limit Cycles in a Rijke Tube", Proceedings of the 2002 IEEE International Conference on Control Applications, 1147-1152, Glasgow, Scotland, 18-20 September, 2002.
213. Entezam, B., Van Moorhem, W. K., and Majdalani, J., "Two-dimensional Numerical Verification of the Unsteady Thermoacoustic Field inside a Rijke Pulse Combustor", *Numerical Heat Transfer, Part A*, **41**, 245-262, 2002.
214. Finlinson, J. C., Nelson, M. A., and Beckstead, M. W., "Characterization of a Modified Rijke Burner for Measurement of Distributed Combustion", 24th JANNAF Combustion Meeting, 13-25, 1987.
215. Matveev, K., "Thermoacoustic Instabilities in the Rijke Tube: Experiments and Modeling", California Institute of Technology, Pasadena, California, USA, 2003.

216. Bittanti, S., De Marco, A., Poncia, G., and Prandoni, W., "Identification of a Model for Thermoacoustic Instabilities in a Rijke Tube", *IEEE Transactions on Control Systems Technology*, **10**, 4, 490-502, 2002.
217. Matveev, K. I., "Energy consideration of the nonlinear effects in a Rijke tube", *Journal of Fluids and Structures*, **18**, 783-794, 2003.
218. Wylie, E. B., and Streeter, V. L., *Fluid Transients*, McGraw-Hill Inc., USA, 1978.
219. Simonson, M., Tuovinen, H., and Emanuelsson, V., "Formation of Hydrogen Cyanide in Fires - A Literature and Experimental Investigation", SP Swedish National Testing and Research Institute, SP REPORT 2000:27, Borås, Sweden, 2000.
220. Purser, D. A., "Toxic product yields and hazard assessment for fully enclosed design fires", *Polymer International*, **49**, 1232-1255, 2000.
221. Ferrari, L. A., Arado, M. G., Giannuzzi, L., Mastrantonio, G., and Guatelli, M. A., "Hydrogen cyanide and carbon monoxide in blood of convicted dead in a polyurethane combustion: a proposition for the data analysis", *Forensic Science International*, **121**, 140-143, 2001.
222. Purser, D. A., "Toxicity Assessment of Combustion Products". In *SFPE Handbook of Fire Protection Engineering* (P. J. DiNenno, Ed.), National Fire Protection Association, Inc, 2-83 -- 2-171, Quincy, Massachusetts, USA, 2002.
223. Nelson, G. L., "Carbon Monoxide and Fire Toxicity: A Review and Analysis of Recent Work", *Fire Technology*, **34**, 1, 39-58, 1998.
224. Gann, R. G., "Sublethal Effects of Fire Smoke", *Fire Technology*, **40**, 95-99, 2004.
225. Persson, B., Simonson, M., and Månsson, M., "Utsläpp från bränder till atmosfären", SP Sveriges Provnings- och Forskningsinstitut, SP RAPPORT 1995:70, Borås, Sweden (in Swedish), 1995.
226. Blomqvist, P., Persson, B., and Simonson, M., "Utsläpp från bränder till miljön - Utsläpp av dioxin, PAH och VOC till luften", Räddningsverket (Swedish Rescue Services Agency), P21-407/02, Karlstad, Sweden (in Swedish), 2002.
227. Persson, B. and Simonson, M., "Fire Emissions into the Atmosphere", *Fire Technology*, **34**, 3, 266-279, 1998.
228. Hölemann, H., "Environmental Problems Caused by Fires and Fire-Fighting Agents", *Fire Safety Science - Proceedings of the Fourth International Symposium*, 61-77, Ottawa, Canada, 13-17 June, 1994.
229. Ahrens, M. and Rohr, K. D., "Fire and the Environment: Issues and Events", *Proceedings of the Fire Risk and Hazard Assessment Research Application Symposium*, Baltimore, Maryland, USA, 9-11 July, 2003.
230. Marlair, G., Simonson, M., and Gann, R. G., "Environmental Concerns of Fires: Facts, Figures, Questions and New Challenges for the Future", 10th International Fire Science & Engineering Conference (Interflam 2004), 325-337, Edinburgh, Scotland, 5-7 July, 2004.

231. Wichmann, H., Lorenz, W., and Bahadir, M., "Release of PCDD/F and PAH during Vehicle Fires in Traffic Tunnels", *Chemosphere*, **31**, 2, 2755-2766, 1995.
232. Mauring, T., Personal communication, Åndalsnes, Norway, 2003.
233. Nilsen, A. R., Lindvik, P. A., and Log, T., "Full-scale Fire Testing in Sub Sea Public Road Tunnels", Interflam 2001, 913-924, Edinburgh, Scotland, 17-19 September, 2001.
234. Pitts, W. M., "The Global Equivalence Ratio Concept and the Prediction of Carbon Monoxide Formation in Enclosure Fires", National Institute of Standards and Technology, NIST Monograph 179, Gaithersburg, MD, USA, 1994.
235. Beyler, C. L., "Major Species Production by Diffusion Flames in a Two-layer Compartment Fire Environment", *Fire Safety Journal*, **10**, 47-56, 1986.
236. Gottuk, D. T., "Carbon Monoxide Production in Compartment Fires", *Journal of Fire Protection Engineering*, **4**, 4, 133-150, 1992.
237. Gottuk, D. T. and Lattimer, B. Y., "Effect of Combustion Conditions on Species Production". In *SFPE Handbook of Fire Protection Engineering* (P. J. DiNenno, Ed.), National Fire Protection Association, Inc, 2-54 -- 2-82, Quincy, Massachusetts, USA, 2002.
238. Babrauskas, V., Parker, W. J., Mulholland, G., and Twilley, W. H., "The phi meter: A simple, fuel-independent instrument for monitoring combustion equivalence ratio", *Rev. Sci Instrum.*, **65**, 7, 2367-2375, 1994.
239. Ingason, H., "Fire Dynamics in Tunnels". In *The Handbook of Tunnel Fire Safety* (R. O. Carvel and A. N. Beard, Eds.), Thomas Telford Publishing, 231-266, London, 2005.
240. Gottuk, D. T., Roby, R. J., and Beyler, C. L., "The Role of Temperature on Carbon Monoxide Production in Compartment Fires", *Fire Safety Journal*, **24**, 315-331, 1995.
241. Tsuchiya, Y., "CO/CO₂ Ratios in Fire", Fire Safety Science - Proceedings of the Fourth International Symposium, 515-526, Ottawa, Canada, 13-17 June, 1994.
242. Beyler, C. L., "Major Species Production by Solid Fuels in a Two Layer Compartment Fire Environment", Fire Safety Science - Proceedings of the First International Symposium, 431-440, Gaithersburg, USA, 7-11 October, 1985.
243. Varon, J., Marik, P. E., Fromm, R. E., and Gueler, A., "Carbon Monoxide Poisoning: A Review for Clinicians", *The Journal of Emergency Medicine*, **17**, 1, 87-93, 1999.
244. Brandt, A. B., "Presentation of test result from large scale fire tests at the Runehamar tunnel", International Symposium on Catastrophic Tunnel Fires (CTF), SP Report 2004:05, 117-120, Borås, Sweden, 20-21 November, 2003.
245. Lighty, J. S. and Pershing, D. W., "Control of Pollutant Emissions from Waste Burning", University of Utah, Project number AQ93-4, 1993.
246. Risholm-Sundman, M., and Vestin, E., "Emissions during combustion of particleboard and glued veneer", *Holz als Roh- und Werkstoff*, **63**, 179-185, 2005.

247. Grønli, M., "A Theoretical and Experimental Study of the Thermal Degradation of Biomass", In *Department of Thermal Energy and Hydropower*, The Norwegian University of Science and Technology, Trondheim, Norway, 1996.
248. Zevenhoven, R., Axelsen, E. P., Kilpinen, P., and Hupa, M., "Nitrogen oxides from nitrogen-containing waste fuels at FBC conditions - Part 1", The 39th IEA FBC meeting, Madrid, Spain, 22-24 November, 1999.
249. Tuovinen, H. and Blomqvist, P., "Modelling of Hydrogen Cyanide Formation in Room Fires", SP Swedish National Testing and Research Institute, SP REPORT 2003:10, Borås, Sweden, 2003.
250. Hansson, K.-M., Samuelsson, J., Tullin, C., and Åmand, L.-E., "Formation of HNCO, HCN, and NH₃ from the pyrolysis of bark and nitrogen-containing model compounds", *Combustion and Flame*, **137**, 265-277, 2004.
251. ISO/TS 13571:2002(E), "Life-threatening components of fire - Guidelines for the estimation of time available for escape using fire data", First ed., 2002-08-01, ISO, 2002.
252. Lönnermark, A. and Ingason, H., "Large Scale Fire Tests in the Runehamar Tunnel - Gas Temperature and Radiation", International Symposium on Catastrophic Tunnel Fires (CTF), SP Report 2004:05, p. 93-103, Borås, Sweden, 20-21 November, 2003.
253. Harmathy, T. Z., *Fire Safety Design and Concrete*, Longman Scientific & Technical, 1993.
254. Boström, L., "Spalling of Tunnel Structure Linings - New Swedish Results", International Symposium on Catastrophic Tunnel Fires (CTF), 69-79, Borås, Sweden, 2003.
255. Boström, L., "Methodology for Measurement of Spalling of Concrete", Fire and Materials 2005, 121-129, Fisherman's Wharf, San Francisco, USA, 31 Jan. - 1 Feb., 2005.
256. Høj, N. P. and Pedersen, L., "Full Scale Tests for Assessment of Fire Risk", Third International Conference on Safety in Road and Rail Tunnels, 225-236, Nice, France, 9-11 March, 1998.
257. Persson, H., "Basutrustning för skumsläckning - Försöksresultat och rekommendationer som underlag för dimensionering och utförande", SP Swedish National Testing and Research Institute, SP RAPPORT 1990:36, Borås, Sweden (in Swedish), 1990.
258. Lemaire, T., "Runehamar Tunnel Fire Tests: Radiation, Fire Spread and Back Layering", International Symposium on Catastrophic Tunnel Fires (CTF), SP Report 2004:05, 105-116, Borås, Sweden, 20-21 November, 2003.
259. Frantzich, H., "Problems of evacuation in catastrophic tunnel fires", International Symposium on Catastrophic Tunnel Fires (CTF), 177-185, Borås, Sweden, 2003.
260. Setoyama, S., Ichikawa, A., Shimizu, K., Gunki, S., and Kimura, T., "Effective Operation of Water Spray System for a Tunnel Fire", Proceedings of the Fifth International Conference on Safety in Road and Rail Tunnels, 547-551, Marseille, France, 6-10 October, 2003.

261. Yoshimochi, T., Gunki, S., Kobayashi, A., and Yokota, M., "Full Scale Testing and Maintenance of Water Spraying Equipment in a Large Tunnel", Proceedings of the Fifth International Conference on Safety in Road and Rail Tunnels, 565-572, Marseille, France, 6-10 October, 2003.
262. Arvidson, M., "Alternative Fire Sprinkler Systems for Roadway Tunnels", Proceedings of the International Symposium on Catastrophic Tunnel Fires, 193-201, Borås, Sweden, 20-21 November, 2003.